

**INTERACTIONS OF IRON DINITROSYL COMPOUNDS  
WITH IMIDAZOLE AND ITS DERIVATIVES**

MASTER OF SCIENCE

McMASTER UNIVERSITY

(Chemistry)

Hamilton, Ontario

**TITLE: INTERACTIONS OF IRON DINITROSYL COMPOUNDS WITH  
IMIDAZOLE AND ITS DERIVATIVES**

**AUTHOR:** Christopher T.C. McCrory, B.Sc. (McMaster University)

**SUPERVISOR:** Professor L. Li

**Number of Pages:** xi, 108

## ABSTRACT

Nitric oxide has been implicated in a number of biological processes, the majority of them involving iron nitrosyl complexes. The urgency then is to further study and characterize these complexes to further the understanding of biological mechanisms. However, the chemical sensitivity of these species precludes the purification and isolation of these compounds which, unfortunately, has directed the trend to merely detecting the presence of these compounds rather than isolating them. To this day, a large number of Electron Paramagnetic Resonance (EPR) detectable, biological compounds have not been isolated.

To this end, the series of biologically relevant compounds of the form  $\text{Fe}(\text{NO})_2(\text{L})_2$  [ L = imidazole **1**, 1-methylimidazole (1-MeIm) **2**, 4-methylimidazole (4-MeIm) **3**, benzimidazole (benzim) **4**, and 5,6-dimethylbenzimidazole (5,6-benzim) **5** ] have been synthesized by direct reaction of the appropriate imidazole ligand with  $\text{Fe}(\text{NO})_2(\text{CO})_2$ . The compounds were extremely air sensitive, both in solution and as a dry solid. This hindered attempts to purify these compounds and so, infra red (IR), nuclear magnetic resonance (NMR) and EPR spectroscopic studies were undertaken of 2:1 reaction mixtures of the appropriate imidazole ligand and  $\text{Fe}(\text{NO})_2(\text{CO})_2$ . These studies revealed that the rapid substitution of the carbonyl ligands is facilitated by a catalytic, 17-electron, electron transfer chain mechanism (ETC), where the imidazole ligand acts to oxidize the 18-electron complex into the active 17-electron  $\text{Fe}(\text{NO})_2(\text{CO})_2^+$  species.

In the course of the EPR study of **2**, crystals formed that were suitable for single-crystal, X-ray diffraction. The compound crystallizes with a monoclinic unit cell, in the C2/c

space group with unit cell dimensions:  $a = 13.985(5)$  Å,  $b = 11.529(5)$  Å,  $c = 15.471(4)$  Å,  $\alpha = 90^\circ$ ,  $\beta = 91.72(2)^\circ$ ,  $\gamma = 90^\circ$ ,  $V = 2493(2)$  Å<sup>3</sup>,  $Z = 8$ . During the course of study of **6**, crystals suitable for single crystal X-ray diffraction were obtained. The compound crystallizes with a monoclinic unit cell, in the P2/c space group and unit cell dimensions:  $a = 11.707(9)$  Å,  $b = 8.1783(5)$  Å,  $c = 17.2489(13)$  Å,  $\alpha = 90^\circ$ ,  $\beta = 106.562(1)^\circ$ ,  $\gamma = 90^\circ$ ,  $V = 1583.0(2)$  Å<sup>3</sup>,  $Z = 2$ .

A relatively new mass spectrometry (MS) procedure was utilized for the reaction mixtures of **1 - 5**, which involved a combination of electrochemical oxidation and electrospray. The method proved very useful, yielding data that could not be obtained by other MS techniques. Oligomeric species of the form L-[Fe(NO)<sub>2</sub>L]<sub>x</sub> ( $x = 2,3,4,5$  or  $6$ ), were also detected by MS for each compound reaction mixture. The oligomers involved linear chains of iron dinitrosyl fragments linked via the imidazole nitrogens. However, it is believed that these oligomers are produced as a result of the conditions met by the mass spectrometer.

A reaction of Fe(NO)<sub>2</sub>(PPh<sub>3</sub>)(CO) with 1-MeIm was also performed in hopes of producing a more stable mono-substituted complex. However, the reaction also proceeded via an Electron Transfer Chain (ETC) pathway to produce Fe(NO)<sub>2</sub>(PPh<sub>3</sub>)<sub>2</sub> **6**.

## ACKNOWLEDGEMENTS

I would like to thank my supervisor, Dr. Lijuan Li for her guidance and patience over the past couple of years. It was an interesting experience starting up a lab.

I would like to thank my coworkers: Guodong Zheng, Roger Liu and especially Nada Reginato who made the lab a fun place to work.

Thanks go to Dr. Donald Hughes and Mr. Brian Sayer for the NMR time and advice, and to George Timmins for the IR and EPR help. Thanks also to Dr. Jim Britten and Mark Stradiotto for their time and advice for X-ray crystallography work.

I would also like to thank Randy, Pippa and Buck and the rest of the Pheonix all stars, with whom I have achieved critical mass on numerous occasions.

Finally, I would like to thank my parents and my brother Ian for their love, support and guidance over the years. I need no other role models.

## TABLE OF CONTENTS

1. Introduction	1
1.1 The Role of Nitric Oxide in Living Systems	2
1.2 Biological Roles of Nitric Oxide	2
1.2.1 Indirect effects of NO	3
1.2.2 Direct Effects of NO	4
1.3 Structure and Bonding in Metal Nitrosyl Complexes	5
1.4 The Chemistry of Metal Nitrosyl Complexes	7
1.4.1 Formation of Metal Nitrosyls	7
1.4.2 The Reactivity of Metal Nitrosyls	9
1.4.3 Iron dinitrosoylcarbonyl	11
1.5 Research Objectives	15
2. Results and Discussion	16
2.1 Mechanism of iron dinitrosoyl compounds with imidazole ligands	16
2.2 Infrared Spectroscopy	23
2.3 Nuclear Magnetic Resonance Spectroscopy	25
2.4 EPR Spectroscopy	29
2.5 X-Ray Crystallography	37
2.6 Mass Spectrometry	55
3. Experimental	83
4. Future Work and Conclusions	91
Appendix A. Structure factor tables for 2	93
Appendix B. Structure factor tables for 6.	99
References	107

## LIST OF SCHEMES

Scheme 1.1	Proposed mechanism of formation of $\text{Fe}(\text{NO})_2(\text{CO})_2$ .	13
Scheme 2.1	Enhanced rate of CO substitution by oxidation of $[(\text{MeCp})\text{Mn}(\text{CO})_3]$ to the 17 electron $[(\text{MeCp})\text{Mn}(\text{CO})_3]^+$ intermediate.	17
Scheme 2.2	Enhanced rate of CO substitution by oxidation of $[(\text{MeCp})\text{Mn}(\text{CO})_2(\text{MeCN})]$ to the 17 electron $[\text{Mn-NCMe}]^+$ intermediate .	18
Scheme 2.3	Enhanced rate of CO substitution <i>via</i> oxidation of $\text{Fe}(\text{NO})_2(\text{CO})(\text{PPh}_3)$ to $\text{Fe}(\text{NO})_2(\text{CO})(\text{PPh}_3)^+$ by TCNE.	19
Scheme 2.4	Mechanistic pathway for formation of the $\text{Fe}(\text{NO})_2(\text{L})_2$ [ $\text{L}$ = imidazole, 1-MeIm, 4-MeIm, Benzim, 5,6-dimethylbenzim] series of compounds.	21
Scheme 2.5	Mechanistic pathway for formation of the $\text{Fe}(\text{NO})_2(\text{L})_2$ [ $\text{L}$ = $\text{PPh}_3$ ] from the reaction of $\text{Fe}(\text{NO})_2(\text{CO})(\text{PPh}_3)$ and 1-MeIm.	22

## FIGURES

Figure 1.1	The NO/NO <sub>2</sub> conversion and NO <sub>2</sub> removal processes in the troposphere	1
Figure 1.2	Molecular Bonding Scheme for Metal Nitrosyls	6
Figure 1.3	Nitrosyl Bending in Metal complexes. A: Linear "3 electron" bonding. B: Bent "1 electron bonding"	7
Figure 1.4	Linear-bent interchange of [Ir(NO)(η <sup>3</sup> -C <sub>3</sub> H <sub>5</sub> )(PPh <sub>3</sub> ) <sub>2</sub> ] <sup>+</sup> .	9
Figure 1.5.	Linear-bent interchange by chemical addition	10
Figure 1.6	Reaction of a nucleophile with the nitrogen of NO.	11
Figure 1.7.	Ortep diagram of [Fe(NO) <sub>2</sub> (CO)] <sub>2</sub> dppne, shown with 50 % thermal ellipsoids (above) and crystal packing diagram (below).	14
Figure 1.8.	Ortep diagram of [Fe(NO) <sub>2</sub> (CO)] <sub>2</sub> dppm, shown with 50 % thermal ellipsoids (above) and crystal packing diagram (below).	14
Figure 2.1	<sup>1</sup> H NMR spectrum of Fe(NO) <sub>2</sub> (1-MeIm) <sub>2</sub> .	27
Figure 2.2	<sup>13</sup> C NMR spectrum of Fe(NO) <sub>2</sub> (1-MeIm) <sub>2</sub> .	28
Figure 2.3.	EPR spectrum (above) and simulation (below) of Fe(NO) <sub>2</sub> (imidazole) <sub>2</sub> .	32
Figure 2.4.	EPR spectrum (above) and simulation (below) of Fe(NO) <sub>2</sub> (1-MeIm) <sub>2</sub> .	33
Figure 2.5.	EPR spectrum (above) and simulation (below) of Fe(NO) <sub>2</sub> (4-MeIm) <sub>2</sub> .	34
Figure 2.6.	EPR spectrum (above) and simulation (below) of Fe(NO) <sub>2</sub> (benzimidazole) <sub>2</sub> .	35
Figure 2.7.	EPR spectrum (above) and simulation (below) of Fe(NO) <sub>2</sub> (5,6-dimethylbenzimidazole) <sub>2</sub> .	36

Figure 2.8.	Ortep diagram of $\text{Fe}(\text{NO})_2(1\text{-MeIm})_2$ shown at 50 % thermal ellipsoids.	40
Figure 2.9.	Crystal packing diagram of $\text{Fe}(\text{NO})_2(1\text{-MeIm})_2$ . Hydrogens are omitted for clarity.	41
Figure 2.10.	X-Ray crystal structure of 6, shown with 50 % thermal ellipsoids. Hydrogen atoms have been omitted for clarity.	42
Figure 2.11.	Crystal packing of 6, viewed down the <i>b</i> axis. Hydrogen atom have been omitted for clarity.	43
Figure 2.12.	Schematic diagram of mass spectrometer ionization apparatus.	55
Figure 2.13.	Mass spectrum of $\text{Fe}(\text{NO})_2(\text{imidazole})_2$	58
Figure 2.14.	Mass spectrum of $\text{Fe}(\text{NO})_2(1\text{-MeIm})_2$	59
Figure 2.15.	Mass spectrum of $\text{Fe}(\text{NO})_2(4\text{-MeIm})_2$	60
Figure 2.16.	Mass spectrum of $\text{Fe}(\text{NO})_2(\text{benzimidazole})_2$	61
Figure 2.17.	Mass spectrum of $\text{Fe}(\text{NO})_2(5,6\text{-dimethylbenzimidazole})_2$	62
Figure 2.18.	Isotopic Ratio of $\text{Fe}(\text{NO})_2(1\text{-MeIm})_2$	63
Figure 2.19.	Ortep diagram of $[\text{Fe}_3(\text{imid})_6(\text{imidH})_2]_x$	70
Figure 2.20.	Daughters of $\text{Fe}(\text{NO})_2(\text{imidazole})_2^+$ 252 ion	71
Figure 2.21.	Daughters of $\text{Fe}(\text{NO})_2(1\text{-MeIm})_2^+$ 280 ion	72
Figure 2.22.	Daughters of $\text{Fe}(\text{NO})_2(4\text{-MeIm})_2^+$ 280 ion	73
Figure 2.23.	Daughters of $\text{Fe}(\text{NO})_2(4\text{-MeIm})_2^+$ 477 ion	74
Figure 2.24.	Daughters of $\text{Fe}(\text{NO})_2(4\text{-MeIm})_2^+$ 674 ion	75
Figure 2.25.	Daughters of $\text{Fe}(\text{NO})_2(\text{benzimidazole})_2^+$ 352 ion	76
Figure 2.26.	Daughters of $\text{Fe}(\text{NO})_2(\text{benzimidazole})_2^+$ 585 ion	77
Figure 2.27.	Daughters of $\text{Fe}(\text{NO})_2(5,6\text{-dimethylbenzimidazole})_2^+$ 408 ion	78

Figure 2.28.	MS Spectrum of $\text{Fe}(\text{NO})_2(1\text{-MeIm})_2$ immediately after exposure to air.	79
Figure 2.29.	MS Spectrum of $\text{Fe}(\text{NO})_2(1\text{-MeIm})_2$ 5 minutes after exposure to air.	80
Figure 2.30.	MS Spectrum of $\text{Fe}(\text{NO})_2(1\text{-MeIm})_2$ 7 minutes after exposure to air.	81
Figure 2.31.	MS Spectrum of $\text{Fe}(\text{NO})_2(1\text{-MeIm})_2$ 10 minutes after exposure to air.	82

## LIST OF TABLES

Table 2.1	Nitrosyl stretching frequencies for compounds 1 - 5.	24
Table 2.2	$g$ values and hyperfine coupling constants for $\text{Fe}(\text{NO})_2(\text{L})_2^+$ compounds. The number in parenthesis is the number of nuclei to which the coupling belongs.	30
Table 2.3	Comparison of iron dinitrosyl bond lengths (in Å).	38
Table 2.4	Crystal data and structure refinement for 2.	44
Table 2.5	Atomic coordinates ( $\times 10^4$ ) and equivalent isotropic displacement parameters ( $\text{\AA}^2 \times 10^3$ ) for 2.	45
Table 2.6	Bond lengths [Å] and angles [deg] for 2.	46
Table 2.7	Anisotropic displacement parameters ( $\text{\AA}^2 \times 10^3$ ) for 2.	47
Table 2.8	Hydrogen coordinates ( $\times 10^4$ ) and isotropic displacement parameters ( $\text{\AA}^2 \times 10^3$ ) for 2.	48
Table 2.9	Crystal data and structure refinement for 6.	49
Table 2.10	Atomic coordinates ( $\times 10^4$ ) and equivalent isotropic displacement parameters ( $\text{\AA}^2 \times 10^3$ ) for 6.	50
Table 2.11	Bond lengths [Å] and angles [°] for 6.	51
Table 2.12	Anisotropic displacement parameters ( $\text{\AA}^2 \times 10^3$ ) for 6.	53
Table 2.13	Hydrogen coordinates ( $\times 10^4$ ) and isotropic displacement parameters ( $\text{\AA}^2 \times 10^3$ ) for 6.	54
Table 2.14	Parent ion peaks for iron nitrosyl imidazole compounds.	68
Table 2.15	Imidazole dimers found in mass spectra.	68
Table 2.16	High MW ions found in Mass spectra of iron dinitrosyl imidazole compounds.	69
Table 2.17	MS/MS of iron dinitrosyl imidazole compounds.	70

## 1. Introduction

It is well known that the earth's atmosphere functions as a an insulating, thermal barrier, much like a greenhouse, and in doing so, provides the warmth necessary for the persistence of life on earth. The destruction of the “natural” protective atmosphere arises from four sources a) increased production of greenhouse gases such as the type of formula  $\text{NO}_x$ , b) increase in acidity of natural rain by nitrogen and sulfur oxides, c) depletion of the protective ozone layer by radical nitrogen oxide species, d) increased levels of secondary pollutants such as peroxyacetyl nitrate (PAN). Figure 1.1 shows the cycle that gives rise to

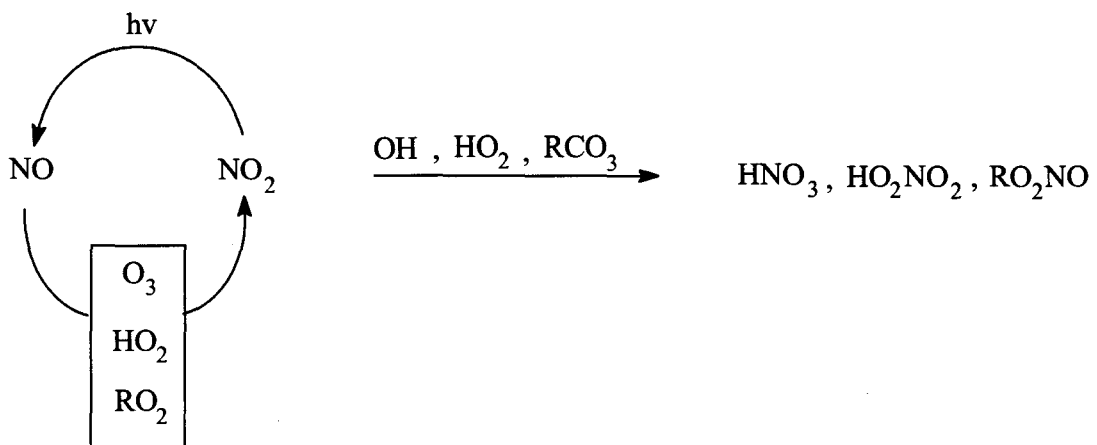


**Figure 1.1.** The NO/NO<sub>2</sub> removal processes in the troposphere

these concerns with regards to NO<sub>x</sub> in the troposphere.

Naturally occurring nitrogen oxides (NO<sub>x</sub>) originate from forest regions, marshlands, and grasslands. Other “natural” sources of NO<sub>x</sub> are derived from forest fires, and lightning where the temperature may reach upwards of 30,000 K.<sup>1</sup> Nearly all of the anthropogenic

$\text{NO}_x$  production occurs as a result of high temperature combustion devices, *via* the oxidation of  $\text{N}_2$  or organic nitrogen compounds. Indeed, it is the brown colour of gaseous  $\text{NO}_2$  that helps contribute to haze associated with smog-induced low visibility in industrialized cities.

The nitric oxide gases are known to cause respiratory problems, while PAN causes eye irritation. Nitrogen dioxide ( $\text{NO}_2$ ) initiates lipid oxidation in biological systems, and its inhalation has been associated with the biosynthesis of carcinogenic nitrosamines. Also, nitrogen oxides have been found to stimulate the nitration of polycyclic aromatic hydrocarbons *in vivo* to produce complexes that display mutagenicity, genotoxicity and carcinogenicity.<sup>2</sup>

However, despite the increasing environmental concern over nitric oxide gases and toxicological health issues, the nitric oxide (NO) molecule has been found to be one of the most important biological molecules ever discovered and has recently been named molecule of the decade.<sup>3</sup> This discovery has lead researchers to aggressively pursue the little known life of NO in living systems.

## 1.2 The Role of Nitric Oxide in Living Systems

The biological activity related to nitric oxide can be divided into two areas, indirect and direct effects. The principal reason that the chemical biology of NO can be partitioned in this manner is because NO has the capacity to react with molecules either directly, or as a pre-formed derivative or a metal complex.

### 1.2.1 Indirect effects of NO

The association of NO with stimulation of cyclic guanosine monophosphate (cGMP) production consequently links NO with a variety of physiological effects.<sup>4</sup> Cyclic GMP can act directly on ion channels and activate protein kinases, which catalyse the phosphorylation or dephosphorylation of proteins.<sup>4</sup> Furthermore, cyclic GMP directly regulates membrane cation channels in retinal photoreceptor cells, mediates smooth muscle relaxation, inhibits platelet aggregation, modulates excretion of Na<sup>+</sup> by the kidney, and helps to regulate cardiac function by modulating Ca<sup>2+</sup> currents.<sup>5</sup> Sodium nitroprusside, Na<sub>2</sub>[NO(CN)<sub>5</sub>Fe]·2H<sub>2</sub>O, which has been marketed as Nipride,<sup>5</sup> is often used to lower blood pressure in humans. Its hypotensive effect is evident within seconds after infusion, and the desired blood pressure is usually obtained in 1-2 minutes. Other nitrosyl compounds such as K[NOBr<sub>5</sub>Ir], K<sub>2</sub>[NOCl<sub>5</sub>Ru] and [NO(NH<sub>3</sub>)<sub>5</sub>Ru]Cl<sub>3</sub> have also shown vasodilatory activity, presumably by releasing NO, but are too toxic for clinical use.

NO plays an important role as a messenger between neurons at synapses in the central nervous system,<sup>3</sup> where it acts as a diffusible, short lived molecule within a local space to help shape the three dimensional network of synaptic responses. It now appears that NO, functioning as a neuromodulator in the hippocampus of the brain plays a fundamental role in the basic neuronal processes that initiate learning and experience.<sup>4</sup>

Nitric oxide is produced by macrophages to kill both invasive cells and in the rejection of tissue grafts.<sup>5</sup> The toxic effect appears to come from inhibition of enzyme activity through nitric oxide bonding to non-heme iron-centers in proteins such as ribonucleotide reductase, and release of intracellular iron from the cells targeted by the

macrophages.

### 1.2.2 Direct Effects of NO

Nitric oxide exists as a persistent, stable radical. However, NO does not rapidly react with most biological substances in a manner analogous to oxygen radicals such as ·OH. Since the lifetime of NO *in vivo* is relatively short (less than 10 sec) only the faster direct reaction of NO, such as with metal centers or other radicals, proves to be important. Reactions with metal centers, mainly iron, are crucial to understanding the bioregulatory behaviour of NO.

Another important direct reaction of metal centers with NO is seen with cytochrome P450. Studies have shown the NO inhibits mammalian P450, which is thought to regulate hormone metabolism and, under infectious conditions, decrease drug metabolism in the liver. The inhibitory mechanism relies on formation of an Fe-NO bond formation which prevents the binding of oxygen, similar to the mechanism for CO inhibition.

Metalloproteins play a major role in controlling concentrations of nitric oxide *in vivo*. Nitric oxide reacts directly with oxyhemoglobin ( $\text{HbO}_2$ ) or oxymyoglobin to form nitrate and methemoglobin (MetHb) or metmyoglobin,<sup>6</sup> which reduces the intracellular concentrations of NO.

The reaction of heme proteins with NO is also important to understanding the mechanism for protection against reactive species in the body. Peroxides are thought to enter a cell and react with heme proteins to form ferryl ( $\text{Fe}=\text{O}$ ) heme complexes. The ferryl heme

protein is then proposed to decompose and generate superoxide anion  $O_2^-$  and release the iron complex. The iron complex can further react with peroxides to generate very potent oxidants such as  $HO_2^-$  and  $H_2O_2$ . NO reacts with the iron complex, which results in the formation of methemoglobin<sup>6</sup> and inhibits the formation of oxidants.

One of the first clues that the immune system utilizes NO to combat pathogens came from electron paramagnetic resonance (EPR) studies in cells showing the formation of  $Cys_2Fe(NO)_2$ .<sup>7</sup> It has been proposed that NO may react directly with ferrodoxin proteins such as aconitase, an enzyme containing a 4Fe-4S cluster that catalyses the isomerization of citrate to isocitrate in the citric acid cycle, destroying the iron-sulfur cluster which results in the loss of enzymatic activity.

### 1.3 Structure and Bonding in Metal Nitrosyl Complexes

The bonding in transition metal carbonyl or nitrosyl complexes may be considered to be made up of two components: (a) donation of electron density from a  $\sigma$ -type orbital on CO or NO onto the metal, and (b) a donation of electron density from the occupied metal  $d$ -orbitals into the  $\pi^*$  antibonding orbitals of the NO or CO ligand. The bonding picture described in Figure 1.2 applies to both nitrosyl and carbonyl bonding interactions. However, there are significant differences in the nature of the electron distributions in the M-NO and M-CO units. One difference stems from the fact that the nitrogen of NO is more electronegative than the carbon of CO,<sup>8</sup> the result being that the NO ligand is a better overall electron acceptor than CO. Another important difference is that in the M-NO unit, the M-N

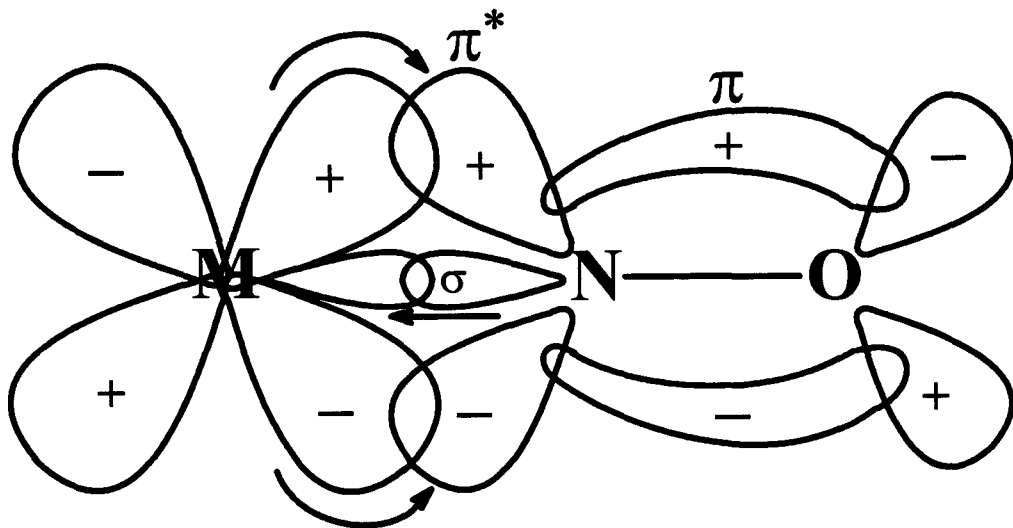


**Figure 1.2.** Molecular Bonding diagram for Metal Nitrosyls

bond is usually strong, and the N-O bond is relatively weak; for carbonyls, the reverse trend is observed. The end result is that the M-N bond is strengthened and shortened by the back-donation while the addition of electron density to the antibonding  $\pi^*$  orbital weakens and lengthens the NO bond. In general, NO is considered to be a weak  $\sigma$ -donor and a strong  $\pi$ -acceptor.

The nitrosyl group can bond to transition metals in a variety of ways, resulting in different geometries about the N atom. One method used to describe the bonding of nitrosyl compounds (the method used in this thesis) is to assign formal oxidation states to the metal and the nitrosyl ligand.<sup>8</sup> With this assignment, a linear M-NO (Figure 1.3 A) unit would occur as the result of a bound  $\text{NO}^+$  ligand (which is isoelectronic with CO and  $\text{N}_2$ ). Coordination of nitric oxide as  $\text{NO}^+$  involves a net donation of three electrons from NO to a metal atom. The extra electron is considered to be in the  $d$  set of orbitals of iron, giving rise to an oxidation state of -2 for  $\text{Fe}(\text{NO})_2(\text{L})_2$  complexes. A bent M-NO (Figure 1.3 B) unit would be the result of a bound  $\text{NO}^-$  ligand. Coordination as  $\text{NO}^-$  involves a net donation of

one electron to the metal.

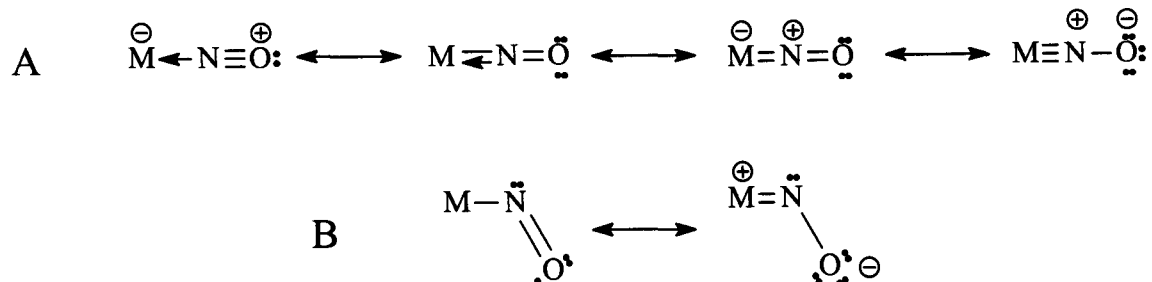


**Figure 1.3.** Nitrosyl Bending in Metal complexes. A: Linear "3 electron" bonding. B: Bent "1 electron bonding"

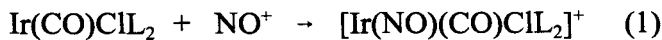
## 1.4 The Chemistry of Metal Nitrosyl Complexes

### 1.4.1 Formation of Metal Nitrosyls

There are a number of ways in which iron nitrosyl complexes are prepared. The earlier syntheses involved the combination of aqueous solutions of Fe(II) salts, anionic ligands and a source of NO gas.<sup>9</sup> These methods produced useful EPR results, but the shortcoming of this earlier work was that isolation and purification of the compounds was not accomplished.

The most successful formation of metal nitrosyl complexes is by displacement of ligands in the coordination sphere of a metal. Again, this can be accomplished by using NO gas to displace a ligand equivalent to that of a 3-electron donor.<sup>10</sup> Nitric oxide gas can also displace two-electron ligands in some monometallic compounds, with subsequent formation of a bimetallic species (presumably because of the extra electron afforded by NO); it can also add to a bi- or polymetallic complex with the subsequent cleavage of metal-metal bonds.<sup>11</sup>

Nitrosonium salts have also been used for the synthesis of metal nitrosyls.  $\text{NO}^+$  forms simple 1:1 adducts with some coordinatively unsaturated metal complexes (Equation 1).<sup>12</sup>



$\text{NO}^+$  also readily displaces CO (or other 2-electron ligands such as carbon disulfide) in a number of coordinatively saturated complexes to generate their nitrosyl analogues (eq 2, 3),<sup>12</sup>

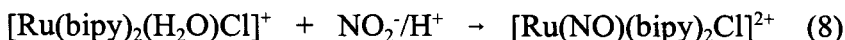


and a variety of nitrosyl halides have been used extensively in formation of metal complexes.<sup>13</sup>

Inorganic nitrites have also been used to obtain metal nitrosyl complexes. The most common nitrite sources for the synthesis of monometallic and cluster complexes are  $\text{PPN}(\text{NO})_2$  and sodium nitrite (eq 4, 5).



The fact that, in acidic media, the nitrite ion equilibrates with the  $\text{NO}^+$  cation has been exploited (6) for nitrosylation (7, 8).



Other metal nitrosylation reactions have been accomplished by reactions with azides, organic nitroso ligands, hydroxylamine and protonation of aminato-type ligands.<sup>12</sup>

### 1.4.2 The Reactivity of Metal Nitrosyls

The M-NO moiety exhibits a wide range of reactivity, including simple conformational changes and reactions at the N and O atoms. In simplistically viewing the linear NO ligand as an electrophile (formally  $\text{NO}^+$ ), it should be rendered prone to nucleophilic attack at the nitrosyl nitrogen. Conversely, the bent NO ligand (formally  $\text{NO}^-$ ) should undergo electrophilic attack at the nitrogen atom. The NO groups can also serve as “spectator” ligands, while still conferring unique chemical reactivity to metal centers.

In solution, a number of compounds have shown the ability to convert from linear to bent conformations. For example, the five coordinate  $[\text{RuCl}(\text{NO})_2(\text{PPh}_3)_2]\text{BF}_4^-$  complex possesses both linear and bent ligands in the solid state but is fluxional in solution due to a rapid, intramolecular interconversion.<sup>14</sup>

The compound  $[\text{Ir}(\text{NO})(\eta^3\text{-C}_3\text{H}_5)(\text{PPh}_3)_2]^+$  (Figure 1.4) in solution also shows a linear-bent NO interchange,<sup>15</sup> in the absence of interchange occurs without an accompanying  $\eta^3\text{-}\eta^1$  allyl fluxional process. Both linear and bent nitrosyl forms of the complex have been crystallized as their  $\text{PF}_6^-$  and  $\text{BF}_4^-$  salts.

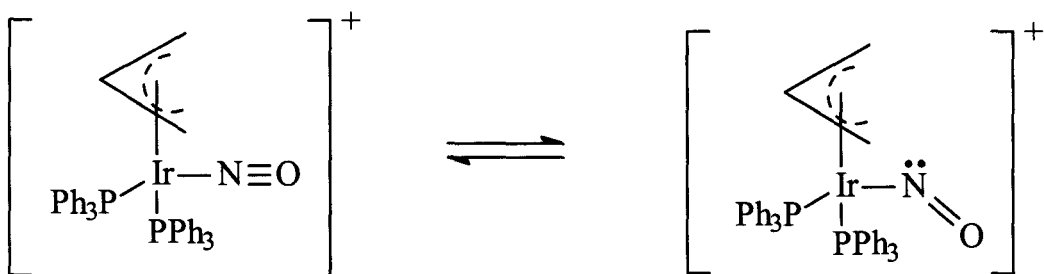


**Figure 1.4** Linear-bent interchange of  $[\text{Ir}(\text{NO})(\eta^3\text{-C}_3\text{H}_5)(\text{PPh}_3)_2]^+$ .

The linear-to-bent NO conformational changes may be induced chemically by the

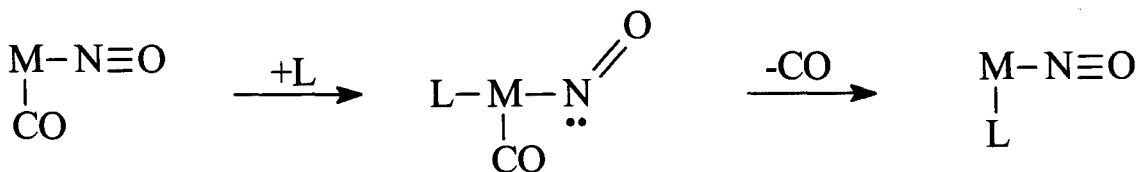


**Figure 1.5.** Linear-bent interchange by chemical addition.

addition of neutral or anionic nucleophiles (L) to the metal center as shown in Figure 1.5. For example,  $[\text{Co}(\text{NO})(\text{das})_2]^{2+}$  (das = O-phenylenabis(dimethyl)arsine) has a linear ( $179^\circ$ ) nitrosyl. Addition of thiocyanide to this complex gives rise to  $[\text{Co}(\text{NO})(\text{das})_2(\text{NCS})]^{2+}$  with a bent nitrosyl ( $132^\circ$ ).<sup>16</sup>

Lewis acids such as  $\text{AlMe}_3$ ,  $\text{Cp}_3\text{Er}$  and  $\text{Cp}_3\text{Yb}$  can react with the oxygen of nitrosyls, forming the corresponding adducts.<sup>17,18</sup> When the Lewis acid binds with the nitrosyl oxygen, electron density is drained away from the NO group, and the metal compensates by donating more electron density into the  $\pi^*$  orbitals of NO. Thus, the  $\nu_{\text{NO}}$  is lowered, by an amount determined by the strength of the interaction between the NO ligand and the lewis acid.

The oxygen of the NO ligand can also be removed by oxygen acceptors (eq 9).<sup>19</sup>



If the MNO group is sufficiently electron rich, it may undergo electrophilic attack by protons. The bent NO is formally  $sp^2$  hybridized and possesses a lone pair of electrons (eq 10, 11).<sup>20</sup>



Nucleophiles can react with the nitrogen of NO if the M-NO unit is essentially linear.

It has been proposed<sup>21</sup> that addition of hydride anion to  $[\text{CpRe(NO)(CO)(PPh}_3)]^+$  results in the formation of a formyl complex *via* an HNO intermediate, which isomerizes to the formyl product as shown in Figure 1.6.

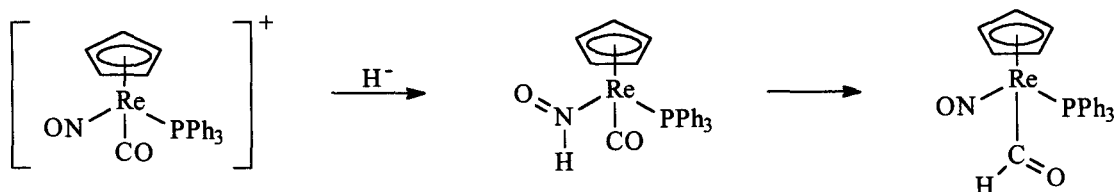
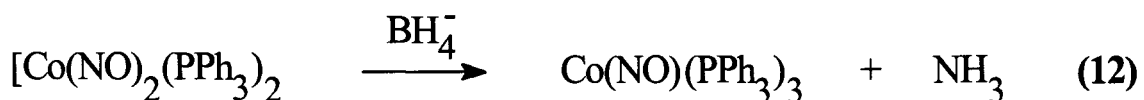


**Figure 1.6.** Reaction of a nucleophile with the nitrogen of NO.

Similarly, the reaction of a cobalt dinitrosyl complex with borohydride leads to reduction of the NO ligand and the formation of ammonia (12).<sup>22</sup>



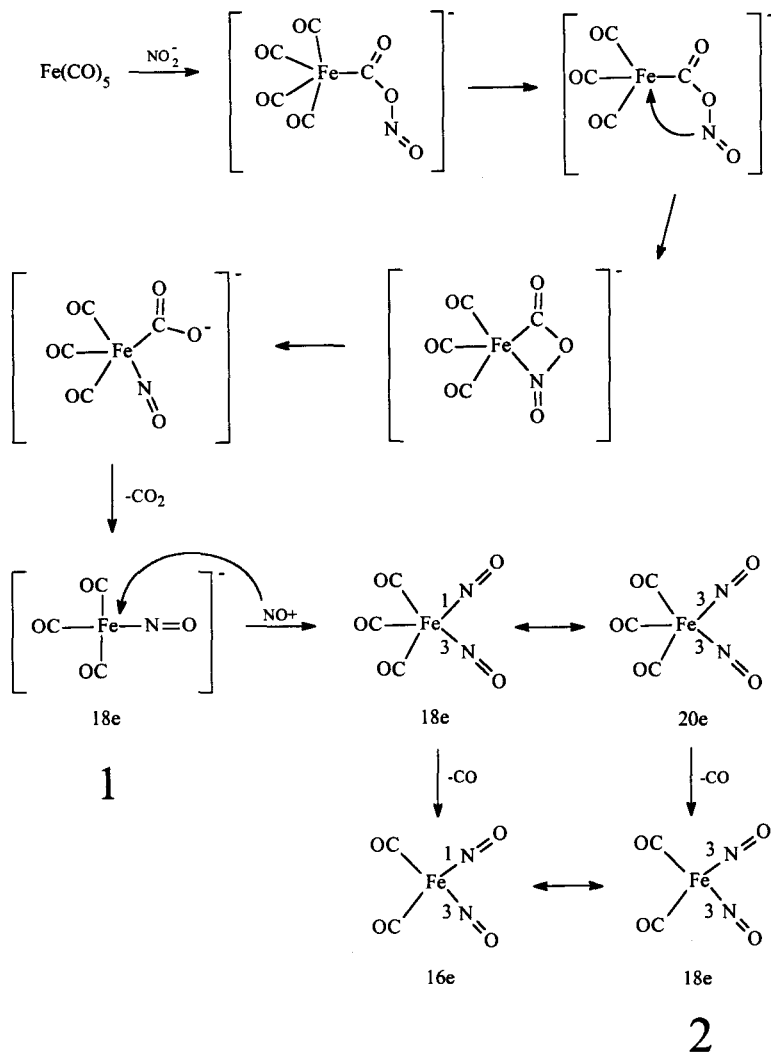
### 1.4.3 Iron dinitrosyl dicarbonyl

The formation of a volatile iron nitrosyl-carbonyl was first observed by Mond and Wallis.<sup>23</sup> It is a deep red compound, with a melting point of 18.4 °C and a density of 1.56 g.cm<sup>-3</sup>.  $\text{Fe}(\text{NO})_2(\text{CO})_2$  is diamagnetic, having a filled  $d^{10}$  shell. It is insoluble in water but

very soluble in organic solvents. The liquid starts decomposing at 50 °C,<sup>24</sup> leading to Fe<sub>2</sub>O<sub>3</sub> and other products. Fe(NO)<sub>2</sub>(CO)<sub>2</sub> is unstable in air and decomposes slowly at room temperature by oxidation. With NaOH or NaOCH<sub>3</sub> in CH<sub>3</sub>OH disproportionation of Fe occurs yielding [Fe(CO)<sub>3</sub>NO]<sup>-</sup> and [Fe(CH<sub>3</sub>OH)<sub>5</sub>NO]<sup>2+</sup>, CO and NO<sup>-</sup>. The Formation of Fe(NO)<sub>2</sub>(CO)<sub>2</sub> by Fe(CO)<sub>5</sub> and nitrite is shown in Scheme 1.1. The reaction takes place initially in methanol. At step 1 in the scheme, Na[Fe(CO)<sub>3</sub>NO] is formed. The methanol is distilled off and the salt dried, at which point water and more nitrite is added to the salt, and the resulting slurry is acidified with CO<sub>2</sub> to produce the starting material **2** in the scheme.

The geometry of the iron centre is reflected in the nature of the ligands attached.<sup>25</sup> For example, the Fe(NO)<sub>2</sub> unit has a large angle for N-Fe-N. The configuration develops because a better  $\pi$  overlap between the Fe and N orbitals is achieved at wider angles. In general, strong  $\pi$ -acids (L) will necessarily have a large L-Fe-L angle. Conversely, the much weaker  $\pi$ -acids, such as Cl-, will have a smaller L-Fe-L angle. The poor  $\pi$ -acceptors rely mainly on  $\sigma$  interactions, which operate at more acute angles. The geometry can also be reflected in the electronic configuration of the iron center. The oxidation of the  $d^{10}$  Fe(NO)<sub>2</sub> complex to  $d^9$  causes geometric distortions,<sup>26</sup> involving a change in shape from tetrahedral to more of a trigonal pyramid, with a missing ligand at the apex. The single electron is occupied in the  $d_z^2$  orbital, which pushes the ligands down. The change from  $d^9$  to  $d^8$  further distorts the four coordinate complex towards a square planar conformation.<sup>25</sup> The Fe(NO)<sub>2</sub>(L)<sub>2</sub> [L = PR<sub>3</sub>, NR<sub>3</sub>] compounds formed by reaction of Fe(NO)<sub>2</sub>(CO)<sub>2</sub> and L have been shown to proceed by a conventional associative mechanism.<sup>27</sup> The conventional process is slow, requiring stirring overnight to replace the first carbonyl and requiring

heating at 85 °C overnight to replace the second carbonyl.<sup>28</sup> A number of Fe(NO)<sub>2</sub>(X)<sub>2</sub> [X



**Scheme 1.1.** Proposed mechanism of formation of  $\text{Fe}(\text{NO})_2(\text{CO})_2$ .

$= \text{PR}_3]$ <sup>29</sup> and  $[\text{Fe}(\text{NO})_2(\text{CO})_2]\text{Y}$  [ $\text{Y} = \text{dppe}$  or  $\text{dppm}$ <sup>30</sup>] compounds have been previously synthesized, and the ortep diagrams of  $[\text{Fe}(\text{NO})_2(\text{CO})_2]\text{dppe}$  and  $\text{dppm}$  are shown in Figures 1.7 and 1.8, respectively. Each iron is situated in a pseudo-tetrahedral environment.

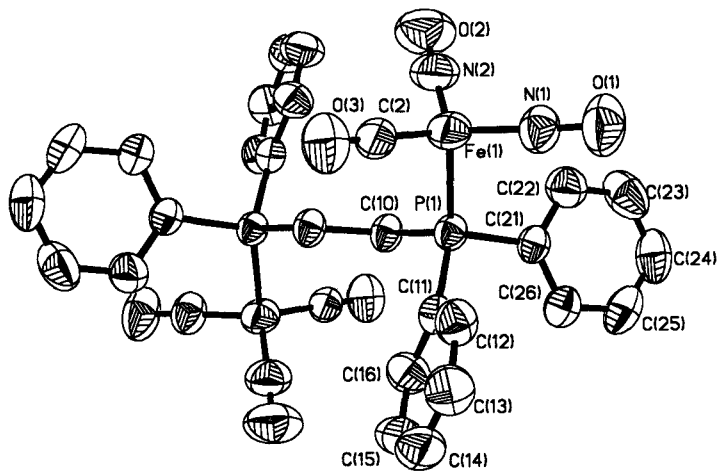


**Figure 1.7.** Ortep diagram of  $[Fe(NO)_2(CO)]_2dppe$ , shown with 50% thermal ellipsoids.

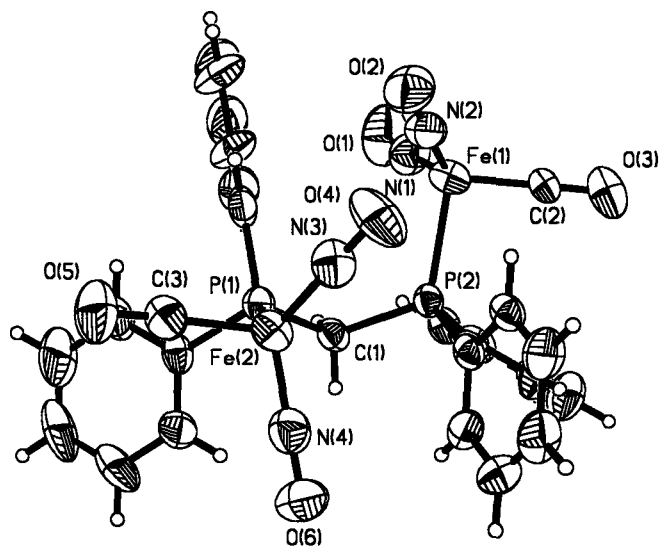


**Figure 1.8.** Ortep diagram of  $[Fe(NO)_2(CO)]_2dppm$ , shown with 50 % thermal ellipsoids.

## 1.5 Research Objectives

Nitric oxide's rapid reactivity with oxygen and other substances in water suggests that, in some instances, NO transport may be affected by metal ion complexation. The trend has been to detect the presence of these compounds rather than isolate them. To this day, a large number of biologically detectable EPR compounds have not been isolated. In fact, the majority of compounds made are made with P and S ligands, and a number of reviews describing these compounds are in the literature.<sup>31,32</sup> It has been our goal to synthesize and fully characterize a series of non-heme, non sulfur iron dinitrosyl compounds, an area of synthesis which has not previously attracted much attention. We focussed on the synthesis of biologically relevant compounds that mimic histidine iron compounds, by using a series of imidazoles (histidine is an imidazole containing amino acid), including imidazole, 1-methylimidazole, 4-methylimidazole, benzimidazole, and 5,6-dimethylbenzimidazole. These were reacted with dinitrosyldicarbonyliron to form disubstituted complexes of the form  $\text{Fe}(\text{NO})_2(\text{L})_2$  [ L = imidazole **1**, 1-methylimidazole **2**, 4-methylimidazole **3**, benzimidazole **4**, and 5,6-dimethylbenzimidazole **5**]. We emphasized characterization of **1-5** by IR, Mass spectrometry, NMR and X-ray crystallography. EPR studies are compared with previous EPR studies of biological iron dinitrosyl mimics.

## 2. Results and Discussion

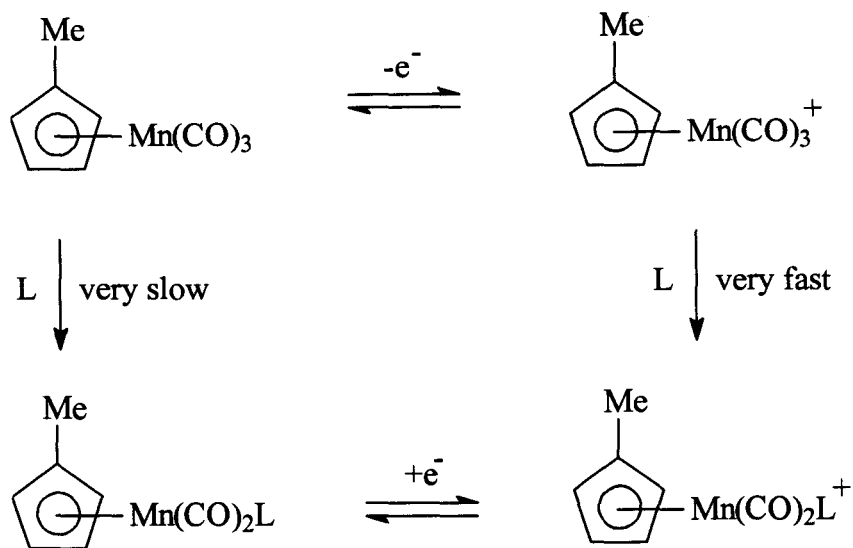
### 2.1 Mechanism of Reaction of iron dinitrosyl compounds with imidazole ligands.

Synthesis of the  $\text{Fe}(\text{NO})_2(\text{L})_2$  [ $\text{L}$  = imidazole **1**, 1-methylimidazole **2**, 4-methylimidazole **3**, benzimidazole **4**, 5,6-dimethylbenzimidazole **5**] series of compounds were carried out under inert atmosphere, utilizing rigorously dried and degassed solvents. The reaction mixtures consisted of a 2:1 molar ratio of the appropriate imidazole ligand with a solution of  $\text{Fe}(\text{NO})_2(\text{CO})_2$  dissolved in THF, ether, or dichloromethane. Upon addition of ligand, the solution turned from red to green within two minutes, with fierce gas evolution. As well, an EPR detectable signal was observed for each reaction mixture of **1 - 5**. These observations indicate that the reaction rate is much greater than that of conventional substitution and therefore the mechanism of substitution proceeds by a pathway other than that of conventional associative substitution.

To determine the mechanism of reaction, attention must first be focussed on the formation of an EPR detectable species in each reaction mixture. The signal, centered approximately at  $g = 2.03\text{G}$ , is consistent with a 17 electron complex that has the unpaired electron situated mainly on iron. A 19 electron complex is ruled out, as these complexes typically have isotropic g-factor values  $< 2.000\text{G}$ .

A variety of 17 electron complexes have been previously studied.<sup>33</sup> For example, the complex  $[(\text{MeCp})\text{Mn}(\text{CO})_3]$ , while normally inert to CO substitution (it does not react

thermally with  $\text{PPh}_3$  over 3 days at  $140^\circ\text{C}$ ), does undergo substitution of one or two CO

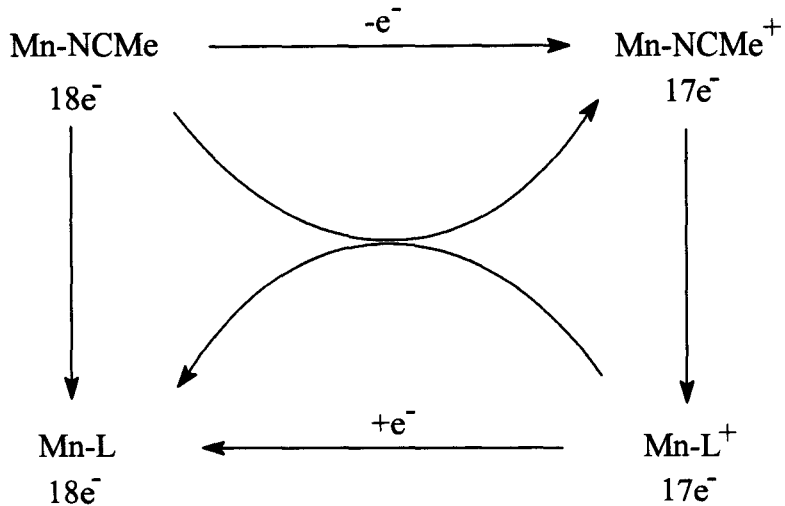


**Scheme 2.1.** Enhanced rate of CO substitution by oxidation of  $[(\text{MeCp})\text{Mn}(\text{CO})_3]$  to the 17 electron  $[(\text{MeCp})\text{Mn}(\text{CO})_3]^+$  intermediate.

ligands within milliseconds at room temperature upon oxidation in the presence of  $\text{P}(\text{OEt})_3$ .<sup>34</sup>

The chemistry involved is illustrated in Scheme 2.1. Kochi and co-workers<sup>35,36</sup> have established that rapid ligand substitution occurs when a slight oxidizing current is applied (or a small amount of a chemical oxidizing agent is added) to a MeCN solution of  $[(\text{MeCp})\text{Mn}(\text{CO})_2(\text{MeCN})]$ . The electrochemical investigation showed that the reaction occurs by a “catalytic electron-transfer chain process”<sup>35</sup> (ETC) defined in Scheme 2.2. The catalytic cycle is initiated by oxidation of a small amount of reactant  $[\text{Mn-NCMe}]$  to yield the 17 electron  $[\text{Mn-NCMe}]^+$ , which rapidly substitutes  $\text{PR}_3$  for MeCN to give  $[\text{Mn-L}]^+$ . It happens that the reactant  $[\text{Mn-NCMe}]$  is more easily oxidized than is the product  $[\text{Mn-L}]$ , which ensures that  $[\text{Mn-NCMe}]^+$  is continuously regenerated by electron transfer from  $[\text{Mn-NCMe}]$  to  $[\text{Mn-L}]^+$ .

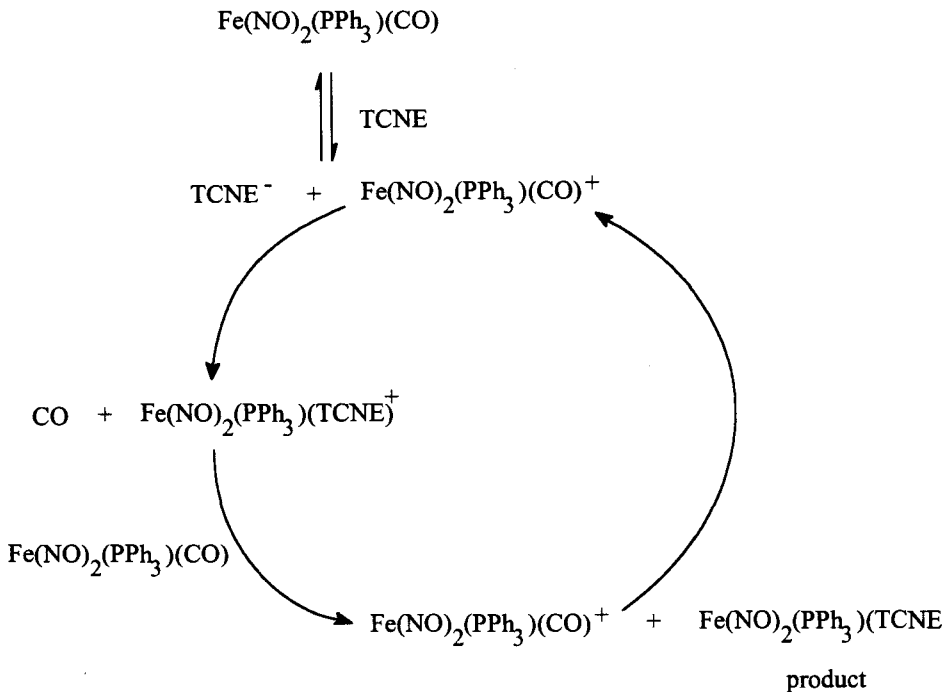
Another such reaction is that of  $\text{Fe}(\text{NO})_2(\text{CO})(\text{PPh}_3)$  with TCNE (Scheme 2.3) as



**Scheme 2.2.** Enhanced rate of CO substitution by oxidation of  $[(\text{MeCp})\text{Mn}(\text{CO})_2(\text{MeCN})]$  to the 17 electron  $[\text{Mn-NCMe}]^+$  intermediate .

reported by Li and coworkers.<sup>37</sup> Generally substitution of one CO of  $\text{Fe}(\text{NO})_2(\text{CO})_2$  usually calls for overnight stirring and replacing the second carbonyl requires heating to 85 °C for 16 h.<sup>38</sup> However, substitution of CO by TCNE was complete in 1-2 h.<sup>37</sup> The reaction was monitored by EPR and both TCNE<sup>-</sup> and  $\text{Fe}(\text{NO})_2(\text{PPh}_3)(\text{L})^+$  radicals were observed (L may be CO or solvent). They suggested that a “radical mechanism involving a 17-electron intermediate”, as shown in Scheme 3, was responsible for the enhancement of the rate of substitution without the use of an oxidizing agent such as  $\text{Co}(\text{cp})_2$ , or an oxidizing potential. The TCNE ligand acts both as the oxidizing agent, and as the ligand to replace CO. Indeed, it has been shown that the reaction of  $[\text{Fe}(\text{NO})_2\text{CO}]_2\text{dppe}$  with TCNE also produces TCNE<sup>-</sup> in solution, and the mechanism proceeds *via* a 17-electron intermediate described in Scheme 2.3.

With no apparent added source of oxidizing agent, and no applied oxidizing current,



**Scheme 2.3.** Enhanced rate of CO substitution *via* oxidation of  $\text{Fe}(\text{NO})_2(\text{CO})(\text{PPh}_3)$  to  $\text{Fe}(\text{NO})_2(\text{CO})(\text{PPh}_3)^+$  by TCNE.

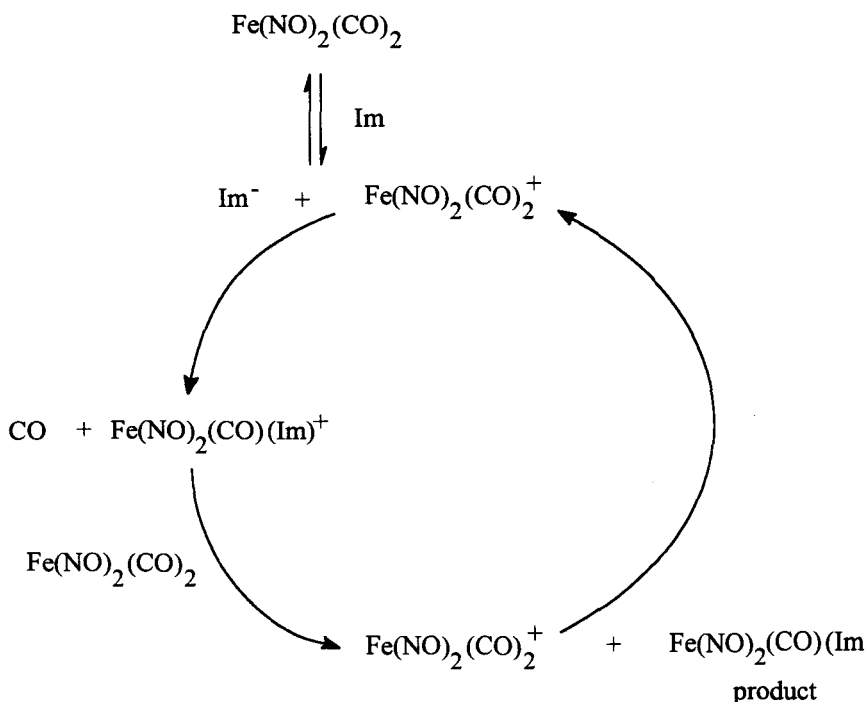
the formation of compounds 1 - 5 proceed *via* a 17 electron ETC pathway similar to that of Li. Scheme 2.4 describes the mechanistic pathway associated with the ETC substitution of CO by the series of imidazole ligands. The first run through will produce the mono-substituted  $\text{Fe}(\text{NO})_2(\text{CO})(\text{L})$  complex, a compound which had been detected previously<sup>39</sup> by IR spectroscopy during reaction of  $\text{Fe}(\text{NO})_2(\text{CO})_2$  and 1-MeIm. A second run through of the cycle, replacing  $\text{Fe}(\text{NO})_2(\text{CO})_2$  with  $\text{Fe}(\text{NO})_2(\text{CO})(\text{L})$  results in the di-substituted product. However, the proposed mechanism involves the formation of an  $\text{Im}^+$  compound, which has not been detected by EPR.

The final product was chemically sensitive to a variety of conditions. In air it

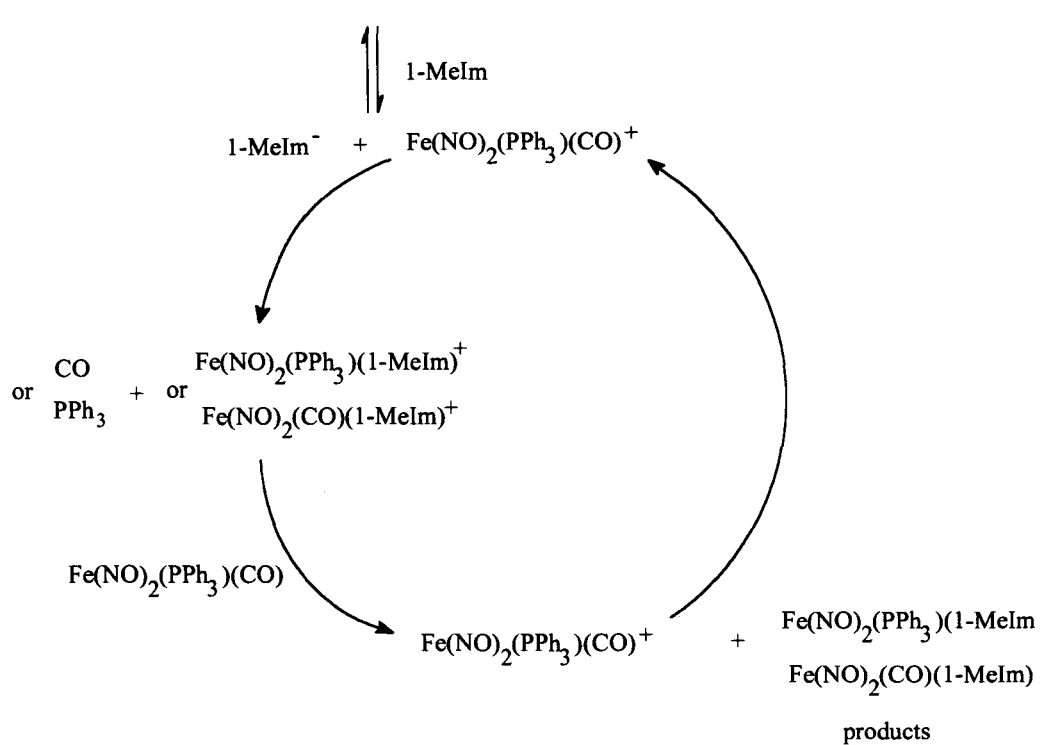
immediately turned from the characteristic green colour of the  $\text{Fe}(\text{NO})_2(\text{L})_2$  complex to a clear brown solution, and further, to a clear solution with an orange precipitate within 7-10 minutes. Removal of solvent by reduced pressure afforded a green solid. Non-polar solvents such as ether and paraffin oil did not dissolve the product, however, the supernatant solution acquired a slight brownish tinge. The green solid did dissolve in chloroform and dichloromethane and created a clear brown solution that did not show precipitation after several days. NMR spectroscopy of deuterated chloroform solutions revealed extremely broadened lines, but nothing discernable. Methanol dissolved the green solid and retained the distinctive green colour in solution, however, this was short lived and the solution turned brown after 30 minutes. NMR spectroscopy of deuterated MeOH solutions also produced spectra with very broadened lines which could not be interpreted. The instability of these complexes may be due to the inability of the poor  $\pi$ -accepting ability of the imidazole ligands to stabilize the lower oxidation state of iron.<sup>40</sup>

In an effort to try to stabilize the final products, the compound  $\text{Fe}(\text{NO})_2(\text{CO})(\text{PPh}_3)$  was used, with the strong  $\pi$ -accepting  $\text{PPh}_3$  ligand as a stabilizer. Iron dinitrosyl products with a  $\text{PR}_3$  ligand are relatively more stable as a solid than the starting material,  $\text{Fe}(\text{NO})_2(\text{CO})_2$ , and it was hoped that this ligand would increase the stability of a mono-substituted imidazole compound. Addition of 1-MeIm to a solution of  $\text{Fe}(\text{NO})_2(\text{CO})(\text{PPh}_3)$

produced violent gas evolution, and a darkening of the solution from red to a very dark red/green colour, which had been observed in the formation of complexes **1-5**. Crystals were obtained which revealed  $\text{Fe}(\text{NO})_2(\text{PPh}_3)_2$  (**6**). This result was not expected, however it is easily explained using a variation of the mechanism shown in Scheme 2.4. Scheme 2.5 details the ETC pathway for formation of **6**. The first time through the cycle, both  $\text{Fe}(\text{NO})_2(\text{PPh}_3)(\text{Im})$  and  $\text{Fe}(\text{NO})_2(\text{CO})(\text{Im})$  are produced. The formation of  $\text{Fe}(\text{NO})_2(\text{CO})(\text{Im})$  releases free  $\text{PPh}_3$  into solution which, after a second run through the cycle, can react with  $\text{Fe}(\text{NO})_2(\text{PPh}_3)(\text{Im})$  to give **6**.



**Scheme 2.4.** Mechanistic pathway for formation of the  $\text{Fe}(\text{NO})_2(\text{L})_2$  [ $\text{L}$  = imidazole, 1-MeIm, 4-MeIm, Benzim, 5,6-dimethylbenzim] series of compounds.



**Scheme 2.5.** Mechanistic pathway for formation of the  $\text{Fe}(\text{NO})_2(\text{L})_2$  [ $\text{L} = \text{PPh}_3$ ] from the reaction of  $\text{Fe}(\text{NO})_2(\text{CO})(\text{PPh}_3)$  and 1-MeIm.

## **2.2 Infrared Spectroscopy**

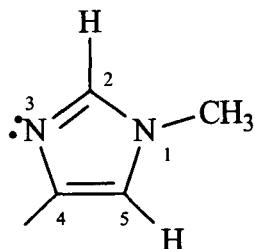
While the MNO group is expected to exhibit  $\nu_{\text{NO}}$ ,  $\nu_{\text{MN}}$  and  $\nu_{\text{MNO}}$ , only  $\nu_{\text{NO}}$  has been identified in most cases in the vibrational spectra of metal nitrosyl complexes.<sup>41</sup> In most nitrosyl complexes, the N-O stretching frequency is observed as an intense and characteristic band in the region 1525-1940 cm<sup>-1</sup>, which is associated with monodentate nitrosyl groups. Assuming the nitrosonium coordination model, the free NO<sup>+</sup> stretching of 2250 cm<sup>-1</sup> would be expected to drop on coordination with a metal atom. This is caused by the increase in back donation of electron density from M to NO and population of the  $\pi^*$  orbital, which weakens the N-O bond. Conversely, a net donation of electron density from the NO group to the metal center should result in a stronger N-O bond, and hence a higher  $\nu_{\text{NO}}$ . The magnitude of this decrease depends on the nature of the metal atom and the degree of  $\sigma$ - and  $\pi$ - bonding involved. This simplistic view is useful when monitoring the progress of a chemical reaction. Linear M-N-O groups absorb in the region 1650-1940 cm<sup>-1</sup>, including M-N-O angles from 160 to 180°, for which the NO ligand has a formal positive charge. The stretches for the bent groups (M-N-O angle 120°) occur at lower wavenumbers (1525-1690 cm<sup>-1</sup>).<sup>42</sup>

Fe(NO)<sub>2</sub>(CO)<sub>2</sub> have intense stretching frequencies for both NO (1810, 1767 cm<sup>-1</sup>) and CO (2087, 2038 cm<sup>-1</sup>). Upon addition of the imidazole ligands, the  $\nu_{\text{NO}}$ 's are lowered by approximately 140 wavenumbers and no carbonyl stretching frequencies are observed. This indicated that two Im ligands had replaced the two CO ligands. The nitrosyls fall into the region of 1650-1940cm<sup>-1</sup>, indicating they are linear. Table 2.1 lists the NO stretching frequencies observed for complexes 1 - 5.

**Table 2.1** Nitrosyl stretching frequencies for compounds **1 - 5**.

Compound	$\nu_{NO}$ (cm <sup>-1</sup> )
<b>1</b> Fe(NO) <sub>2</sub> (imidazole) <sub>2</sub>	1680, 1622
<b>2</b> Fe(NO) <sub>2</sub> (1-MeIm) <sub>2</sub>	1673, 1616
<b>3</b> Fe(NO) <sub>2</sub> (4-MeIm) <sub>2</sub>	1677, 1620
<b>4</b> Fe(NO) <sub>2</sub> (Benzimidazole) <sub>2</sub>	1682, 1625
<b>5</b> Fe(NO) <sub>2</sub> (5,6-dimethylbenzim) <sub>2</sub>	1683, 1625

### 2.3 Nuclear Magnetic Resonance Spectroscopy



Numbering Scheme for 1-MeIm

The solids of the  $\text{Fe}(\text{NO})_2(\text{L})_2$  [ $\text{L}$  = imidazole **1**, 1-methylimidazole **2**, 4-methylimidazole **3**, benzimidazole **4**, 5,6-dimethylbenzimidazole **5**] could not be purified by conventional means. The NMR spectroscopy was therefore carried out using reaction mixtures of the imidazole series of compounds in deuterated solvents, such as *d*-chloroform and *d*-methanol (the deuterated solvents were rigorously dried over  $\text{CaH}_2$ ). Analysis of the spectra proved difficult, as obvious line broadening occurred from paramagnetic species in solution. Repeated attempts produced only one spectrum, that of **2**, which could be deciphered. The proton spectrum of **2**, shown in Figure 2.1, reveals a mixture of 1-MeIm and  $\text{Fe}(\text{NO})_2(1\text{-MeIm})_2$  in solution. The broad signal at 8.79 ppm is attributed to H2 and H4 of **2** (see 1-MeIm diagram above for numbering scheme). It is believed that the resonances of H2 and H4 are similar, and with line broadening, only one broad signal is observed. The 1-MeIm ligand act as an electron donor, and so the protons of H2 and H4 are deshielded upon complexation with the iron and are shifted further downfield with respect to the free 1-MeIm molecule. The signal at 4.99 ppm is assigned to H5, which is not subjected to any deshielding by complexation. The broad peak at 3.97 ppm is assigned to the  $\text{CH}_3$  group. The peaks at

7.68, 7.10, 6.87, and 3.68 ppm are assigned to H<sub>2</sub>, H<sub>4</sub>, H<sub>5</sub>, and CH<sub>3</sub> of the free 1-MeIm ligand, respectively.

The <sup>13</sup>C spectrum, shown in Figure 2.2, also reveals a mixture of 1-MeIm and Fe(NO)<sub>2</sub>(1-MeIm)<sub>2</sub> in solution. The small signals at 226.2 and 225.6 ppm are attributed to either of the C<sub>2</sub> and C<sub>4</sub> carbons. Again, these atoms are affected by the deshielding which occurs upon complexation. Definitive assignment of these two atom resonances was not made. The peak at 143.4 ppm is assigned to the C<sub>5</sub> carbon and the broad peak at 38.3 ppm is attributed to the CH<sub>3</sub> carbon. The resonance peaks at 143.6, 134.2, 123.1, and 34.2 ppm arise from the C<sub>2</sub>, C<sub>4</sub>, C<sub>5</sub> and CH<sub>3</sub> carbons of the free 1-MeIm ligand, respectively.

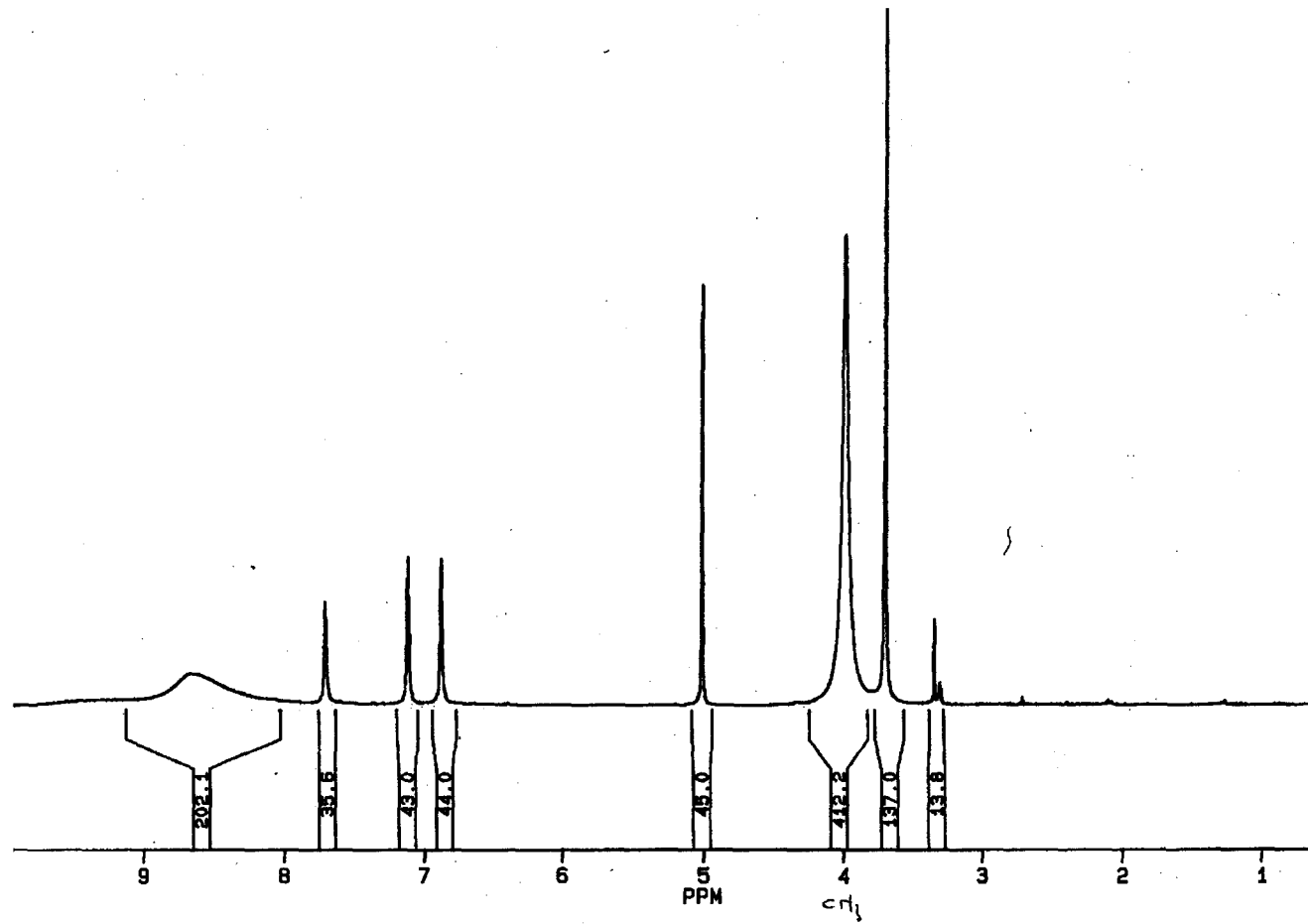


**Figure 2.1.**  $^1\text{H}$  NMR spectrum of  $\text{Fe}(\text{NO})_2(1\text{-MeIm})_2$  in deuterated methan

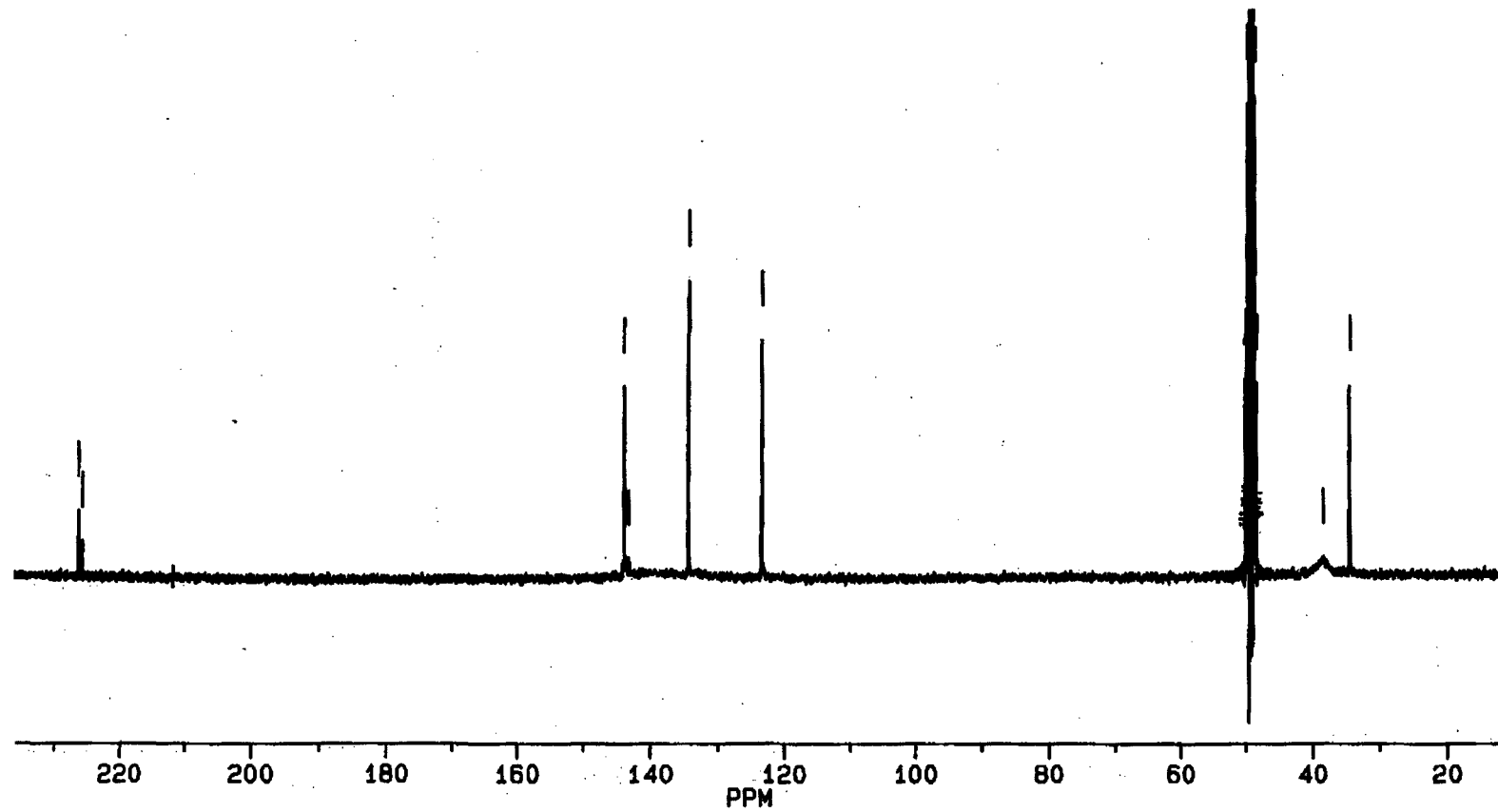


**Figure 2.2.**  $^{13}\text{C}$  NMR spectrum of  $\text{Fe}(\text{NO})_2(1\text{-MeIm})_2$  in deuterated methan

## **2.4 EPR Spectroscopy**

Electron paramagnetic resonance spectroscopy (EPR) has been one of the most commonly employed techniques for the characterization of iron dinitrosyl complexes. Although solution EPR cannot be used to determine the geometry of complexes, the spectra are useful as a means of confirming the presence of the desired product. For example, Martini and co-workers<sup>42</sup> reported a study on a mixture of urea and an Fe(NO)<sub>2</sub> complex. Urea (H<sub>2</sub>N-CO-NH<sub>2</sub>) can be expected to bind through either its carbonyl oxygen atom, or one of the two nitrogen groups. The spectrum of Fe(NO)<sub>2</sub>(urea)<sub>2</sub> revealed a five line spectrum ( $g = 2.034$ ,  $a_{\text{n}} = 2.2\text{G}$ ) which indicated the interaction of the unpaired electron with only two equivalent nuclei of <sup>14</sup>N of the nitrosyls. The urea molecules are therefore bound to the Fe(NO)<sub>2</sub><sup>+</sup> group by the carbonyl oxygen. In a similar aqueous study with imidazole,<sup>43</sup> the spectrum obtained consisted of nine hyperfine components spaced about 2.5 G apart, and indicated a compound with two equivalent <sup>14</sup>N nuclei from the nitrosyl groups and two equivalent <sup>14</sup>N nuclei from the imidazole groups, each with the same hyperfine coupling constant.

In the course of study of Fe(NO)<sub>2</sub>(CO)<sub>2</sub> with imidazole ligands, neutral compounds of the form Fe(NO)<sub>2</sub>(L)<sub>2</sub> [L = imidazole **1**, 1-methylimidazole **2**, 4-methylimidazole **3**, benzimidazole **4**, 5,6-dimethylbenzimidazole **5**] were expected to be produced. However, NMR characterization proved difficult because of extensive line broadening. This suggested that a paramagnetic species was present in solution. EPR studies did reveal that a paramagnetic species was present in solution, which is believed to be a 17 electron, iron dinitrosyl intermediate involved in the formation of the 18 electron, Fe(NO)<sub>2</sub>(L)<sub>2</sub> complex.

The g-values and hyperfine coupling constants observed for compounds **1 - 5** are listed in Table 2.2. Spectra simulation have been performed and are consistent with experimental data. Figures 2.3-2.7 show the experimental (top) and simulated (bottom) spectra for each compound.

**Table 2.2.** g values and hyperfine coupling constants for  $\text{Fe}(\text{NO})_2(\text{L})_2^+$  compounds. The number in parentheses is the number of nuclei to which the coupling belongs.

Compound	g-value	$a_n$
$\text{Fe}(\text{NO})_2(\text{imidazole})_2$	2.0344	3.3 (1), 2.4 (1), 2.1 (2)
$\text{Fe}(\text{NO})_2(1\text{-MeIm})_2$	2.0275	2.9 (2), 2.6 (2)
$\text{Fe}(\text{NO})_2(4\text{-MeIm})_2$	2.0336	3.1 (1), 2.5 (1), 2.2 (2)
$\text{Fe}(\text{NO})_2(\text{benzimidazole})_2$	2.0341	3.8 (1), 2.4 (1), 1.9 (2)
$\text{Fe}(\text{NO})_2(5,6\text{-dimethylbenzim})_2$	2.0344	3.9 (1), 2.2 (2)

Compounds **1-5** are all centred around 2.03 G, which is typical for iron dinitrosyl radicals with an unpaired electron localized on Fe as discussed by Li and co-workers.<sup>44</sup> The EPR spectra of compound **1**, displayed in figure 2.3, shows a signal at 2.0343 G, that consists of 10 lines. Simulation reveals that the signal arises from the two equivalent  $^{14}\text{N}$  nuclei of the nitrosyl ligands with a hyperfine coupling constant of 2.1 G and two inequivalent  $^{14}\text{N}$  nuclei from the imidazole ligands with a coupling constant of 3.2 and 2.4 G. This experiment was

carried out in tetrahydrofuran, whereas previous studies by Martini<sup>45</sup> were carried out in aqueous solution which affects the g-value. The nine line spectrum reported was not symmetric and obviously consisted of four nuclei that were not mutually equivalent as they have suggested. Simulations were not performed by Martini confirm the coupling constants. Compound **2**, whose EPR spectrum is shown in Figure 2.4, produces a signal centred at 2.0275 G, and is comprised of nine lines. Simulation reveals two equivalent <sup>14</sup>N nuclei from the nitrosyl ligands and two equivalent 1-MeIm ligands with coupling constants of 2.6 and 2.9 G, respectively. Compound **3** (Figure 2.5) produces a 10 line spectrum centred at 2.0337 G. The spectrum contains two equivalent <sup>14</sup>N nitrosyl groups, with a coupling constant of 2.2 G, and two inequivalent 4-MeIm ligands with coupling constants of 3.1 and 2.5 G. The spectrum of compound **4**, shown in Figure 2.6, is centred at 2.0341 G and consists of eleven lines. Simulation revealed a compound with two equivalent <sup>14</sup>N nuclei from the nitrosyls, with hyperfine coupling of 1.9 G and two inequivalent <sup>14</sup>N nuclei from the BenzIm groups with hyperfine coupling equal to 3.8 and 2.4 G. The EPR spectrum of **5**, shown in Figure 2.7, was centred at 2.035 G and consisted of 9 lines. The simulation for this spectrum revealed that only three <sup>14</sup>N nuclei were producing the hyperfine interactions. Two equivalent nitrosyl groups gave rise to a coupling of 2.2 G, and only one <sup>14</sup>N nucleus produces a coupling of 3.9 G. The reaction mixture of Fe(NO)<sub>2</sub>(CO)<sub>2</sub> and 5,6-dimethylbenzimidazole was in a 1:2 ratio to facilitate the substitution of two carbonyls by the imidazole ligands. It is unknown as to why only one 5,6-dimethylbenzimidazole ligand was involved in substitution.



**Figure 2.3.** EPR spectrum (above) and simulation (below) of  $\text{Fe}(\text{NO})_2(\text{imidazole})_2$ .

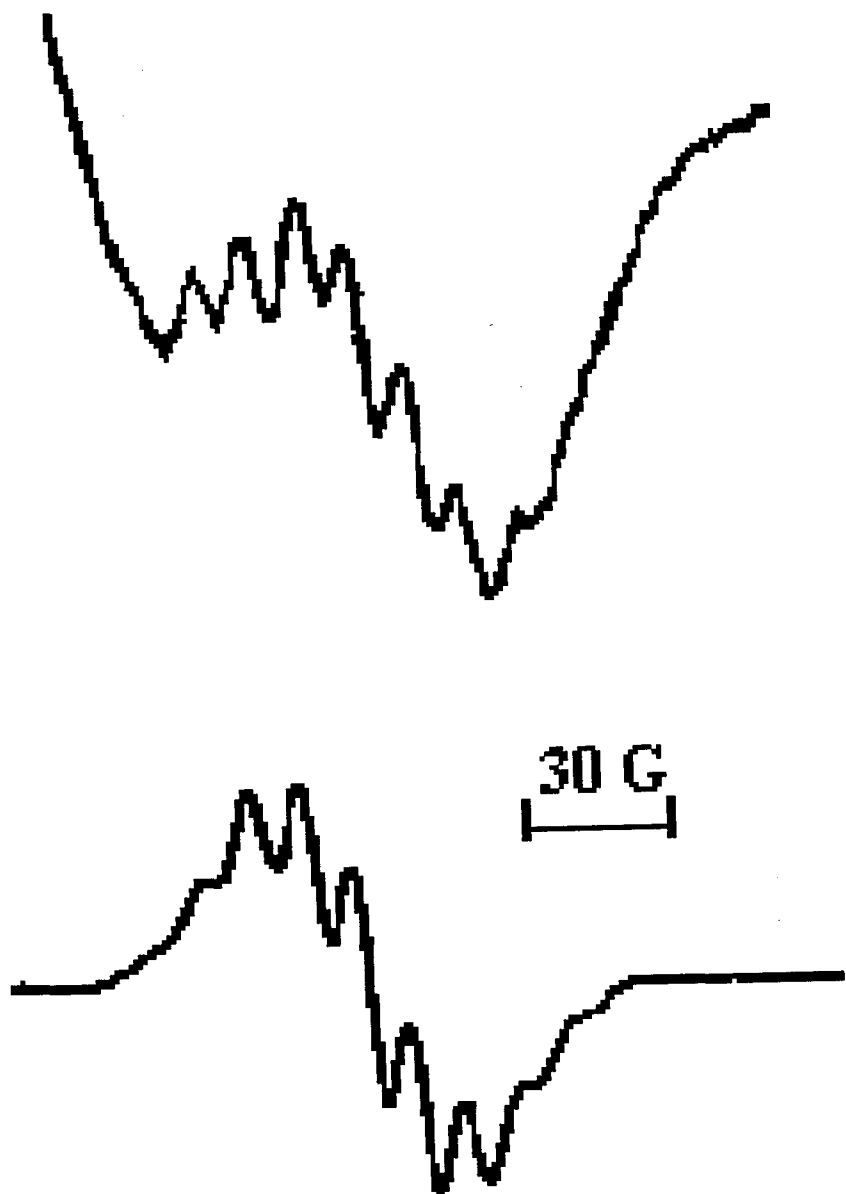


**Figure 2.4.** EPR spectrum (above) and simulation (below) of  $\text{Fe}(\text{NO})_2(1\text{-MeIm})_2$ .

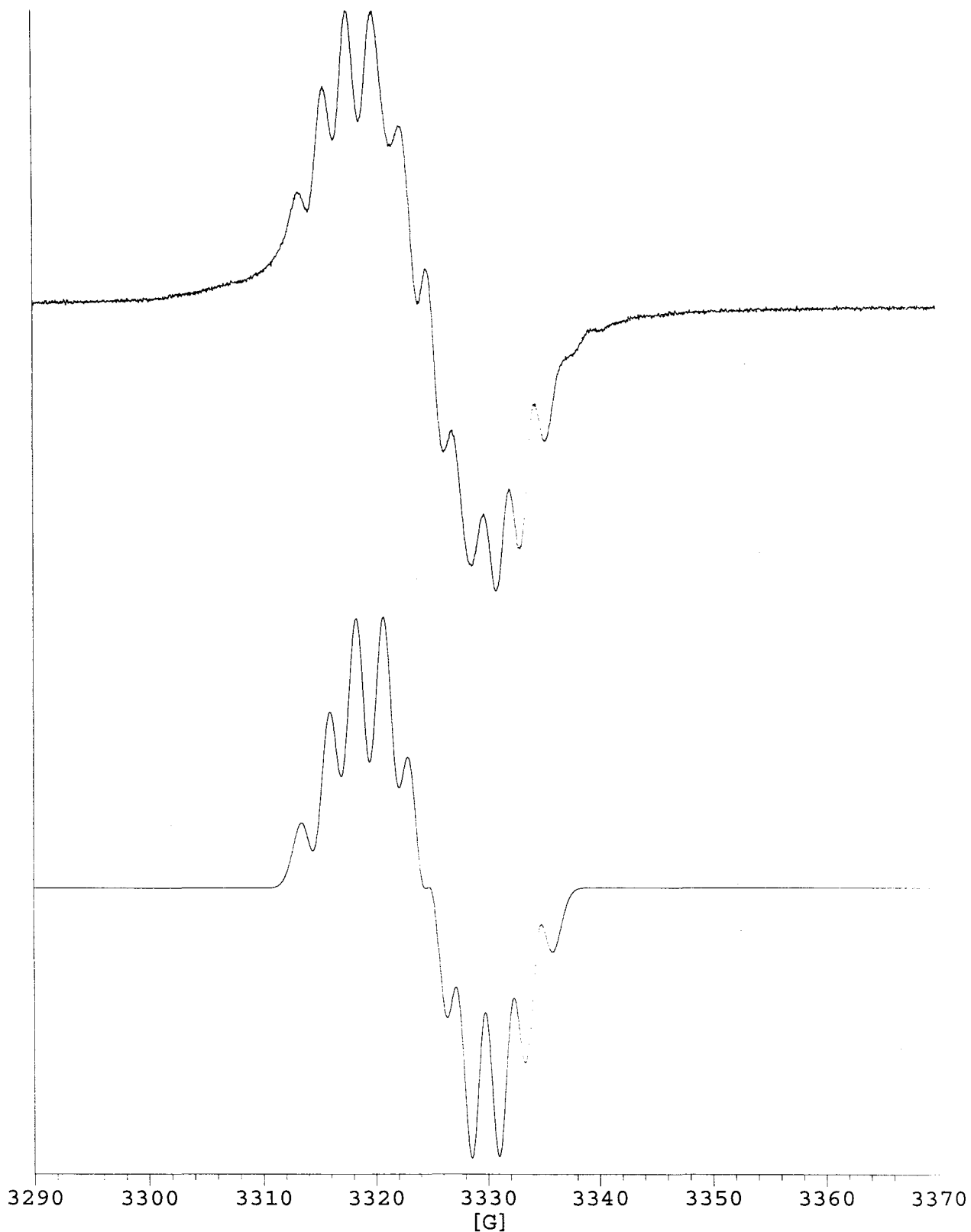


**Figure 2.5.** EPR spectrum (above) and simulation (below) of  $\text{Fe}(\text{NO})_2(4\text{-MeIm})_2$ .

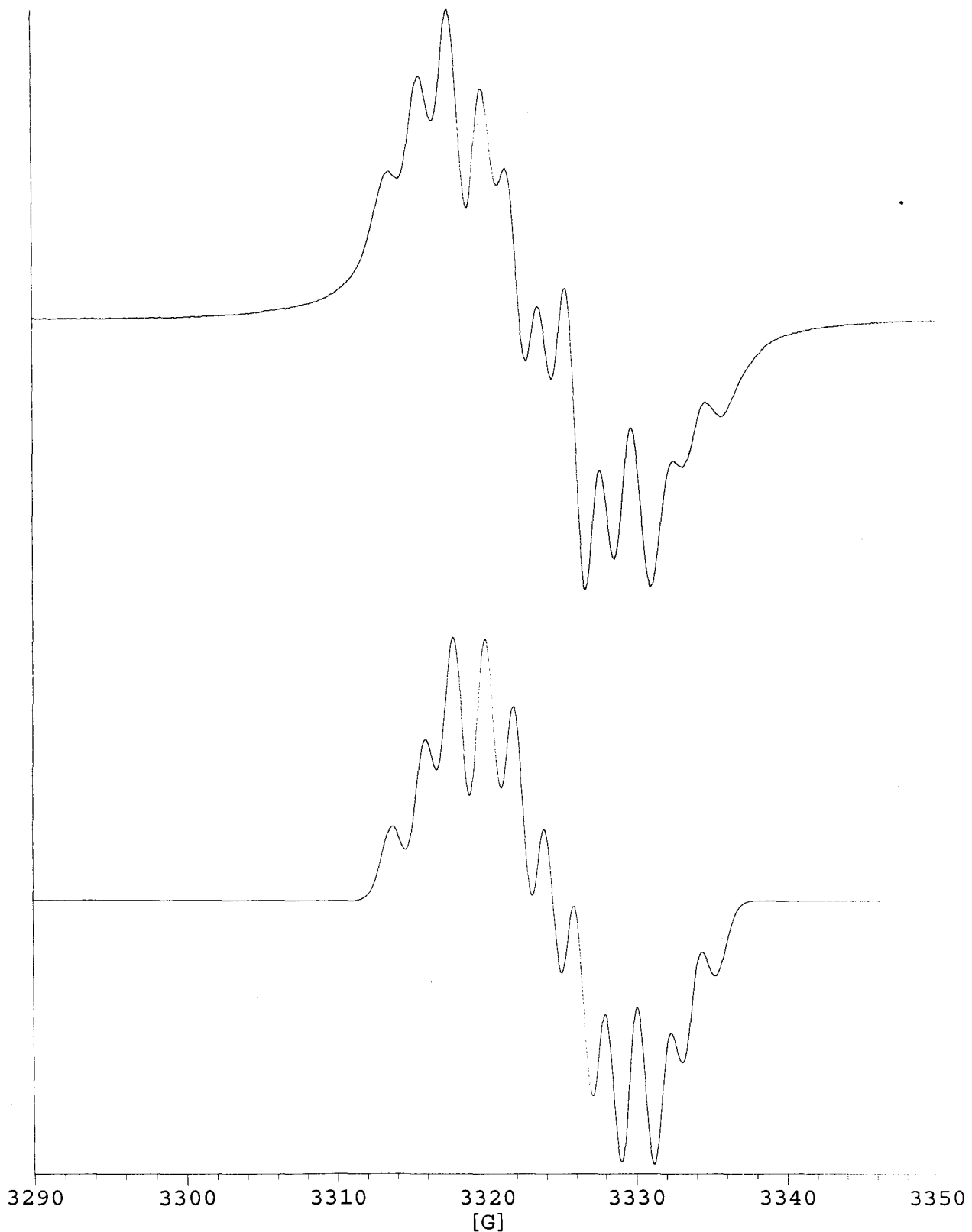


**Figure 2.6.** EPR spectrum (above) and simulation (below) of  $\text{Fe}(\text{NO})_2(\text{benzimidazole})_2$ .

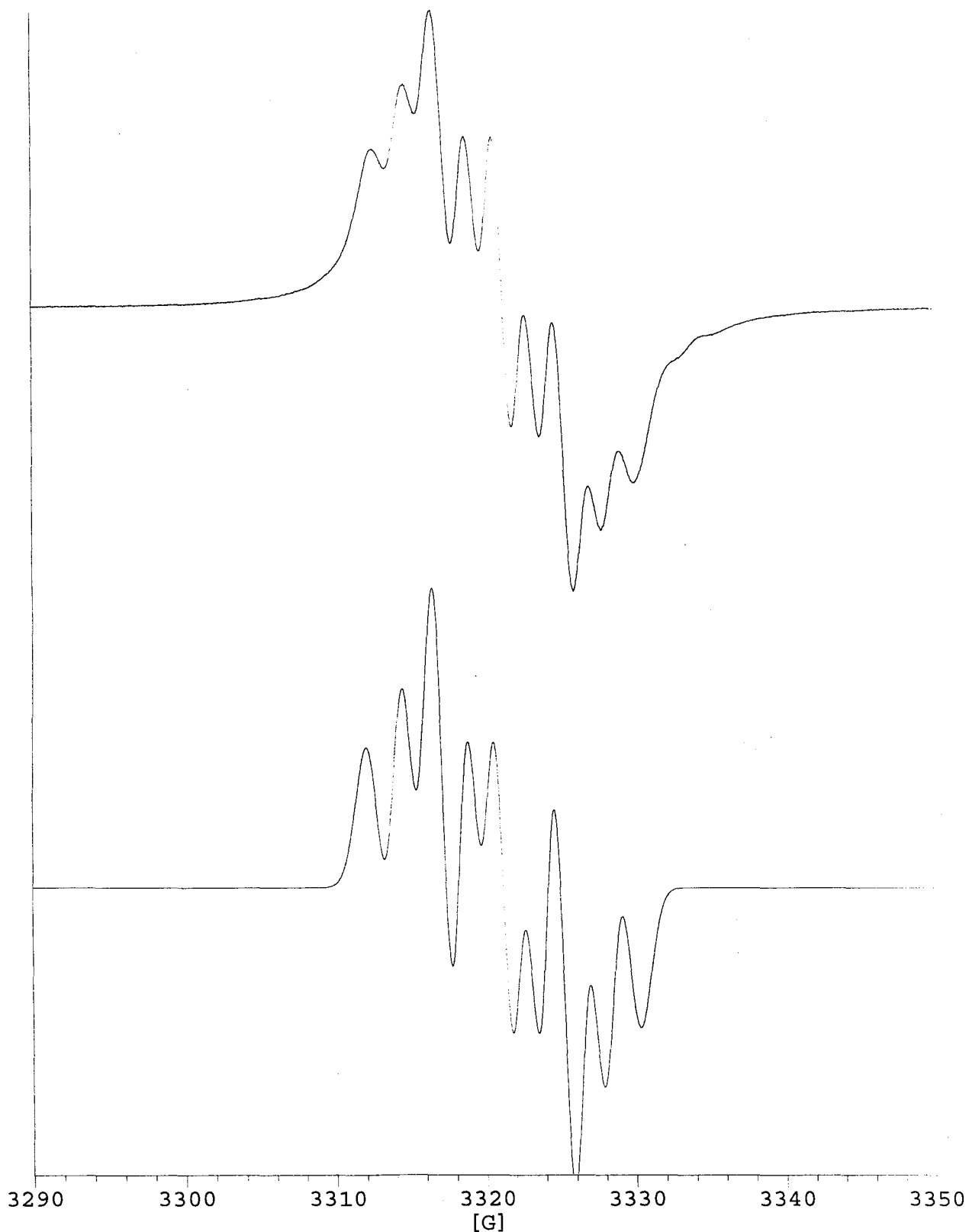


**Figure 2.7.** EPR spectrum (above) and simulation (below) of  $\text{Fe}(\text{NO})_2(5,6\text{-dimethylbenzimidazole})_2$ .

## 2.5 X-Ray Crystallography

Single crystals of **2** were obtained from ether solution. The crystals were placed in a petri dish containing dry paraffin oil. The oil had been dried over sodium metal and purged with nitrogen for one week prior to use. A single green crystal, 0.06 x 0.25 x 0.30mm was mounted on a glass fibre, with the paraffin oil as the adhesive. The X-ray crystal structure of **2**,  $\text{Fe}(\text{NO})_2(1\text{-methylimidazole})_2$  is shown in Figure 2.8. It crystallized as a monoclinic system, with a space group of C2/c and with the following dimensions:  $a = 13.985(5) \text{ \AA}$ ,  $b = 11.529(5) \text{ \AA}$ ,  $c = 15.471(4) \text{ \AA}$ ,  $\alpha = 90^\circ$ ,  $\beta = 91.72(2)^\circ$ ,  $\gamma = 90^\circ$ ,  $V = 2493(2) \text{ \AA}^3$ ,  $Z = 8$ .

The iron atom is situated in a *pseudo-tetrahedral* environment, with two coordinated NO groups attached through the nitrogen and two coordinated 1-methylimidazole ligands attached by the  $sp^2$  hybridized nitrogen. The nitrosyls are linear, having angles of  $167.5(3)^\circ$  and  $170.1(3)^\circ$ . They are situated with an angle of  $116.5^\circ$  between  $\text{N}_1\text{-Fe-N}_2$ . The  $\text{O}_1\text{-Fe-O}_2$  angle is  $107.3^\circ$ , and so forms an "attracto" conformation where  $\text{O-M-O} < \text{N-M-N}$ . This is in accord with the proposal that for complexes with N-M-N bond angles of less than  $130^\circ$ , the two O atoms bend towards each other.<sup>46</sup> The angle between  $\text{N}_3\text{-Fe-N}_5$  is  $91.20^\circ$ . The nitrosyl groups are much better  $\pi$ -acceptors than the 1-MeIm ligands and will necessarily have a larger angle between them than the corresponding 1-MeIm ligands.<sup>47</sup>

Since the 1-MeIm ligand is a poorer  $\pi$ -acceptor than  $\text{PR}_3$ , dppe or dppm, the imidazole complex would be expected to have shorter Fe-N(O) and longer N-O bond distances than the phosphorous complexes. The  $\pi$ -acidity of the P ligand would compete with the  $\pi$ -accepting ability of N(O) and would, in effect, cancel each other out. The imidazole complex would not be able to compete with the Fe-N(O) backbonding, resulting

in a shorter Fe-N(O) and longer N-O bond. Table 2.3 compares the bond distances of some iron dinitrosyl complexes. The dppe and dppm complexes follow this trend loosely, with somewhat longer Fe-N bonds and only slightly longer N-O bonds. The PPh<sub>3</sub> complex does not follow this trend, with bond distances similar to that of the 1-MeIm complex.

**Table 2.3. Comparison of iron dinitrosyl bond lengths (in Å).**

	Fe(NO) <sub>2</sub> (1-MeIm) <sub>2</sub>	[Fe(NO) <sub>2</sub> (CO)] <sub>2</sub> dppe	[Fe(NO) <sub>2</sub> (CO)] <sub>2</sub> dppm	Fe(NO) <sub>2</sub> (PPh <sub>3</sub> ) <sub>2</sub>
Fe-N (avg)	1.649	1.680	1.685	1.651
N-O (avg)	1.189	1.170	1.171	1.188

If a plane were to pass horizontally through each of the flat 1-MeIm ligands, the two planes would be skewed 106.7° from each other. The methyl groups on the N4 and N6 atoms 1-MeIm point to the same side of the molecule, bestowing close to a C<sub>s</sub> symmetry rather than a C<sub>2</sub> symmetry. A crystal packing diagram, shown in Figure 2.9, reveals a layering of 1-MeIm ligands (not to be confused with π stacking), a phenomenon previously encountered in iron dinitrosyl compounds.<sup>48</sup> Closer inspection shows that each of two H's of a methyl group is sandwiched between two nitrosyls, the two nitrosyls coming from different molecules. Each hydrogen is in close proximity with the oxygen of the NO ligands, which may prove to be a hydrogen bonding effect and a reason why the remaining four imidazole complexes do not readily form crystals. The third hydrogen of the methyl group is not involved in hydrogen bonding.

The crystal structure of **6** has been previously reported.<sup>49</sup> The unit cell dimensions for both refinements match, however, the quality of the data of the previous study is questionable. Firstly, the thermal parameters were not reported. Secondly, they did not indicate the data to parameter ratio or the 2270 total reflections collected within  $2\theta \leq 54^\circ$ . Only 1198 independent non-zero reflections were used in the refinement. If the total number of parameters was the same as in the refinement of **6** (total of 255 parameters), the data to parameter ratio would be less than 5:1, an unsatisfactory data set by today's standards and prone to large errors. A new definition of  $\text{Fe}(\text{NO})_2(\text{PPh}_3)_2$  is necessary and is described below.

The refinement of **6** used 3208 independent reflections for 255 parameters, or a ratio of 12.5:1. Figure 2.10 shows the *ortep* diagram of **6**,  $\text{Fe}(\text{NO})_2(\text{PPh}_3)_2$ . The iron is situated in a *pseudo-tetrahedral* environment with two coordinated NO groups attached through the nitrogen and two triphenyl phosphine groups attached through the phosphorous atom. The nitrosyls are linear, having angles of  $177.7(4)^\circ$ . The O-Fe-O angle is less than the N-Fe-N angle, and fits the definition of an 'attracto' conformation. The angle of N-Fe-N is  $124.5(3)^\circ$ . The angle of P-Fe-P is  $111.9(6)^\circ$ . The nitrosyl groups are better  $\pi$ -acceptors than the  $\text{PPh}_3$  ligands and therefore have the larger angle between them. In comparison with **2**, the greater  $\pi$ -accepting ability of the  $\text{PPh}_3$  ligand widens the P-Fe-P angle of **6** to  $111.9(6)^\circ$ , whereas the lesser  $\pi$ -acidity of the 1-MeIm group folds in the N<sub>3</sub>-Fe-N<sub>5</sub> angle to  $91.2^\circ$ .

The crystal packing of **6**, shown in Figure 2.11, reveals a layering of nitrosyls and a layering of the phenyl groups as observed in the crystal packing of  $[\text{Fe}(\text{NO})_2(\text{CO})]_2\text{dppe}$  and  $[\text{Fe}(\text{NO})_2(\text{CO})]_2\text{dppm}$ .<sup>50</sup>

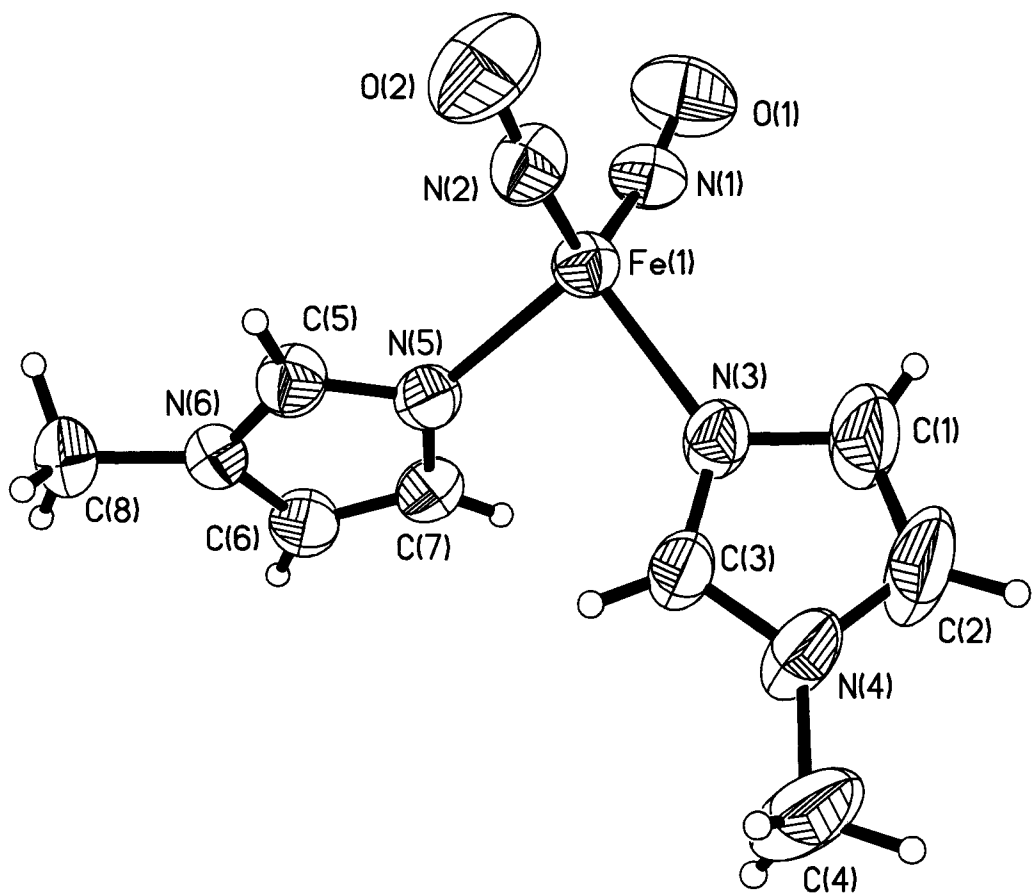


**Figure 2.8.** Ortep diagram of  $\text{Fe}(\text{NO})_2(1\text{-MeIm})_2$  shown at 50 % thermal ellipsoids.

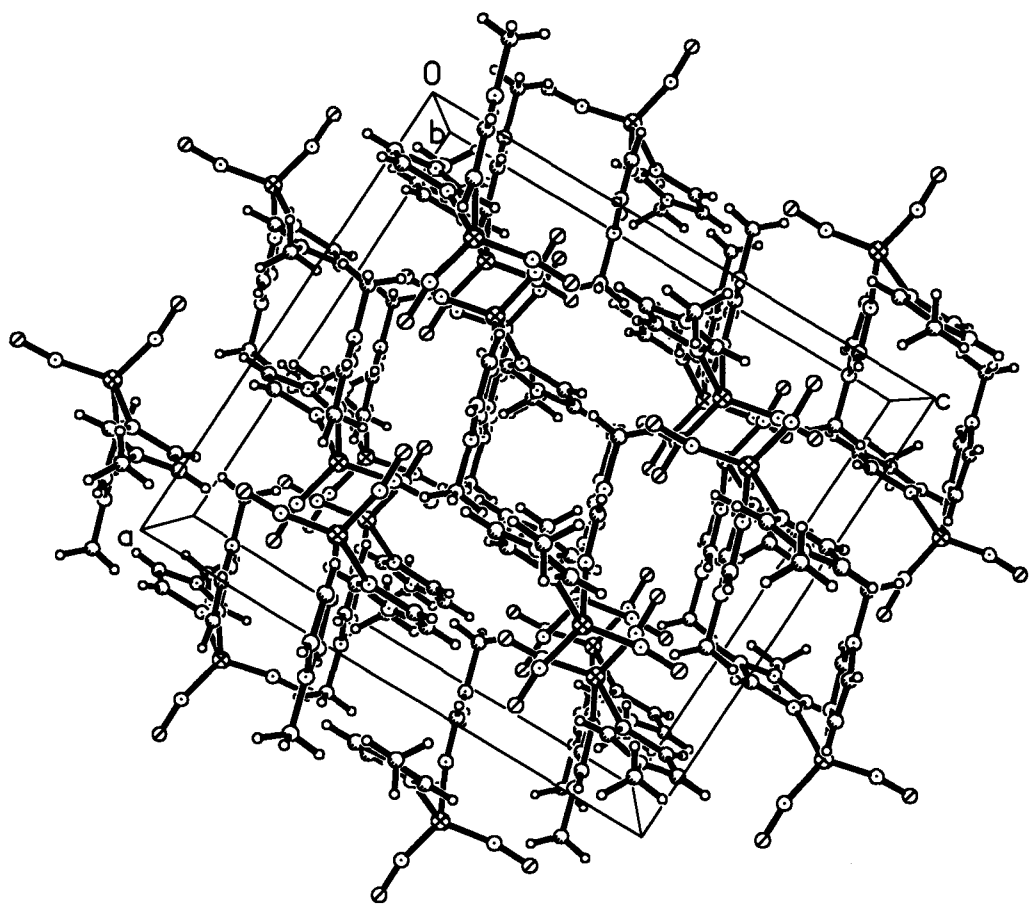


**Figure 2.9.** Crystal packing diagram of  $\text{Fe}(\text{NO})_2(1\text{-MeIm})_2$ .

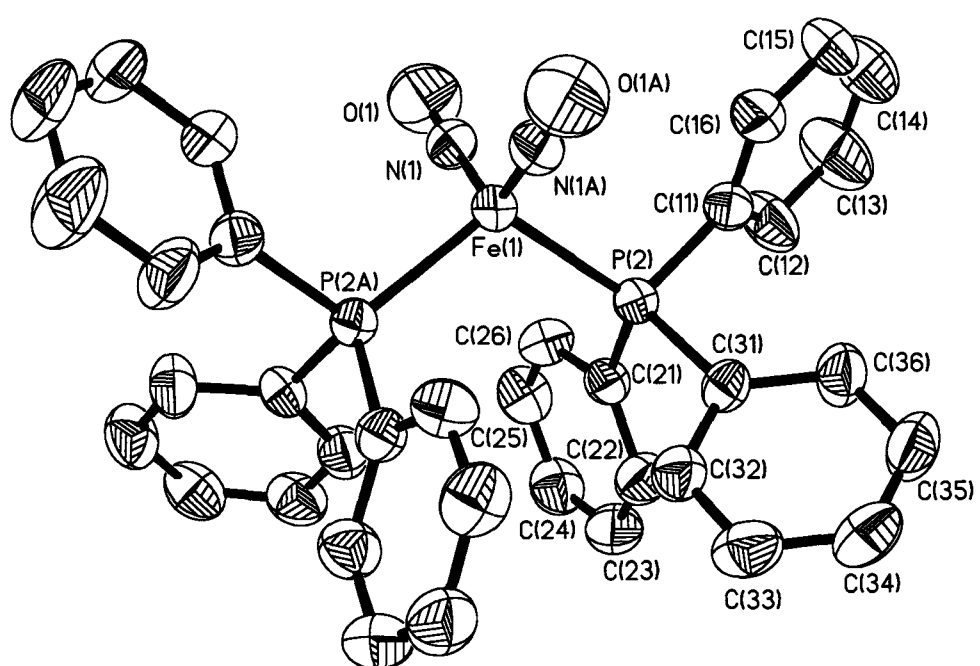


**Figure 2.10.** X-Ray crystal structure of 6, shown with 50 % thermal ellipsoids. Hydrogen atoms have been omitted for clarity.

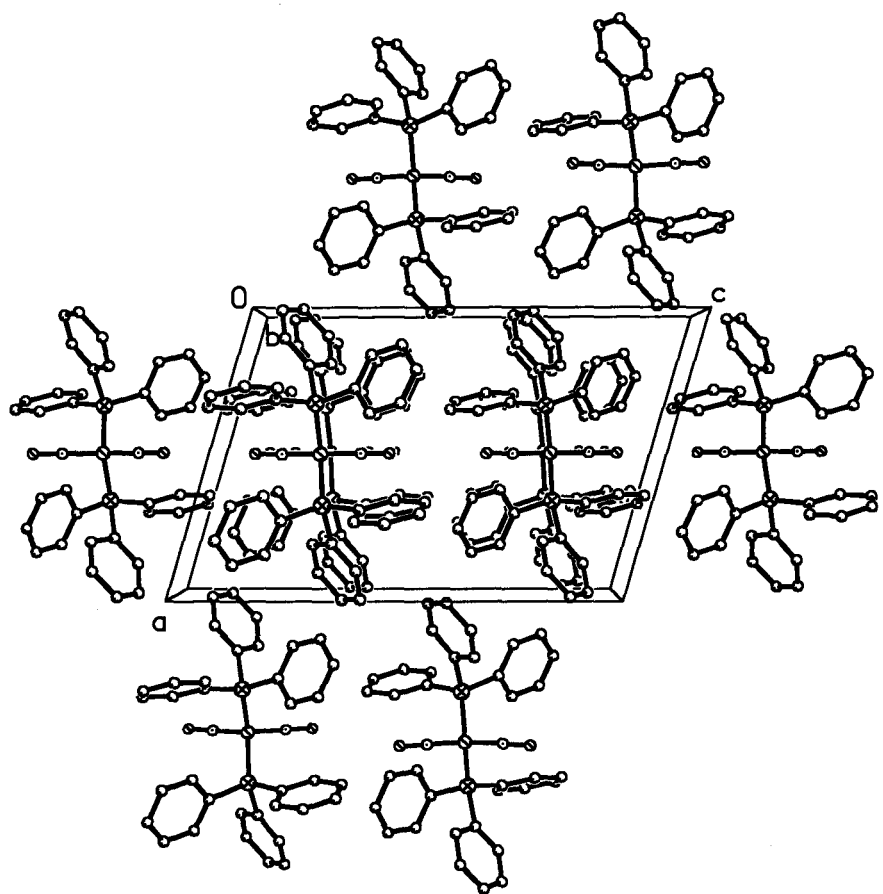


**Figure 2.11.** Crystal packing of **6**, viewed down the *b* axis. Hydrogen atom have been omitted for clarity.

Table 2.4. Crystal data and structure refinement for 2.

Identification code	n2
Empirical formula	C8 H12 Fe N6 O2
Formula weight	280.09
Temperature	300(2) °K
Wavelength	0.71073 Å
Crystal system	Monoclinic
Space group	C2/c
Unit cell dimensions	a = 13.985(5) Å    α = 90°. b = 11.529(5) Å    β = 91.72(2)°. c = 15.471(4) Å    γ = 90°.
Volume, Z	2493(2) Å^3, 8
Density (calculated)	1.492 Mg/m^3
Absorption coefficient	1.210 mm^-1
F(000)	1152
Crystal size	.06 x .25 x .30 mm
Theta range for data collection	2.29 to 26.44 °.
Limiting indices	-17<=h<=17, -14<=k<=14, -13<=l<=19
Reflections collected	9872
Independent reflections	2408 [R(int) = 0.0439]
Absorption correction	None
Refinement method	Full-matrix least-squares on F^2
Data / restraints / parameters	2408 / 0 / 179
Goodness-of-fit on F^2	1.112
Final R indices [I>2sigma(I)]	R1 = 0.0419, wR2 = 0.0928
R indices (all data)	R1 = 0.0633, wR2 = 0.1034
Largest diff. peak and hole	0.330 and -0.237 e.Å^-3

Table 2.5. Atomic coordinates ( $\times 10^4$ ) and equivalent isotropic displacement parameters ( $\text{Å}^2 \times 10^3$ ) for 2.  $U(\text{eq})$  is defined as one third of the trace of the orthogonalized  $U_{ij}$  tensor.

	x	y	z	$U(\text{eq})$
Fe(1)	2025(1)	7309(1)	2075(1)	40(1)
N(1)	3140(2)	6942(3)	1892(2)	49(1)
N(2)	1799(2)	7754(2)	3062(2)	51(1)
N(3)	1083(2)	6097(2)	1588(2)	47(1)
N(4)	-259(2)	5243(3)	1185(2)	65(1)
N(5)	1505(2)	8530(2)	1227(2)	42(1)
N(6)	1202(2)	10293(2)	751(2)	42(1)
O(1)	3975(2)	6742(3)	1919(2)	82(1)
O(2)	1782(2)	8090(3)	3787(2)	87(1)
C(1)	1193(3)	4930(4)	1650(4)	83(2)
C(2)	371(4)	4402(4)	1411(4)	99(2)
C(3)	196(2)	6247(3)	1308(2)	49(1)
C(4)	-1253(3)	5084(4)	889(3)	94(2)
C(5)	1317(2)	9618(3)	1437(2)	46(1)
C(6)	1327(3)	9610(3)	44(2)	51(1)
C(7)	1502(3)	8535(3)	340(2)	48(1)
C(8)	1019(3)	11536(3)	767(2)	57(1)

Table 2.6. Bond lengths [Å] and angles [deg] for 2.

---

<b>Fe(1)-N(1)</b>	<b>1.648 (3)</b>
<b>Fe(1)-N(2)</b>	<b>1.650 (3)</b>
<b>Fe(1)-N(5)</b>	<b>2.044 (3)</b>
<b>Fe(1)-N(3)</b>	<b>2.048 (3)</b>
<b>N(1)-O(1)</b>	<b>1.189 (3)</b>
<b>N(2)-O(2)</b>	<b>1.188 (4)</b>
<b>N(3)-C(3)</b>	<b>1.313 (4)</b>
<b>N(3)-C(1)</b>	<b>1.358 (5)</b>
<b>N(4)-C(3)</b>	<b>1.332 (4)</b>
<b>N(4)-C(2)</b>	<b>1.350 (6)</b>
<b>N(4)-C(4)</b>	<b>1.462 (5)</b>
<b>N(5)-C(5)</b>	<b>1.323 (4)</b>
<b>N(5)-C(7)</b>	<b>1.372 (4)</b>
<b>N(6)-C(5)</b>	<b>1.321 (4)</b>
<b>N(6)-C(6)</b>	<b>1.364 (4)</b>
<b>N(6)-C(8)</b>	<b>1.457 (4)</b>
<b>C(1)-C(2)</b>	<b>1.343 (6)</b>
<b>C(6)-C(7)</b>	<b>1.341 (5)</b>
<b>N(1)-Fe(1)-N(2)</b>	<b>116.57 (14)</b>
<b>N(1)-Fe(1)-N(5)</b>	<b>112.76 (12)</b>
<b>N(2)-Fe(1)-N(5)</b>	<b>107.78 (13)</b>
<b>N(1)-Fe(1)-N(3)</b>	<b>111.28 (13)</b>
<b>N(2)-Fe(1)-N(3)</b>	<b>114.43 (13)</b>
<b>N(5)-Fe(1)-N(3)</b>	<b>91.20 (11)</b>
<b>O(1)-N(1)-Fe(1)</b>	<b>167.5 (3)</b>
<b>O(2)-N(2)-Fe(1)</b>	<b>170.1 (3)</b>
<b>C(3)-N(3)-C(1)</b>	<b>104.9 (3)</b>
<b>C(3)-N(3)-Fe(1)</b>	<b>128.5 (2)</b>
<b>C(1)-N(3)-Fe(1)</b>	<b>125.4 (3)</b>
<b>C(3)-N(4)-C(2)</b>	<b>106.4 (3)</b>
<b>C(3)-N(4)-C(4)</b>	<b>126.9 (4)</b>
<b>C(2)-N(4)-C(4)</b>	<b>126.7 (4)</b>
<b>C(5)-N(5)-C(7)</b>	<b>104.3 (3)</b>
<b>C(5)-N(5)-Fe(1)</b>	<b>124.4 (2)</b>
<b>C(7)-N(5)-Fe(1)</b>	<b>129.5 (2)</b>
<b>C(5)-N(6)-C(6)</b>	<b>106.8 (3)</b>
<b>C(5)-N(6)-C(8)</b>	<b>125.7 (3)</b>
<b>C(6)-N(6)-C(8)</b>	<b>127.5 (3)</b>
<b>C(2)-C(1)-N(3)</b>	<b>109.6 (4)</b>
<b>C(1)-C(2)-N(4)</b>	<b>107.0 (4)</b>
<b>N(3)-C(3)-N(4)</b>	<b>112.1 (3)</b>
<b>N(6)-C(5)-N(5)</b>	<b>112.4 (3)</b>
<b>C(7)-C(6)-N(6)</b>	<b>106.6 (3)</b>
<b>C(6)-C(7)-N(5)</b>	<b>109.9 (3)</b>

Table 2.7. Anisotropic displacement parameters ( $\text{Å}^2 \times 10^3$ ) for 2.

The anisotropic displacement factor exponent takes the form:

$$-2 \pi^2 [ h^2 a^*{}^2 U_{11} + \dots + 2 h k a^* b^* U_{12} ]$$

	U11	U22	U33	U23	U13	U12
Fe(1)	39(1)	41(1)	38(1)	1(1)	1(1)	-2(1)
N(1)	41(2)	61(2)	45(2)	3(1)	-1(1)	-1(1)
N(2)	59(2)	46(2)	48(2)	-2(1)	6(1)	-6(1)
N(3)	40(2)	38(2)	63(2)	-5(1)	6(1)	2(1)
N(4)	44(2)	49(2)	101(3)	-26(2)	12(2)	-11(1)
N(5)	45(2)	42(2)	41(2)	0(1)	-2(1)	-4(1)
N(6)	43(2)	39(2)	44(2)	2(1)	-2(1)	1(1)
O(1)	44(2)	121(3)	81(2)	2(2)	2(1)	10(2)
O(2)	112(3)	93(2)	56(2)	-29(2)	20(2)	-16(2)
C(1)	61(3)	41(2)	145(5)	-10(2)	-1(3)	11(2)
C(2)	78(3)	36(2)	183(6)	-26(3)	8(3)	-2(2)
C(3)	46(2)	37(2)	64(2)	-8(2)	3(2)	-3(2)
C(4)	53(3)	94(4)	134(4)	-41(3)	1(3)	-27(2)
C(5)	54(2)	46(2)	39(2)	-1(2)	4(2)	-1(2)
C(6)	60(2)	51(2)	40(2)	2(2)	-3(2)	1(2)
C(7)	54(2)	47(2)	44(2)	-9(2)	-3(2)	-1(2)
C(8)	66(2)	40(2)	65(2)	1(2)	-2(2)	7(2)

Table 2.8. Hydrogen coordinates ( $\times 10^4$ ) and isotropic displacement parameters ( $\text{\AA}^2 \times 10^3$ ) for 2.

	x	y	z	U(eq)
H(4A)	-1396 (3)	4270 (4)	856 (3)	141
H(4B)	-1346 (3)	5427 (4)	327 (3)	141
H(4C)	-1670 (3)	5449 (4)	1288 (3)	141
H(8A)	964 (3)	11824 (3)	186 (2)	86
H(8B)	1538 (3)	11922 (3)	1069 (2)	86
H(8C)	434 (3)	11682 (3)	1058 (2)	86
H(1)	1742 (34)	4579 (46)	1771 (30)	105 (17)
H(2)	227 (34)	3634 (47)	1427 (31)	108 (17)
H(3)	-87 (21)	6921 (29)	1214 (19)	39 (9)
H(5)	1274 (23)	9863 (27)	1976 (21)	41 (9)
H(6)	1309 (28)	9881 (33)	-521 (26)	73 (12)
H(7)	1614 (24)	7931 (31)	46 (22)	50 (10)

Table 2.9. Crystal data and structure refinement for 6.

Empirical formula	C36 H30 Fe N2 O2 P2
Formula weight	640.41
Temperature	300(2) K
Wavelength	0.71073 Å
Crystal system	Monoclinic
Space group	P2/c
Unit cell dimensions	a = 11.7076(9) Å α = 90°. b = 8.1783(5) Å, β = 106.5720(10)°. c = 17.2489(13) Å γ = 90°.
Volume, Z	1583.0(2) Å^3, 2
Density (calculated)	1.344 Mg/m^3
Absorption coefficient	0.612 mm^-1
F(000)	664
Crystal size	.08 x .10 x .12 mm
Theta range for data collection	1.81 to 26.39°.
Limiting indices	-14<=h<=14, -8<=k<=10, -21<=l<=21
Reflections collected	12269
Independent reflections	3208 [R(int) = 0.0947]
Absorption correction	None
Refinement method	Full-matrix least-squares on F^2
Data / restraints / parameters	3208 / 0 / 255
Goodness-of-fit on F^2	1.089
Final R indices [I>2sigma(I)]	R1 = 0.0652, wR2 = 0.1049
R indices (all data)	R1 = 0.1310, wR2 = 0.1304
Largest diff. peak and hole	0.257 and -0.303 e.Å^-3

Table 2.10. Atomic coordinates ( $\times 10^4$ ) and equivalent isotropic displacement parameters ( $\text{Å}^2 \times 10^3$ ) for 6. U(eq) is defined as one third of the trace of the orthogonalized  $U_{ij}$  tensor.

	x	y	z	U(eq)
Fe(1)	5000	2938 (1)	7500	38 (1)
N(1)	5017 (3)	1999 (5)	6656 (3)	53 (1)
O(1)	5008 (4)	1279 (5)	6056 (3)	95 (1)
P(2)	3330 (1)	4489 (1)	7111 (1)	37 (1)
C(11)	2049 (4)	3144 (5)	6705 (3)	44 (1)
C(12)	1150 (4)	3494 (7)	6020 (4)	67 (2)
C(13)	185 (6)	2454 (9)	5754 (4)	92 (2)
C(14)	105 (6)	1074 (9)	6154 (5)	88 (2)
C(15)	992 (5)	692 (7)	6849 (4)	72 (2)
C(16)	1966 (4)	1717 (6)	7119 (3)	55 (1)
C(21)	3207 (3)	5938 (5)	6287 (3)	39 (1)
C(22)	2862 (4)	7545 (6)	6308 (3)	53 (1)
C(23)	2829 (5)	8585 (7)	5668 (4)	61 (1)
C(24)	3138 (4)	8051 (7)	5015 (4)	61 (1)
C(25)	3465 (5)	6452 (7)	4974 (3)	58 (1)
C(26)	3519 (4)	5414 (6)	5613 (3)	51 (1)
C(31)	2865 (3)	5677 (5)	7865 (2)	38 (1)
C(32)	3663 (4)	6792 (5)	8343 (3)	50 (1)
C(33)	3363 (5)	7708 (6)	8922 (3)	59 (1)
C(34)	2262 (5)	7537 (6)	9042 (3)	61 (1)
C(35)	1455 (5)	6470 (7)	8578 (3)	64 (2)
C(36)	1753 (4)	5544 (6)	7994 (3)	54 (1)

Table 2.11. Bond lengths [ $\text{\AA}$ ] and angles [ $^\circ$ ] for 6.

---

$\text{Fe(1)-N(1)}$	1.651(4)
$\text{Fe(1)-N(1)\#1}$	1.651(4)
$\text{Fe(1)-P(2)\#1}$	2.2655(11)
$\text{Fe(1)-P(2)}$	2.2655(11)
$\text{N(1)-O(1)}$	1.188(5)
$\text{P(2)-C(21)}$	1.824(4)
$\text{P(2)-C(31)}$	1.827(4)
$\text{P(2)-C(11)}$	1.831(4)
$\text{C(11)-C(12)}$	1.370(7)
$\text{C(11)-C(16)}$	1.386(6)
$\text{C(12)-C(13)}$	1.384(7)
$\text{C(13)-C(14)}$	1.341(9)
$\text{C(14)-C(15)}$	1.380(9)
$\text{C(15)-C(16)}$	1.384(7)
$\text{C(21)-C(22)}$	1.378(6)
$\text{C(21)-C(26)}$	1.382(6)
$\text{C(22)-C(23)}$	1.386(7)
$\text{C(23)-C(24)}$	1.350(7)
$\text{C(24)-C(25)}$	1.370(7)
$\text{C(25)-C(26)}$	1.379(7)
$\text{C(31)-C(36)}$	1.386(6)
$\text{C(31)-C(32)}$	1.394(6)
$\text{C(32)-C(33)}$	1.373(6)
$\text{C(33)-C(34)}$	1.370(7)
$\text{C(34)-C(35)}$	1.365(7)
$\text{C(35)-C(36)}$	1.382(7)
$\text{N(1)-Fe(1)-N(1)\#1}$	124.5(3)
$\text{N(1)-Fe(1)-P(2)\#1}$	107.17(12)
$\text{N(1)\#1-Fe(1)-P(2)\#1}$	103.06(13)
$\text{N(1)-Fe(1)-P(2)}$	103.06(13)
$\text{N(1)\#1-Fe(1)-P(2)}$	107.17(12)
$\text{P(2)\#1-Fe(1)-P(2)}$	111.89(6)
$\text{O(1)-N(1)-Fe(1)}$	177.7(4)
$\text{C(21)-P(2)-C(31)}$	103.6(2)
$\text{C(21)-P(2)-C(11)}$	102.6(2)
$\text{C(31)-P(2)-C(11)}$	102.3(2)
$\text{C(21)-P(2)-Fe(1)}$	117.67(14)
$\text{C(31)-P(2)-Fe(1)}$	119.63(13)
$\text{C(11)-P(2)-Fe(1)}$	108.70(14)
$\text{C(12)-C(11)-C(16)}$	118.1(4)
$\text{C(12)-C(11)-P(2)}$	123.2(4)
$\text{C(16)-C(11)-P(2)}$	118.6(4)
$\text{C(11)-C(12)-C(13)}$	120.7(6)
$\text{C(14)-C(13)-C(12)}$	121.2(6)
$\text{C(13)-C(14)-C(15)}$	119.5(6)

---

C(14)-C(15)-C(16)	119.9(6)
C(15)-C(16)-C(11)	120.6(5)
C(22)-C(21)-C(26)	117.8(4)
C(22)-C(21)-P(2)	123.9(4)
C(26)-C(21)-P(2)	118.2(3)
C(21)-C(22)-C(23)	120.4(5)
C(24)-C(23)-C(22)	120.9(5)
C(23)-C(24)-C(25)	119.8(5)
C(24)-C(25)-C(26)	119.7(5)
C(25)-C(26)-C(21)	121.3(5)
C(36)-C(31)-C(32)	117.3(4)
C(36)-C(31)-P(2)	123.8(3)
C(32)-C(31)-P(2)	118.8(3)
C(33)-C(32)-C(31)	121.3(5)
C(34)-C(33)-C(32)	120.1(5)
C(35)-C(34)-C(33)	120.0(5)
C(34)-C(35)-C(36)	120.1(5)
C(35)-C(36)-C(31)	121.2(5)

---

Symmetry transformations used to generate equivalent atoms:  
#1 -x+1,y,-z+3/2

Table 2.12. Anisotropic displacement parameters ( $\text{Å}^2 \times 10^3$ ) for 6.

The anisotropic displacement factor exponent takes the form:

$$-2 \pi^2 [ h^2 a^{*2} U_{11} + \dots + 2 h k a^* b^* U_{12} ]$$

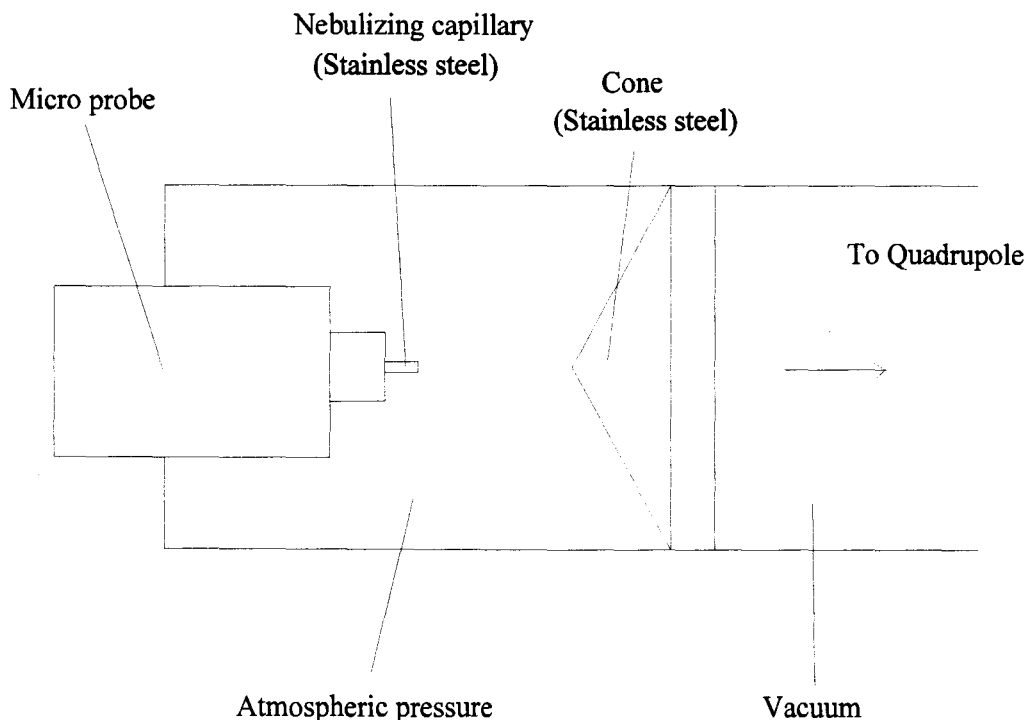
	U11	U22	U33	U23	U13	U12
Fe(1)	33 (1)	33 (1)	50 (1)	0	14 (1)	0
N(1)	49 (2)	45 (2)	71 (3)	-14 (2)	28 (2)	-3 (2)
O(1)	113 (3)	89 (3)	97 (3)	-45 (3)	53 (3)	-15 (2)
P(2)	32 (1)	36 (1)	42 (1)	-2 (1)	10 (1)	-1 (1)
C(11)	41 (2)	40 (3)	51 (3)	-10 (2)	14 (2)	-4 (2)
C(12)	47 (3)	69 (4)	76 (4)	2 (3)	4 (3)	-22 (3)
C(13)	65 (4)	105 (6)	87 (5)	3 (4)	-11 (4)	-36 (4)
C(14)	57 (4)	85 (5)	116 (6)	-19 (4)	14 (4)	-36 (3)
C(15)	61 (4)	54 (4)	108 (5)	-6 (4)	37 (4)	-19 (3)
C(16)	47 (3)	47 (3)	71 (4)	0 (3)	17 (3)	-4 (2)
C(21)	33 (2)	39 (2)	42 (3)	-3 (2)	6 (2)	-4 (2)
C(22)	58 (3)	50 (3)	53 (3)	-1 (3)	20 (3)	5 (2)
C(23)	67 (3)	45 (3)	74 (4)	13 (3)	23 (3)	6 (3)
C(24)	61 (3)	62 (4)	60 (4)	18 (3)	18 (3)	0 (3)
C(25)	61 (3)	68 (4)	44 (3)	5 (3)	15 (3)	-5 (3)
C(26)	58 (3)	44 (3)	53 (3)	-3 (3)	16 (2)	4 (2)
C(31)	33 (2)	42 (2)	37 (2)	0 (2)	7 (2)	7 (2)
C(32)	41 (3)	48 (3)	58 (3)	-8 (2)	11 (2)	1 (2)
C(33)	60 (3)	48 (3)	61 (3)	-13 (3)	6 (3)	4 (3)
C(34)	69 (4)	61 (4)	53 (3)	-14 (3)	17 (3)	15 (3)
C(35)	55 (3)	73 (4)	72 (4)	-15 (3)	32 (3)	6 (3)
C(36)	37 (3)	65 (3)	61 (3)	-17 (3)	15 (3)	-4 (2)

Table 2.13. Hydrogen coordinates ( $\times 10^4$ ) and isotropic displacement parameters ( $\text{Å}^2 \times 10^3$ ) for 6.

	x	y	z	U(eq)
H(12)	1227 (39)	4441 (54)	5731 (27)	59 (15)
H(13)	-334 (62)	2709 (80)	5249 (41)	133 (28)
H(14)	-609 (49)	405 (65)	5991 (33)	94 (18)
H(15)	957 (42)	-260 (60)	7159 (29)	72 (16)
H(16)	2562 (37)	1363 (50)	7579 (26)	52 (14)
H(22)	2693 (31)	7917 (44)	6739 (23)	30 (11)
H(23)	2643 (39)	9670 (56)	5719 (27)	58 (14)
H(24)	3069 (40)	8695 (59)	4543 (31)	75 (16)
H(25)	3733 (40)	6081 (53)	4554 (29)	61 (15)
H(26)	3700 (35)	4351 (50)	5547 (24)	45 (12)
H(32)	4448 (39)	6843 (52)	8254 (25)	58 (13)
H(33)	3922 (41)	8456 (57)	9200 (28)	68 (16)
H(34)	2039 (38)	8036 (55)	9458 (27)	63 (15)
H(35)	676 (52)	6325 (67)	8674 (34)	108 (21)
H(36)	1171 (38)	4898 (50)	7663 (26)	52 (13)

## 2.6 Mass Spectrometry

Analysis of thermally labile organometallic compounds by traditional ionization methods such as electron impact (EI) and chemical ionization (CI) is difficult. Fortunately, the problem has been alleviated to some extent by fast atom bombardment (FAB). For the series of iron dinitrosyl imidazole compounds,  $\text{Fe}(\text{NO})_2(\text{L})_2$  [ $\text{L}$  = imidazole **1**, 1-methylimidazole **2**, 4-methylimidazole **3**, benzimidazole **4**, 5,6-dimethylbenzimidazole **5**], these conventional ionization techniques provide spectra with no observance of  $\text{M}^+$ ,  $\text{M}^+$  being defined as the sought after molecular ion for the four coordinate compounds of **1 - 5**. Recently, techniques have been demonstrated that combine electrospray and electrochemical



**Figure 2.12.** Schematic diagram of mass spectrometer ionization apparatus.

oxidation (ESCI) that produce intact molecular ions ( $M^+$ ) for a variety of organometallic (and organic) compounds.<sup>51</sup> A drawback of this procedure is the complexity of the methodology used to generate the ions, i.e. interfacing an electrochemical cell with the sample introduction system or the use of mobile phase additives such as dichlorodicyanobenzoquinone (DDQ) to promote the oxidation. Smith has recently developed a modification to the ESCI method without the use of an external electrochemical cell or addition of chemical oxidants.<sup>52</sup> Figure 2.12 shows a schematic diagram of the ESCI apparatus used, in which a potential difference is created between the nebulizing capillary tube (4 - 4.5 kV) and the cone (5 - 15 V). A solution containing the compound approaches the capillary tip where the compound is oxidized during a positive ion mode, under atmospheric pressure. It is believed that the ionization occurs at the tip of the nebulizing capillary when the compounds come in contact with the capillary walls.<sup>53</sup> The ionized compounds pass through the cone and are subjected to a vacuum as they flow towards the quadrupole detector. The mass spectroscopy experiments were carried out using reaction mixtures of the imidazole series of compounds that were worked up in a mixture of 90:10 dichloromethane/methanol, the same solvent composition as the carrier mobile phase. The  $M^+$  parent ions observed for compounds **1-5** are listed in Table 2.14. The mass spectra obtained for **1 - 5** are shown in Figures 2.13-2.17, respectively. Figures 2.18a and 2.18b show the simulated and experimental isotopic distribution of the  $M^+$  280 peak for  $\text{Fe}(\text{NO})_2(1\text{-MeIm})_2^+$ , respectively. This distribution was used to determine the iron containing compounds in the spectra.

There are two recurring, interesting aspects in each spectra besides the ( $M^+$ ) peaks:

1) a non iron compound that corresponds to twice the MW of the imidazole ligand plus hydrogen [ 2 Im + H]; and 2) repeating, higher molecular mass peaks beyond M+. The first interesting observation is a dimer of the imidazole ligand linked through a hydrogen atom.

Table 2.15 lists the imidazole dimers

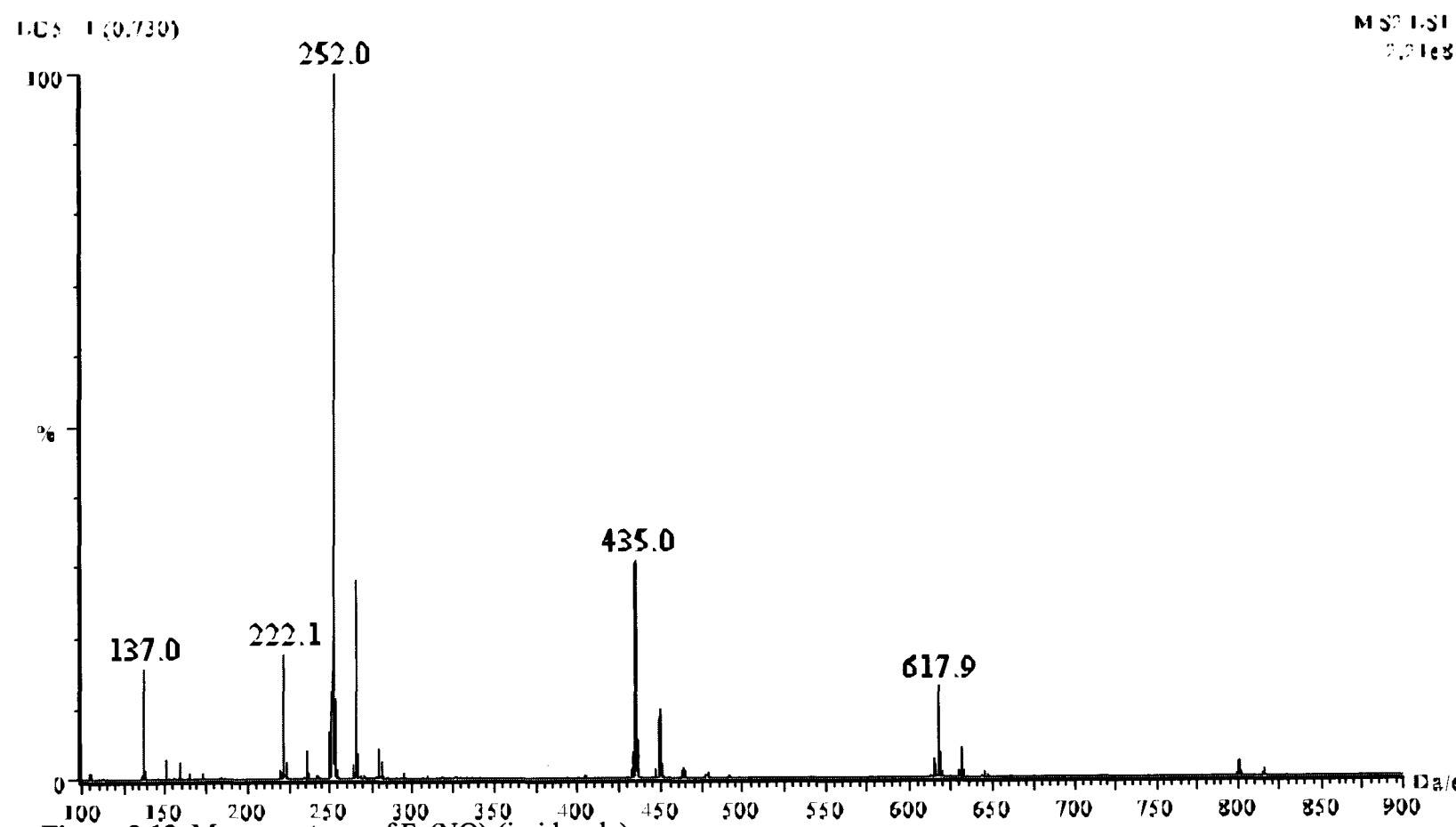


Figure 2.13. Mass spectrum of  $\text{Fe}(\text{NO})_2(\text{imidazole})_2$

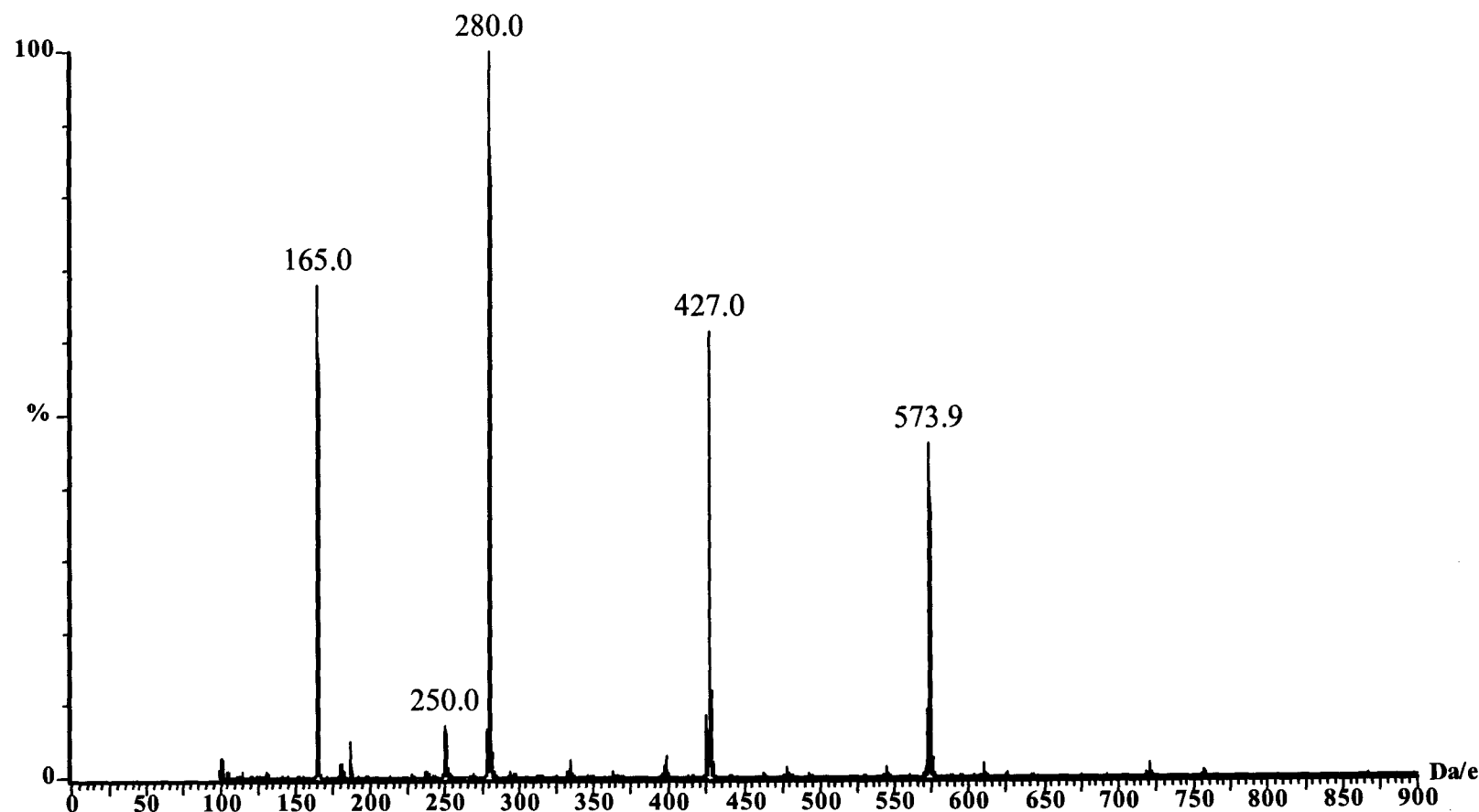


Figure 2.14. Mass spectrum of  $\text{Fe}(\text{NO})_2(1\text{-MeIm})_2$

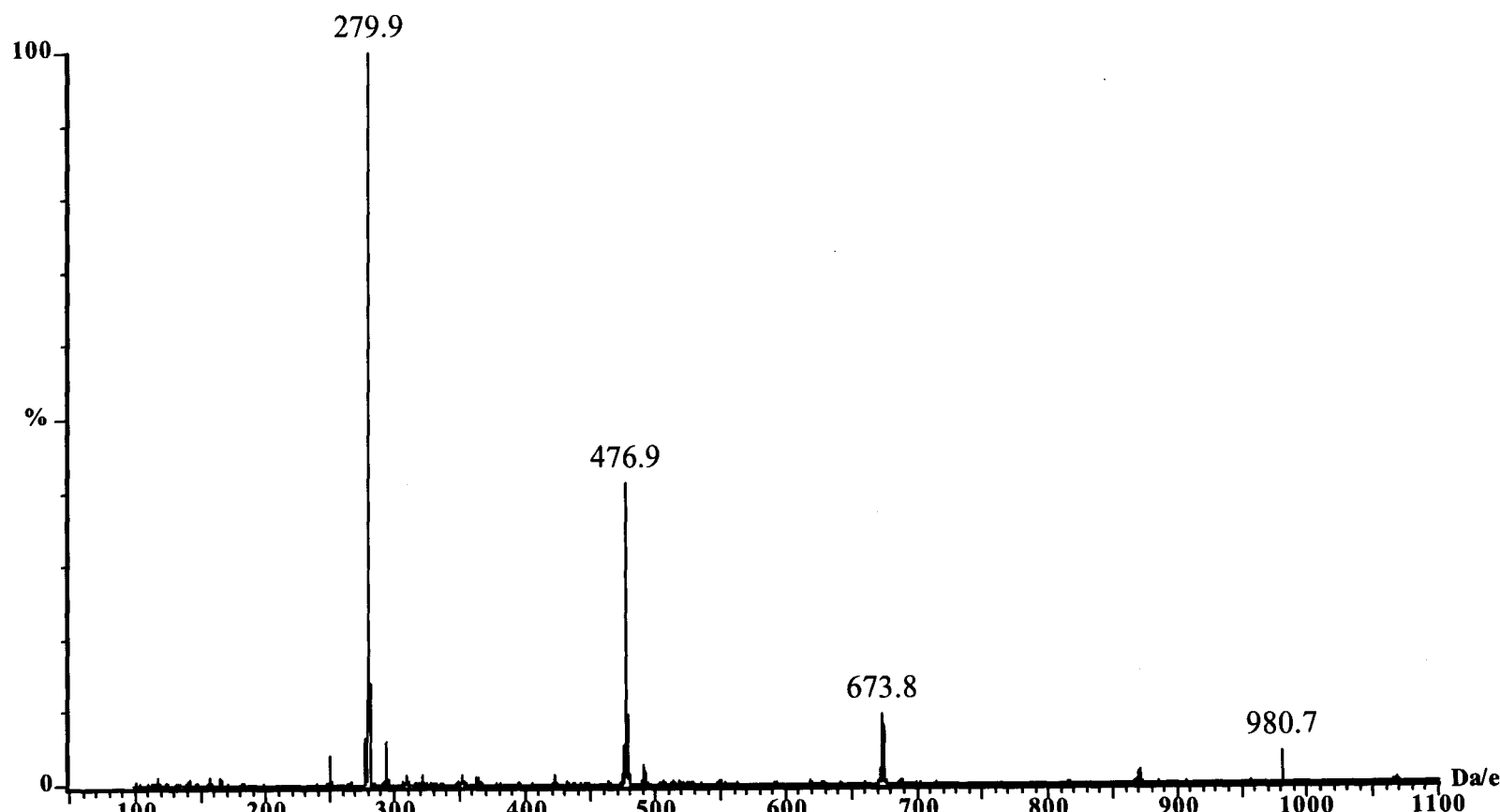
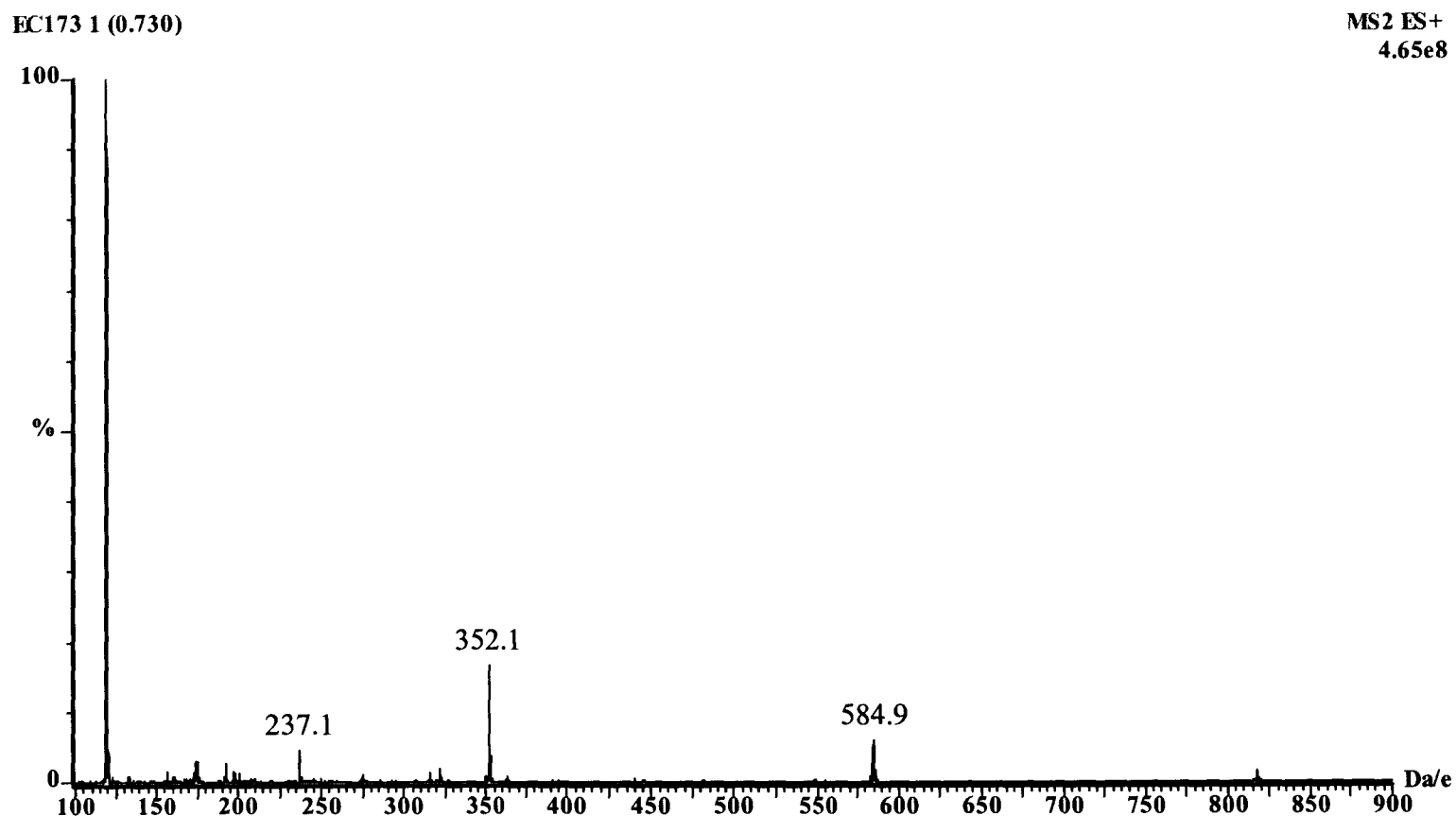
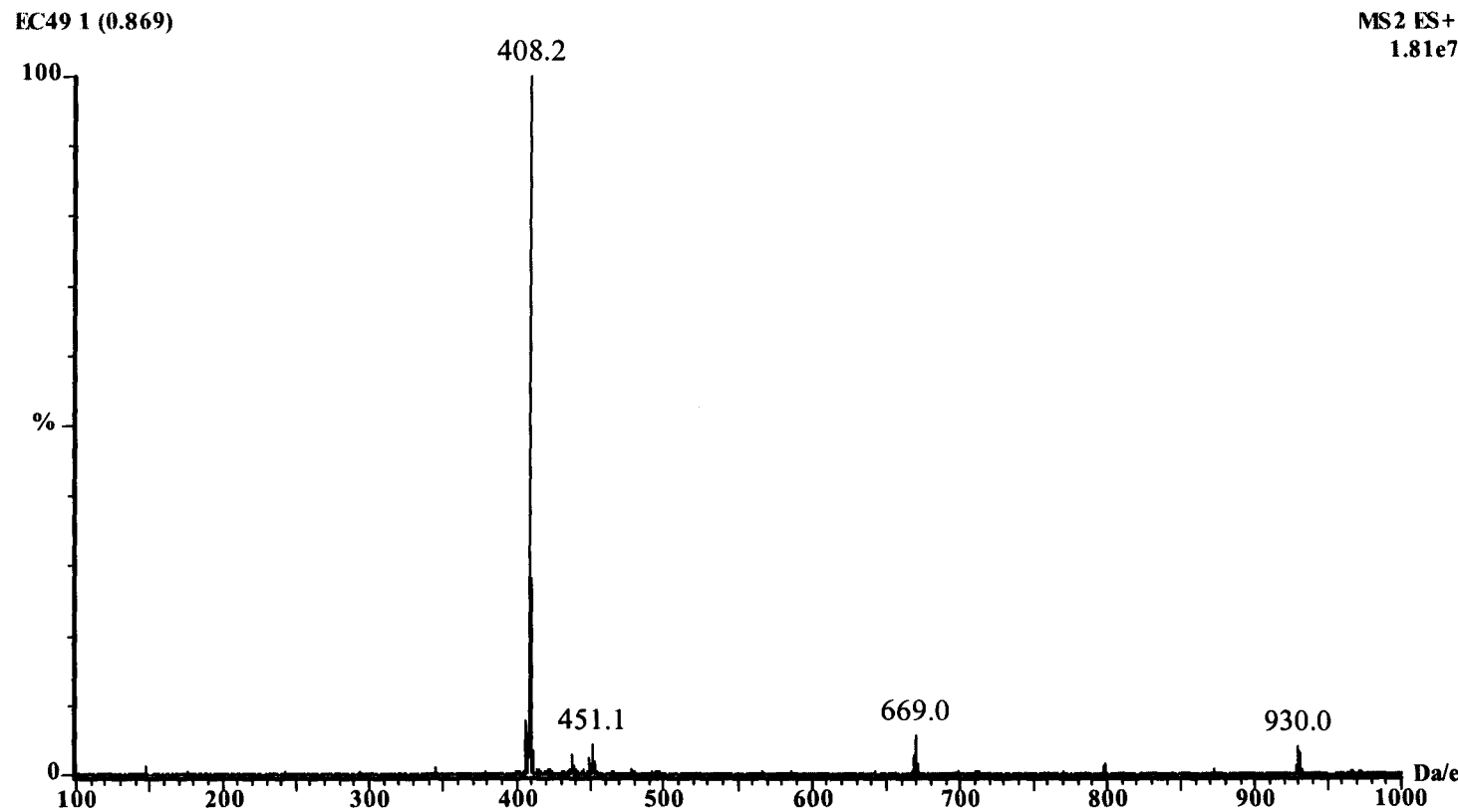


Figure 2.15. Mass spectrum of  $\text{Fe}(\text{NO})_2(4\text{-MeIm})_2$



**Figure 2.16.** Mass spectrum of  $\text{Fe}(\text{NO})_2(\text{benzimidazole})_2$



**Figure 2.17.** Mass spectrum of  $\text{Fe}(\text{NO})_2(5,6\text{-dimethylbenzimidazole})_2$

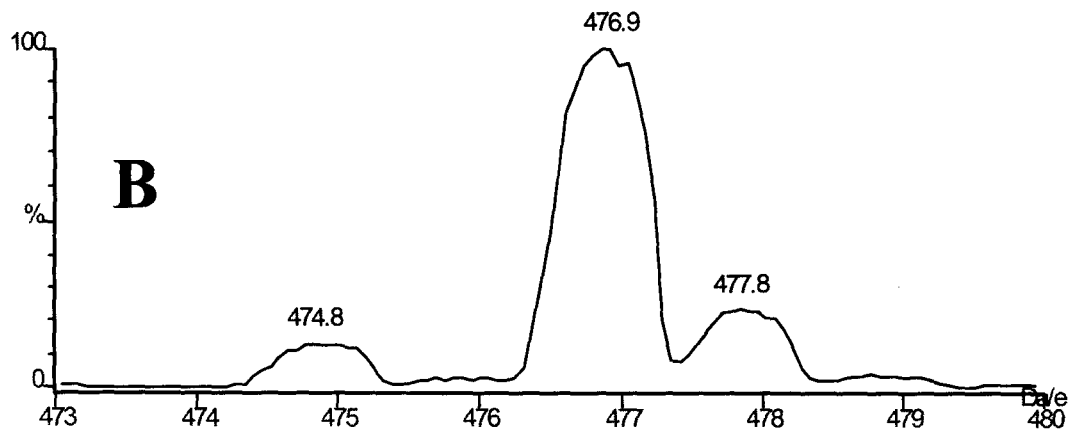
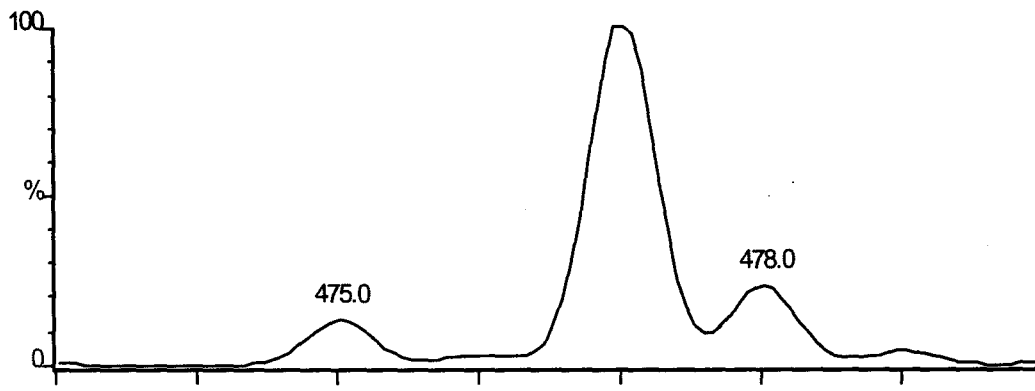


**Figure 2.18.** Isotopic Ratio of  $\text{Fe}(\text{NO})_2(1\text{-MeIm})_2$

found in each spectrum and Scheme 2.6 shows the proposed structures of each dimer formed. The association of imidazole ligands into long chain oligomers has been previously noted<sup>54</sup> and has been deemed responsible for the high melting points of imidazole, 4-MeIm, Benzim, and 5,6-dimethylbenzim (m.p. 90, 66, 170, and 204°C, respectively) relative to N-protected imidazoles (1-MeIm m.p. -6 °C).

The second unforseen feature of each mass spectrum is the appearance of higher weight molecular peaks than the parent ions. Table 2.16 lists the MW peaks greater than M+ observed for each spectrum, and the corresponding repeating mass difference between higher MW values. Each of the peaks beyond M+ is related to the M+ by the addition of a repeating mass unit, or monomer. In other words, each higher mass peak is an oligomer based on the starting M+ peak in each mass spectrum. The repeat mass unit consists of one iron, two nitrosyls, and one deprotonated imidazole ligand. For the case of Fe(NO)<sub>2</sub>(imidazole)<sub>2</sub>, the M+ peak occurs at m/z 252, with accompanying peaks at m/z 435, 618, and 801. The MW 435 peak would then consist of the M+ parent molecule, plus the iron fragment shown in Scheme 2.7. Correspondingly, the peaks at m/z 618 and 801 are larger oligomers consisting of 3 and 4 iron repeat units attached to M+. The concentration of even higher MW species are of very low intensity, and are lost in the baseline noise.

It is believed that these compounds are a direct result of the environmental conditions set by the mass spectrometer.<sup>55</sup> Point in proof, an experiment was carried out involving a series of injections of a reaction mixture of Fe(NO)<sub>2</sub>(CO)<sub>2</sub> with 4-MeIm that was allowed to sit for approximately 10 minutes, 1 hour and one day. All three spectra

obtained were identical. If a polymeric species were formed in solution, a higher molecular weight distribution of ions would be expected after longer periods of time with exposure to the monomer.

Inorganic polymer species with imidazoles and Cu, Co, and Zn have been reported.<sup>56,57,58,59</sup> The iron compound in Figure 2.19,  $[\text{Fe}_3(\text{imid})_6(\text{imidH})_2]_x$ ,<sup>60</sup> consists of chains of tetrahedral iron centers cross-linked *via* octahedral iron ions to generate a 3-D array. All of the iron centers are bridged to four other metal centers *via* imidazolate ions, the two remaining (trans) coordination positions of the octahedral centers being occupied by neutral imidazole molecules. The  $[\text{Fe}(\text{NO})_2(\text{Im})_2]_x$  oligomer is a linear chain. The nitrosyl ligands replace two coordination sites available on iron and prevent the formation of cross linking between the linear chains of Fe-Im-Fe.

The fact that **2** has a repeat unit of mass 147, as shown in Figure 2.14, is unusual. The tertiary N is protected by a methyl group and is not expected to be available to bridge another iron. Even if the methyl group were removed it would still have a repeat unit of mass 183, 36 mass units higher than that observed. Each of the higher MW peaks is an iron containing compound, as confirmed by their isotopic distribution. MS/MS experiments have only been performed on the M+ 280 peak, so composition of the repeat unit is unknown.

Foffani and co-workers<sup>61</sup> have previously reported the fragmentation pattern for  $\text{Fe}(\text{NO})_2(\text{CO})_2$ . The spectrum was obtained with a collision energy of 50 eV. A cascading pattern was observed including ions such as  $\text{Fe}(\text{NO})_2(\text{CO})_2^+$  (large),  $\text{Fe}(\text{NO})_2(\text{CO})^+$  (2<sup>nd</sup> largest),  $\text{Fe}(\text{NO})(\text{CO})_2^+$  (v.small),  $\text{Fe}(\text{NO})_2^+$  (small),  $\text{Fe}(\text{NO})(\text{CO})^+$  (med),  $\text{Fe}(\text{CO})_2^+$

(v.small), Fe(NO)<sup>+</sup> (med), Fe(CO)<sup>+</sup> (large), FeN<sup>+</sup> (med), Fe<sup>+</sup> (largest), NO<sup>+</sup> (large), CO<sup>+</sup> (large). The ms/ms experiments were performed on compounds **1 - 5** with more gentle collision conditions than Foffani's work (collision energies no greater than 35 eV, as compared to 50 eV for Foffani). The spectra obtained for compounds **1 - 5** obviously do not have the same degree of fragmentation with the lower collision energy, but the spectra in Figures 2.20 - 2.27 still provide useful information. We observe the characteristic losses of NO and Im ligands for each compound, the fragment ion MW's of which are listed in Table 2.17.

The ESCI technique was used on the Fe(NO)<sub>2</sub>(1-MeIm)<sub>2</sub> reaction mixture to try to gain insight into the decomposition of the Fe(NO)<sub>2</sub>(L)<sub>2</sub> set of compounds. The dark green mixture was exposed to air and allowed to react, after which, samples of the solution were injected at timed intervals. Figure 2.14 shows the initial spectra before exposure to air. Upon exposure, the solution immediately turned to a clear brown solution. The spectra obtained (Figure 2.28) shows the 280 peak remains the dominant ion peak, with many new peaks appearing lower than 280. Higher MW iron containing peaks are still visible at 427 and 574, but much lower intensity than the 280 peak.

After 5 minutes (Figure 2.29), the solution became cloudy and took on a more orange colour. The M+ 280 was still relatively large, but is no longer the dominant peak. The 165 ion became the largest peak, which corresponds to the 1-MeIm dimer. There are no peaks in the spectrum that are observed as daughters of the 280 peak. An unknown peak appears at 348, almost of the same intensity as the 280 ion. A small peak at 473 is still observed, while the peak at 574 has disappeared.

At seven minutes (Figure 2.30), the solution had cleared and a precipitate settled to the bottom of the flask. The ions of mass greater than 400 are no longer discernable above the baseline, and the spectrum is still complex. A large non-iron peak is visible at 105 and becomes the dominant peak. The 280 ion peak is very small and the 165 peak is just slightly smaller than the 105 peak.

After 10 minutes (Figure 2.31), the solution became almost clear, with an orange precipitate covering the bottom of the flask. The solution contains mainly protonated imidazole ligand. A small amount of the dimer 1-MeIm dimer appears at 165. An unknown peak also remains at m/z 105, but much smaller than m/z 165.

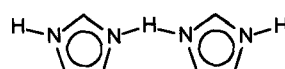
These experiments show no characteristic losses of NO and ligand, as found by ms/ms experiments. This infers that the reaction is not proceeding by way of a dissociative ( $S_N1$  type) substitution mechanism and therefore most likely proceeds *via* an associative ( $S_N2$  type) pathway. There are no soluble iron containing compounds in solution after 7 - 10 minutes, which leaves mainly the 1-MeIm ligand ( $1\text{-MeImH}^+$ , m/z 83) and the dimer complex (shown in Scheme 2.6 B, m/z 165) as the major species in the spectra. The colour of the precipitate after 7 - 10 minutes is orange, and may be an iron oxide. It is thought that upon exposure of the solution to air, oxygen addition occurs at the iron center to produce a bimolecular intermediate compound. A molecular weight peak reflecting a species of this nature has not yet been deciphered in the spectra.

**Table 2.14.** Parent ion peaks for iron nitrosyl imidazole compounds.

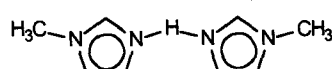
Compound	M <sup>+</sup> (Da/e)
<b>1</b> Fe(NO) <sub>2</sub> (imidazole) <sub>2</sub>	252.0
<b>2</b> Fe(NO) <sub>2</sub> (1-MeIm) <sub>2</sub>	280.0
<b>3</b> Fe(NO) <sub>2</sub> (4-MeIm) <sub>2</sub>	279.9
<b>4</b> Fe(NO) <sub>2</sub> (Benzimidazole) <sub>2</sub>	352.1
<b>5</b> Fe(NO) <sub>2</sub> (5,6-dimethylbenzim) <sub>2</sub>	408.2

**Table 2.15.** Imidazole dimers found in mass spectra.

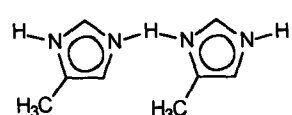
Molecular Weights of Imidazole Dimers		
Original compound	Symbol	Molecular Weight
<b>1</b> Fe(NO) <sub>2</sub> (imidazole) <sub>2</sub>	<b>A</b>	137 (large)
<b>2</b> Fe(NO) <sub>2</sub> (1-MeIm) <sub>2</sub>	<b>B</b>	165 (large)
<b>3</b> Fe(NO) <sub>2</sub> (4-MeIm) <sub>2</sub>	<b>C</b>	165 (v.small)
<b>4</b> Fe(NO) <sub>2</sub> (Benzimidazole) <sub>2</sub>	<b>D</b>	237 (v.small)
<b>5</b> Fe(NO) <sub>2</sub> (5,6-dimethylbenzim) <sub>2</sub>	<b>E</b>	293 (v.small)



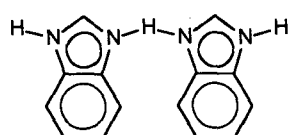
**A**



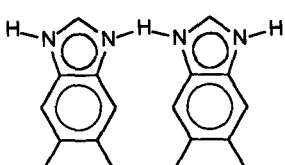
**B**



**C**

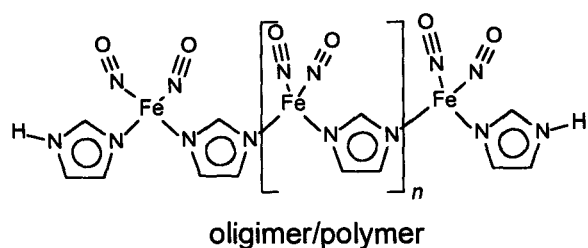
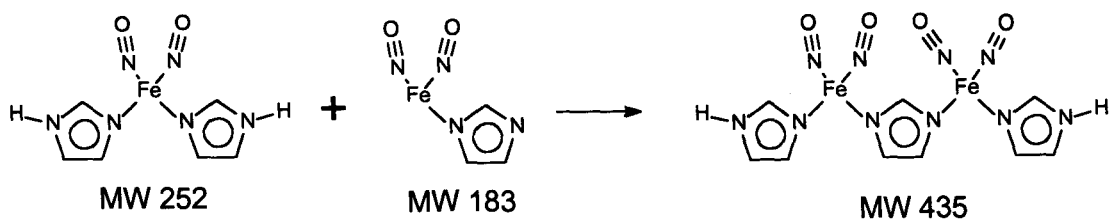


**D**



**E**

**Scheme 2.6.** Proposed structures of imidazole dimers detected in mass spectrometer.



**Scheme 2.7.** Proposed structures of oligomers detected in mass spectrometer.

**Table 2.16.** High MW ions found in Mass spectra of iron dinitrosyl imidazole compounds.

Compound	MW Peaks Observed	MW Repeat Unit
<b>1</b> Fe(NO) <sub>2</sub> (imidazole) <sub>2</sub>	252, 435, 618, 801	183
<b>2</b> Fe(NO) <sub>2</sub> (1-MeIm) <sub>2</sub>	280, 427, 574, 721	147
<b>3</b> Fe(NO) <sub>2</sub> (4-MeIm) <sub>2</sub>	280, 477, 674, 871, 1068	197
<b>4</b> Fe(NO) <sub>2</sub> (Benzimidazole) <sub>2</sub>	352, 585, 818, 1051, 1284	233
<b>5</b> Fe(NO) <sub>2</sub> (5,6-dimethylbenzim) <sub>2</sub>	408, 669, 930	261

**Table 2.17.** MS/MS of iron dinitrosyl imidazole compounds.

Compound	Daughters of	Observed Peaks
<b>1</b> Fe(NO) <sub>2</sub> (imidazole) <sub>2</sub>	252	222 (-NO), 191 (-2NO), 184 (-Im), 154 (-NO, Im)
<b>2</b> Fe(NO) <sub>2</sub> (1-MeIm) <sub>2</sub>	280	280 (M+), 250 (-NO), 220 (-2NO), 168 (-NO, 1-MeIm)
<b>3</b> Fe(NO) <sub>2</sub> (4-MeIm) <sub>2</sub>	280	280 (M+), 250 (-NO), 220 (-2NO), 168 (-NO, 1-MeIm)
	477	477 (M+), 447 (-NO), 417 (-2NO), 395 (-4-MeIm), 365 (-NO, 4-MeIm), 335 (-2NO, 4-MeIm)
<b>4</b> Fe(NO) <sub>2</sub> (Benzimidazole) <sub>2</sub>	352	322 (-NO), 292 (-2NO), 234 (-benzim), 204 (-NO, benzim)
	585	585 (M+), 555 (-NO), 525 (-2NO), 477 (-benzim), 437 (-NO, benzim)
<b>5</b> Fe(NO) <sub>2</sub> (5,6-dimethylbenzim) <sub>2</sub>	408	408 (M+), 378 (-NO), 348 (-2NO), 262 *, 232 (-5,6dimethylbenz), 202 (-NO, -5,6dimethylbenz)

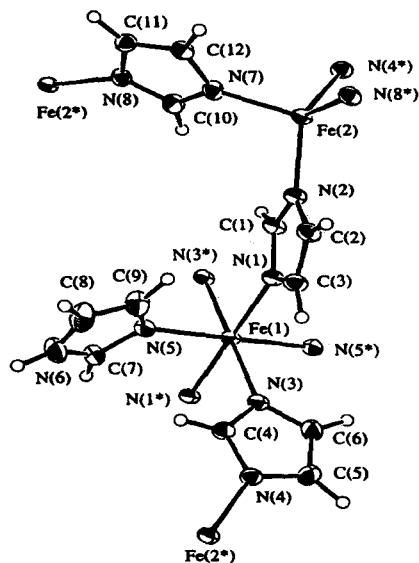


**Figure 2.19.** Ortep diagram of  $[\text{Fe}_3(\text{imid})_6(\text{imidH})_2]_x$

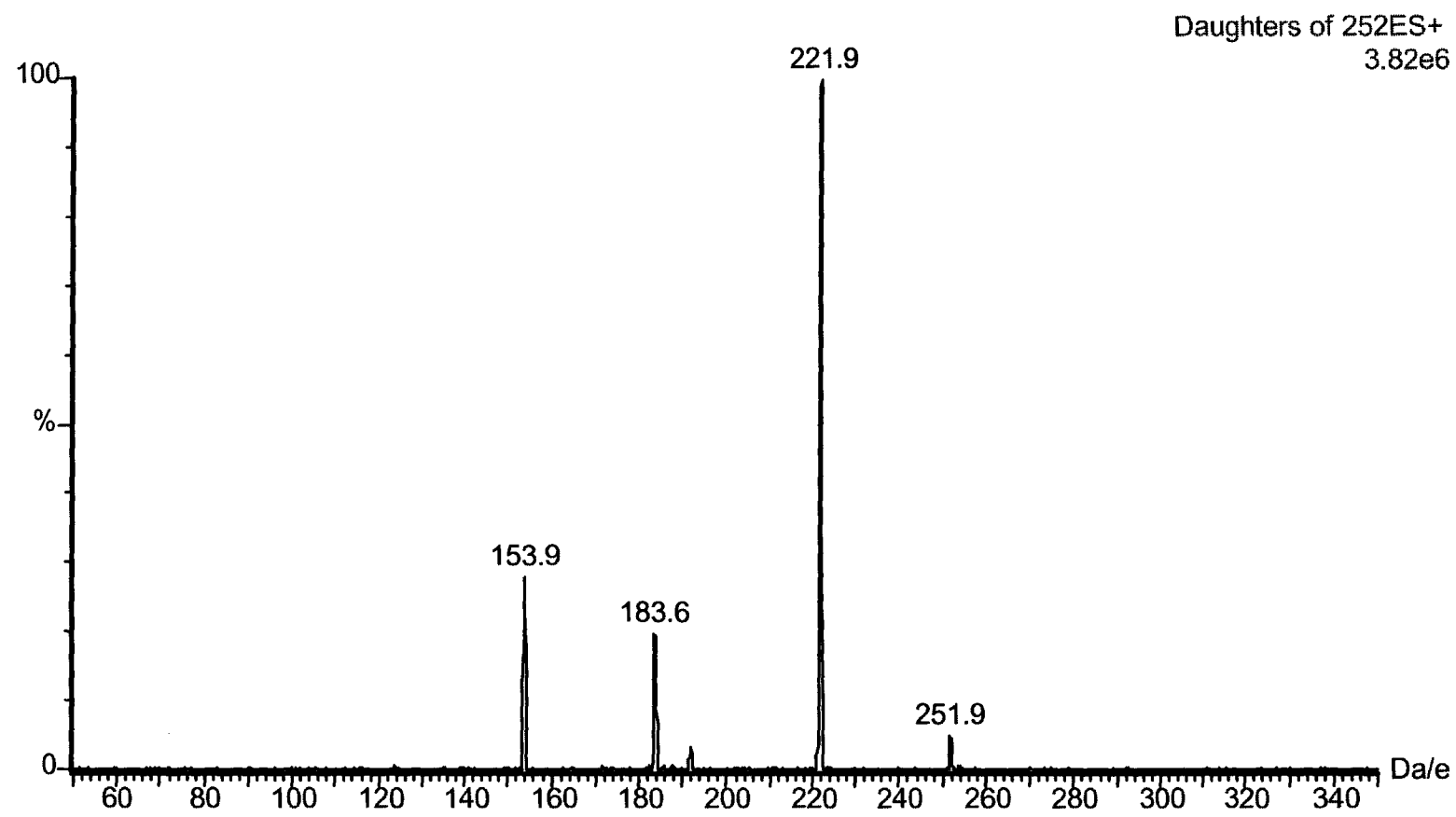
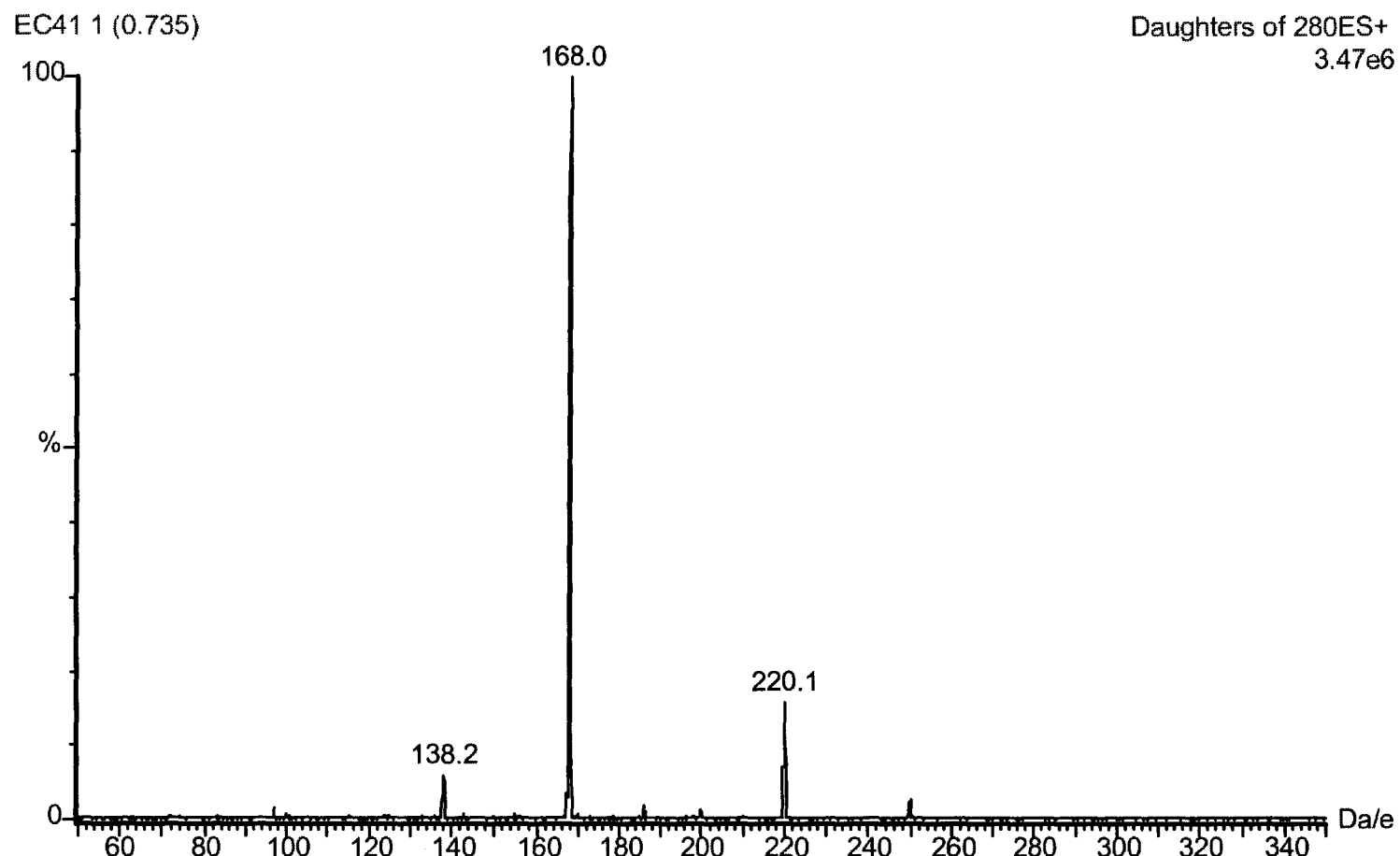
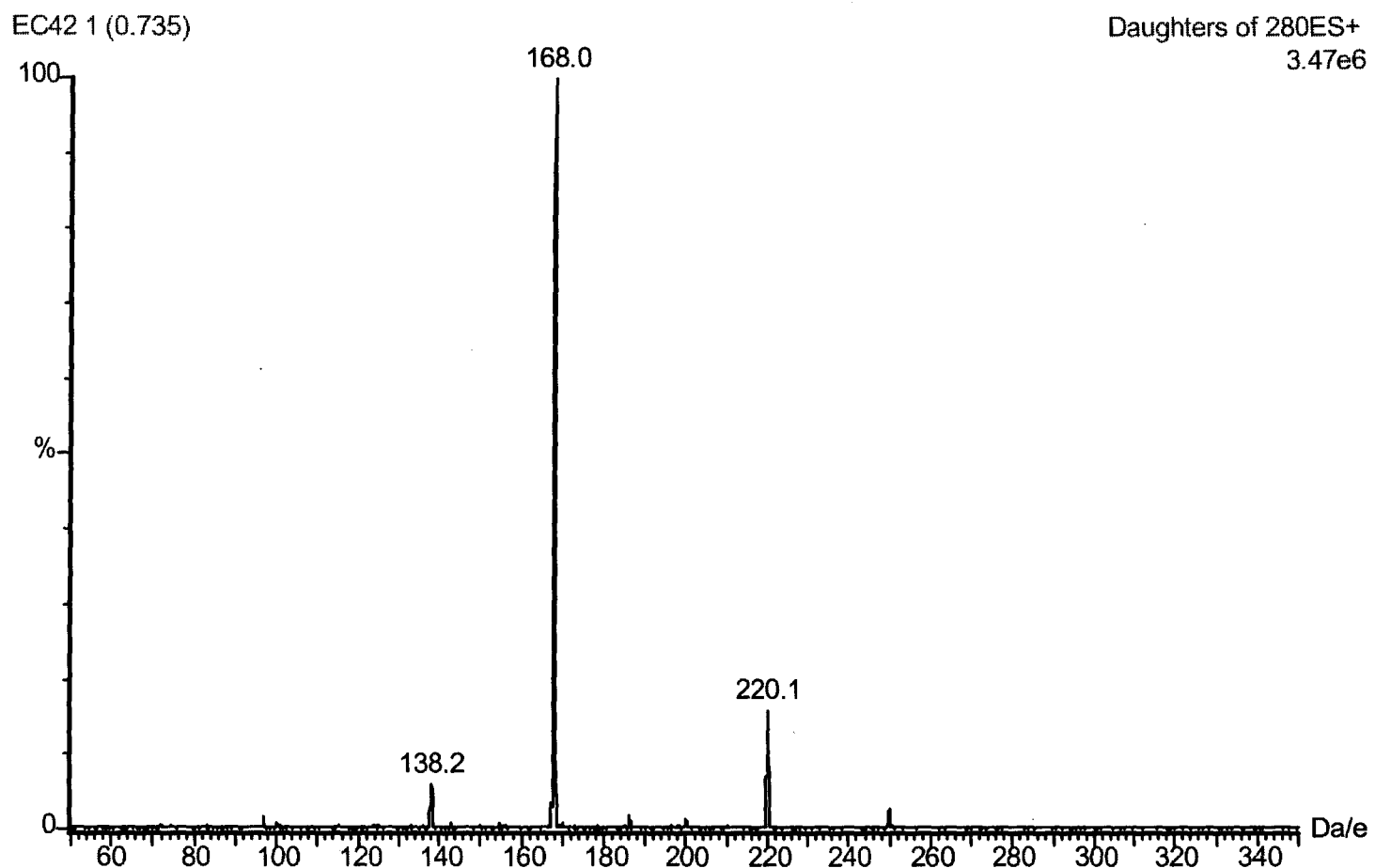


Figure 2.20. Daughters of  $\text{Fe}(\text{NO})_2(\text{imidazole})_2^+$  252 ion



**Figure 2.21.** Daughters of  $\text{Fe}(\text{NO})_2(1\text{-Melm})_2^+$  280 ion



**Figure 2.22.** Daughters of  $\text{Fe}(\text{NO})_2(4\text{-MeIm})_2^+$  280 ion

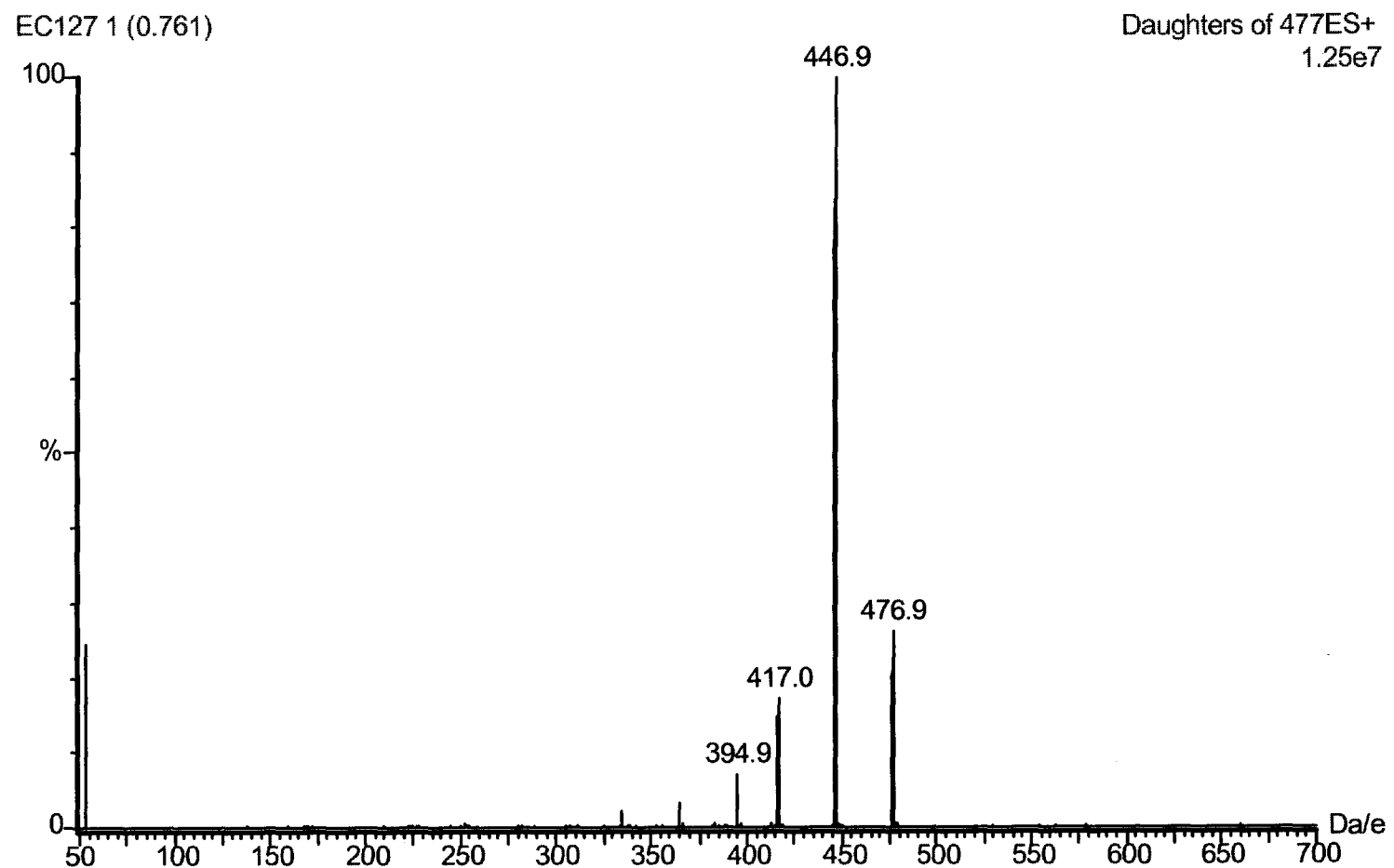


**Figure 2.23.** Daughters of  $\text{Fe}(\text{NO})_2(4\text{-MeIm})_2^+$  477 ion

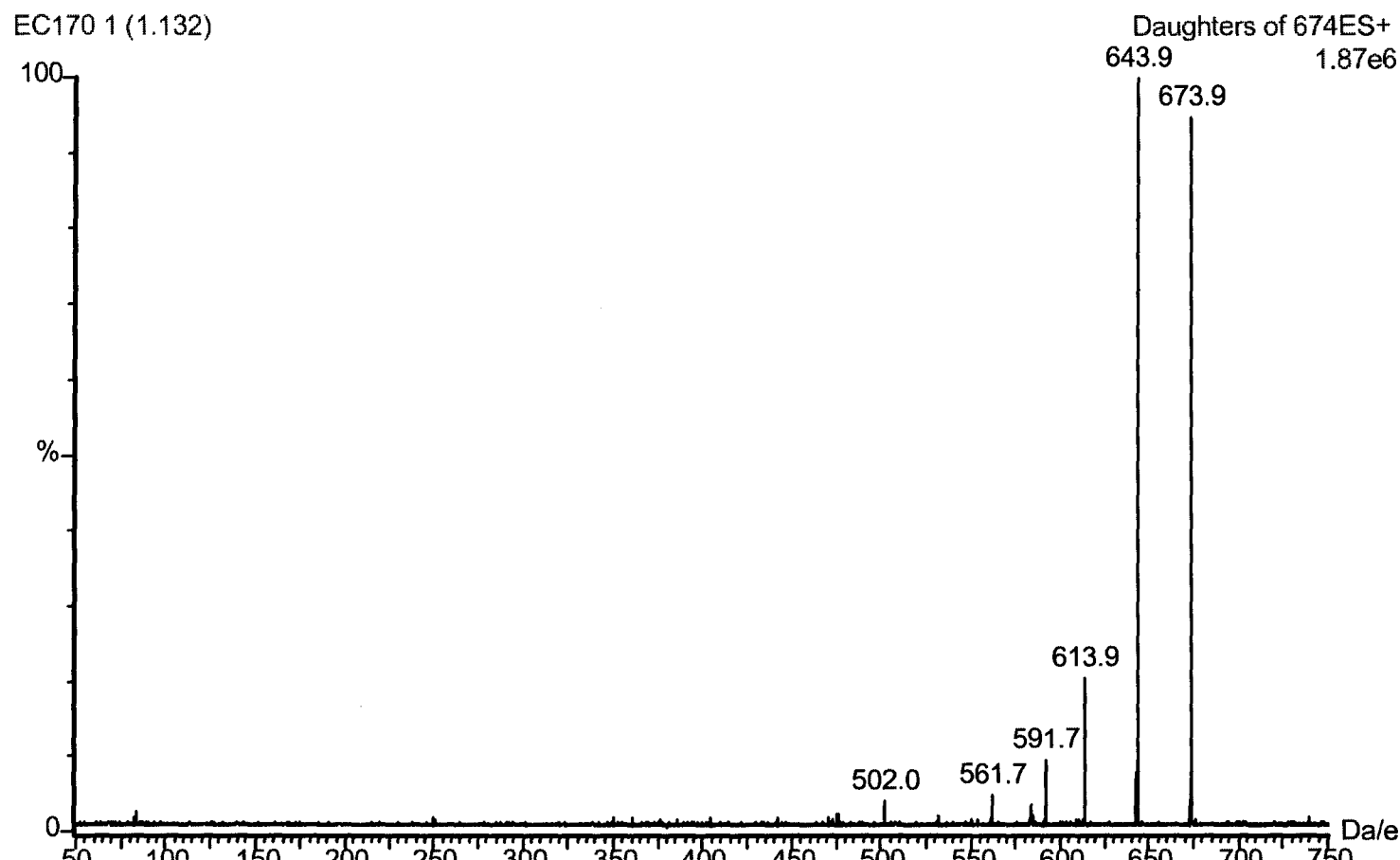


**Figure 2.24.** Daughters of  $\text{Fe}(\text{NO})_2(4\text{-MeIm})_2^+$  674 ion

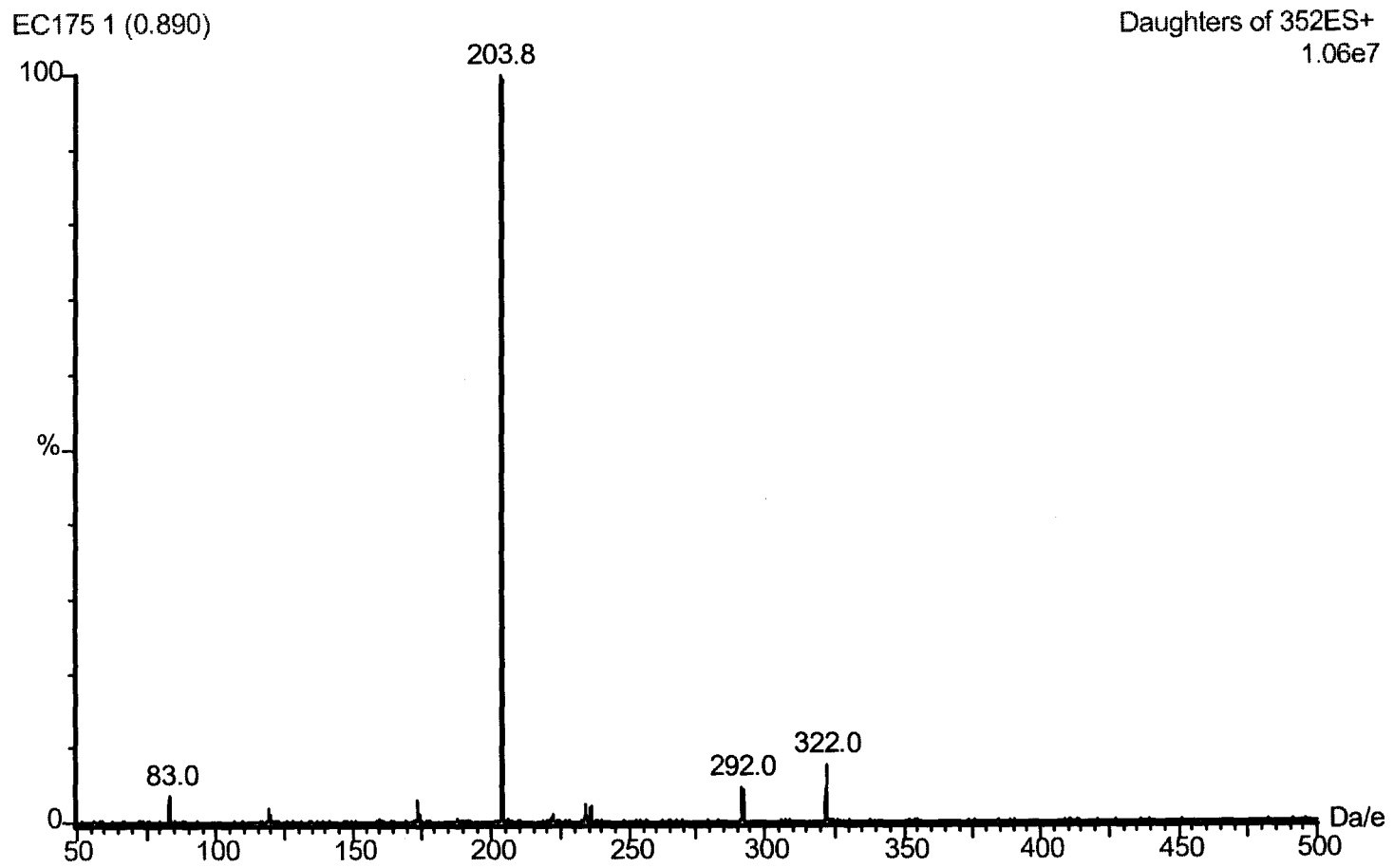


**Figure 2.25.** Daughters of  $\text{Fe}(\text{NO})_2(\text{benzimidazole})_2^+$  352 ion

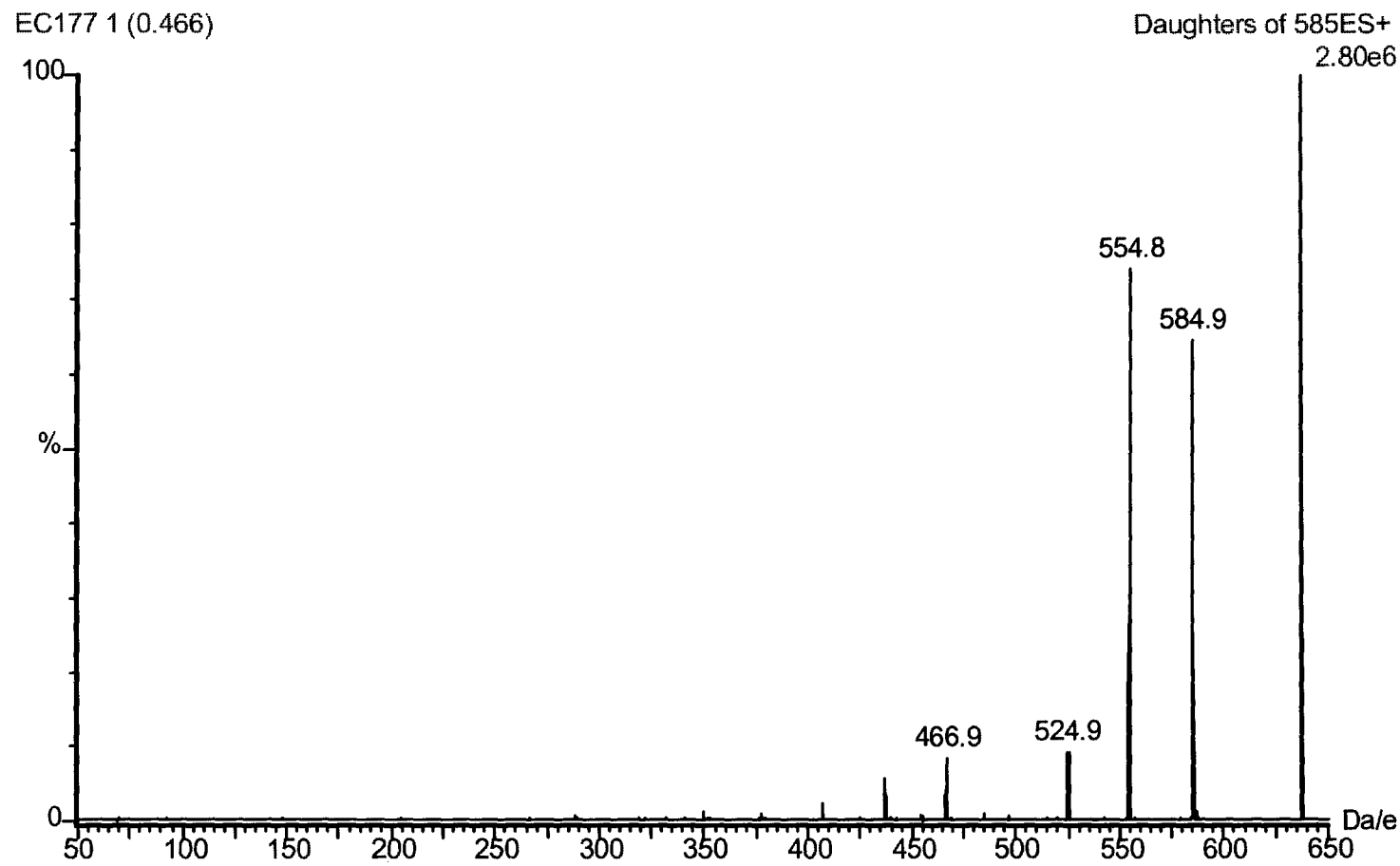


**Figure 2.26.** Daughters of  $\text{Fe}(\text{NO})_2(\text{benzimidazole})_2^+$  585 ion

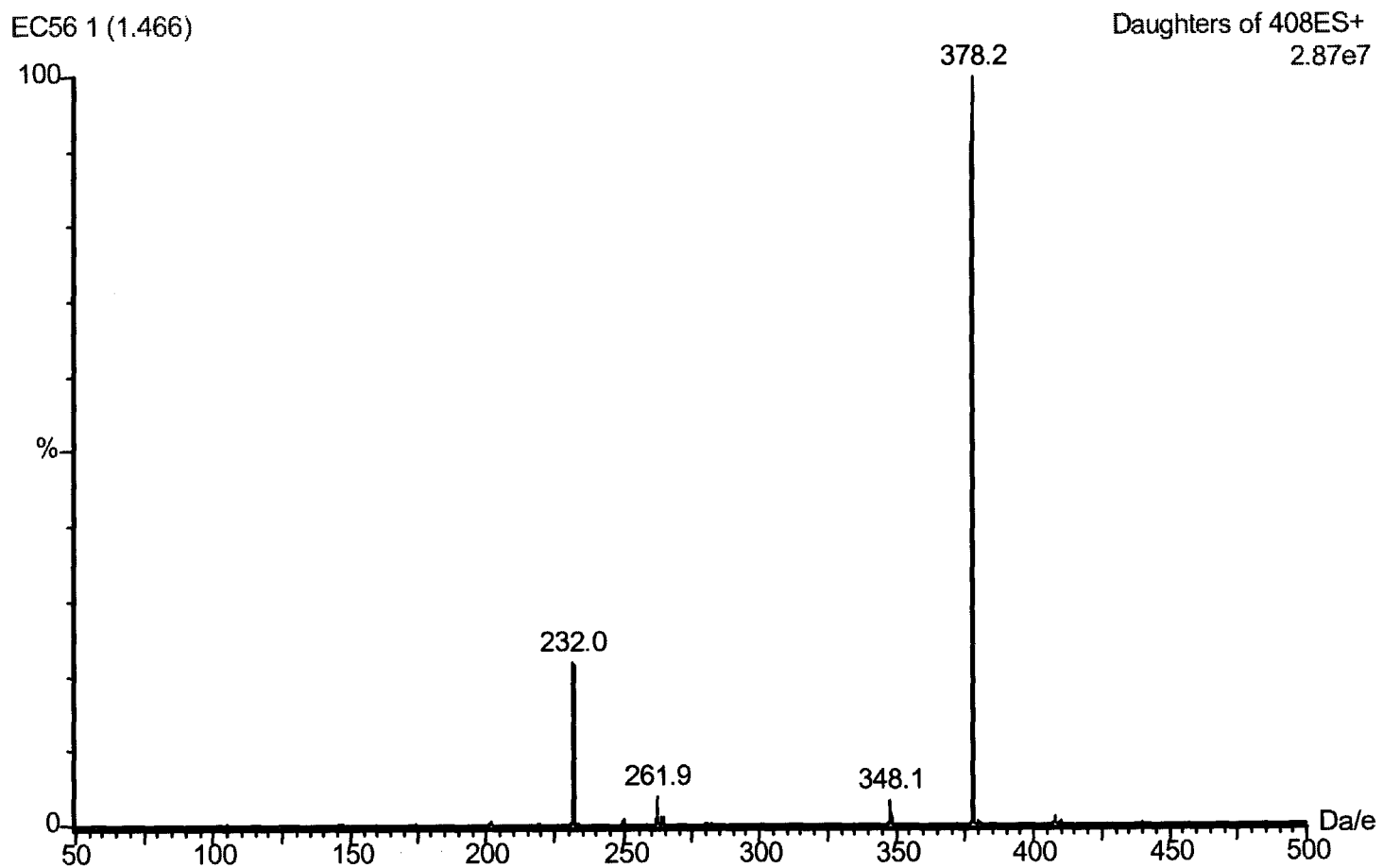


**Figure 2.27.** Daughters of  $\text{Fe}(\text{NO})_2(5,6\text{-dimethylbenzimidazole})_2^+$  408 ion

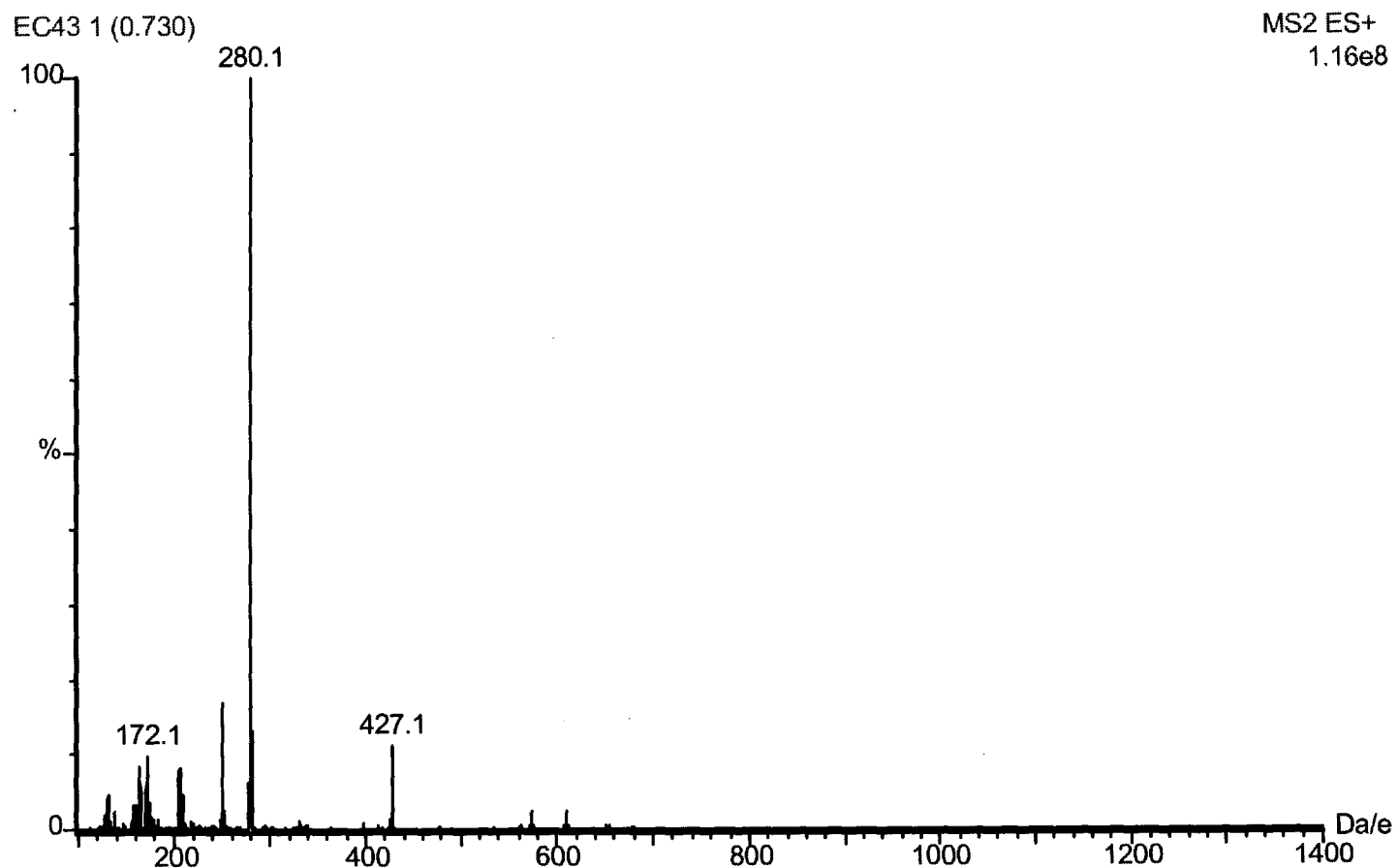


**Figure 2.28.** MS Spectrum of  $\text{Fe}(\text{NO})_2(1\text{-MeIm})_2$  immediately after exposure to air.

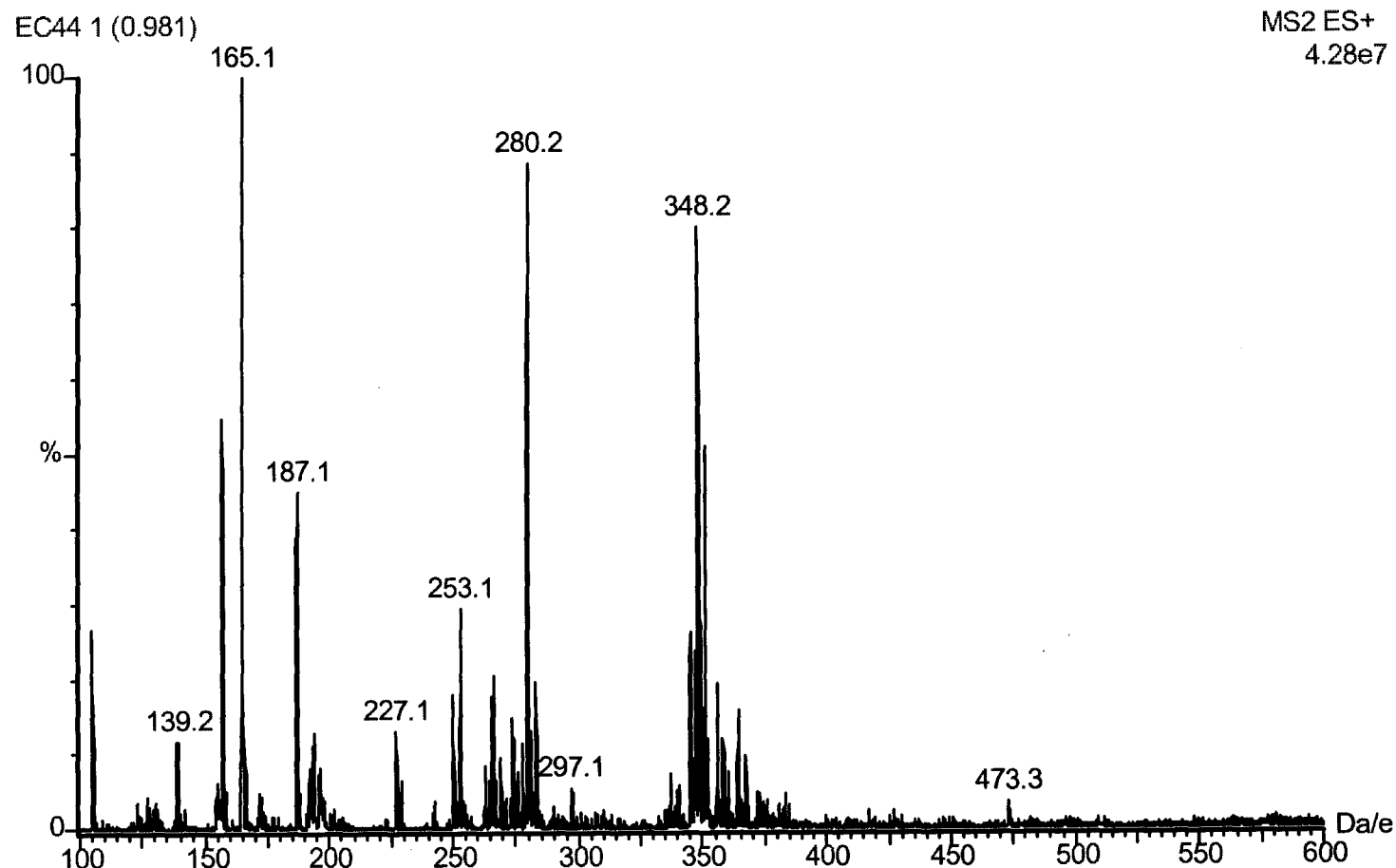


**Figure 2.29.** MS Spectrum of  $\text{Fe}(\text{NO})_2(1\text{-MeIm})_2$ , 5 minutes after exposure to air.

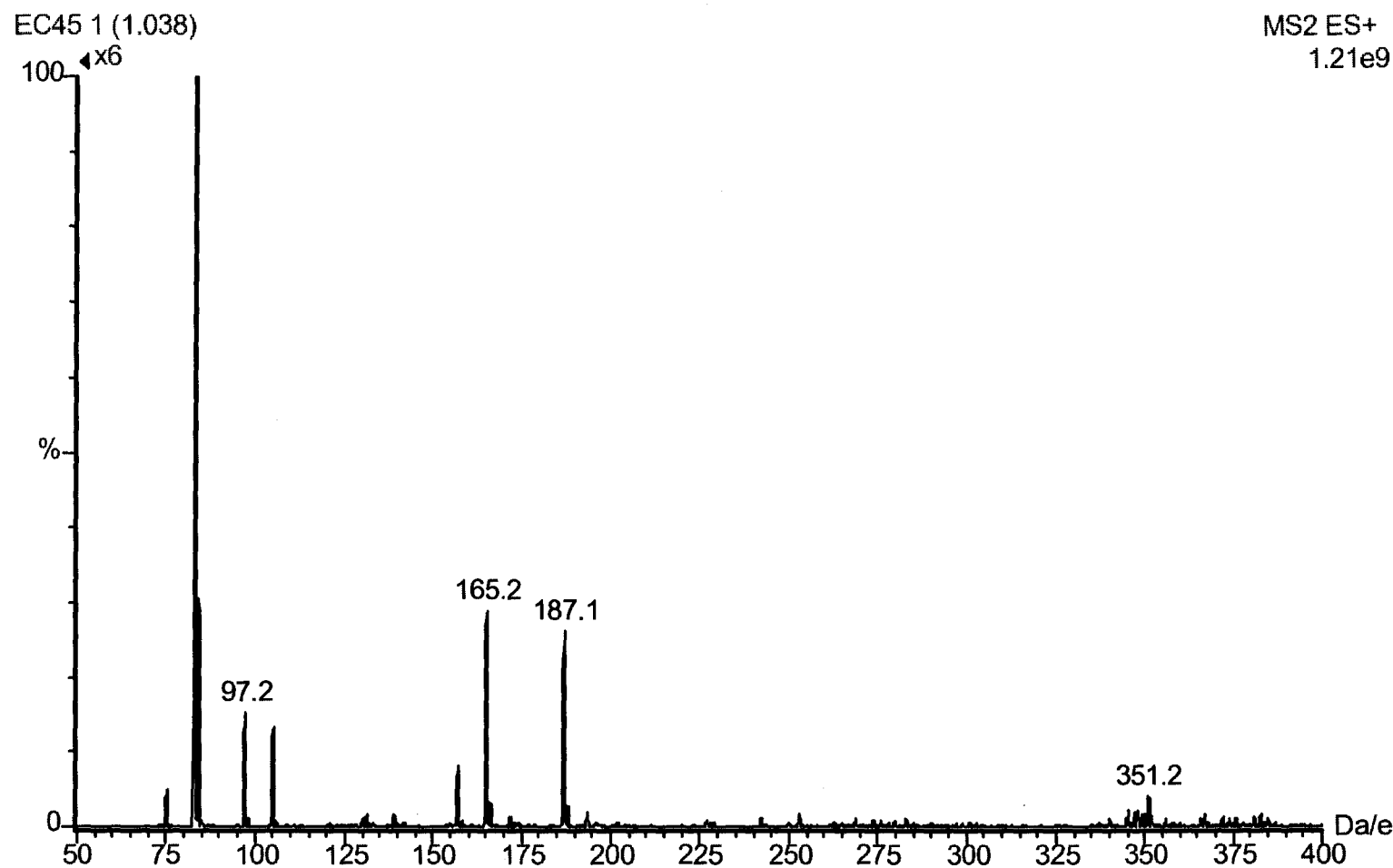


**Figure 2.30.** MS Spectrum of  $\text{Fe}(\text{NO})_2(1\text{-MeIm})_2$ , 7 minutes after exposure to air.

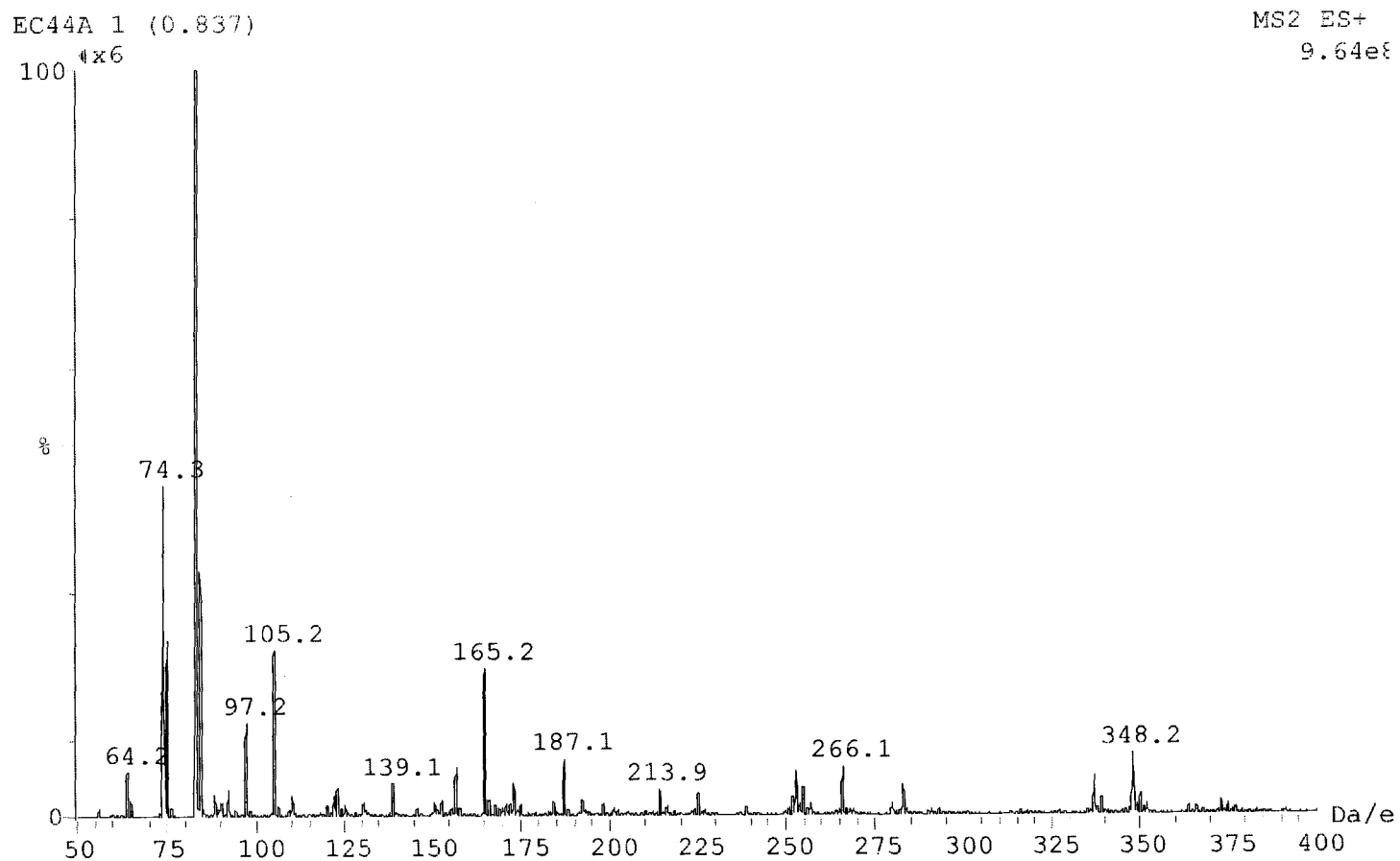


**Figure 2.31.** MS Spectrum of  $\text{Fe}(\text{NO})_2(1\text{-MeIm})_2$ , 10 minutes after exposure to air.

### **3. Experimental**

Tetrahydrofuran (THF) was refluxed over sodium/benzophenone until the mixture became blue/purple. The THF was then distilled and collected under inert nitrogen atmosphere. Diethylether was refluxed over sodium/benzophenone until the mixture became blue. The ether was then distilled and collected under inert nitrogen atmosphere. Dichloromethane and methanol were both refluxed over calcium hydride ( $\text{CaH}_2$ ) for 24hrs. Dichloromethane and MeOH were then distilled and collected under inert nitrogen atmosphere. Pentacarbonyliron(o), imidazole, 1-methylimidazole, 4-methylimidazole, benzimidazole, 5,6-dimethylbenzimidazole and sodium metal were purchased from Sigma-Aldrich Chemicals and used without further purification. Sodium nitrite was purchased from Fischer Scientific and used without further purification.

Dinitrosyldicarbonyliron(o) and subsequent imidazole complexes were air sensitive. Manipulations were carried out either in a glove bag or in a two station dry box (Innovative Technology), both purged with nitrogen dried by passing through a "Lab Clear" gas drying bottle .

#### **3.1 FT-IR Spectroscopy**

IR spectra were recorded on a Bio-Rad FTS-40 spectrometer as KBr pellets or using a  $\text{CaF}_2$  solution cell. Solution IR were performed using 2:1 reaction mixtures of the appropriate imidazole ligand and  $\text{Fe}(\text{NO})_2(\text{CO})_2$ , in THF. The IR spectrum for

$\text{Fe}(\text{NO})_2(\text{CO})_2$  was obtained by dissolving it in ether and using a NaCl solution cell.

### **3.2 Nuclear Magnetic Resonance (NMR)**

All NMR spectra were recorded on either a Bruker AC-200 ( $^1\text{H}$  200MHz,  $^{13}\text{C}$  50MHz) or AC-300 ( $^1\text{H}$  300MHz,  $^{13}\text{C}$  75MHz) spectrometer. Samples were prepared under nitrogen in a glove-bag by performing the reactions in deuterated methanol, in a reaction flask fitted with a young valve and a side arm with an NMR tube attached by a 1/4" Swagelok ultra-torr connector. After CO evolution subsided, the mixture was poured through the side-arm, into the NMR tube, frozen and flame sealed.

$\text{Fe}(\text{NO})_2(\text{CO})_2$  was filtered through glass wool and washed with one ampule of deuterated MeOH. Following this was the imidazole ligand, dissolved in one ampule of d-MeOH.

### **3.3 Electron Paramagnetic Resonance Spectroscopy (EPR)**

All EPR spectra were recorded on a Bruker EMX 8/2.7 spectrometer, operating at a frequency of 9.4 GHz (X-band) with a magnetic field modulation of 100 kHz and equipped with a variable-temperature device. Samples were prepared under nitrogen in a glove bag. A solution of  $\text{Fe}(\text{NO})_2(\text{CO})_2$  dissolved in THF was added through a glass wool filter to a reaction flask fitted with a young valve and a side arm with a quartz micro-EPR tube. A 2 molar equivalent of the appropriate imidazole ligand , dissolved in THF, was then added through a glass wool filter to the reaction flask. Spectra were obtained immediately.

### **3.4 X-ray crystallography**

X-ray crystallographic data for **2** were collected from a single crystal sample, which had been placed on a glass fibre, mounted 6mm above a brass pin, using paraffin oil as the adhesive. The X-ray crystallographic data for **6** were collected from a single crystal sample, which had been mounted on a glass fibre, 6mm above a brass pin, using epoxide glue as the adhesive. Both data sets were collected at -60°C, using a P4 Siemens diffractometer, equipped with a Siemens SMART 1K Charged-Coupled Device (CCD) Area Detector (using the program SMART) and a rotating anode using graphite-monochromated Mo-Kalpha radiation ( $\lambda = 0.71073 \text{ \AA}$ ). The crystal-to-diffractometer distance was 3.9991 cm and the data collection was carried out in 512 X512 pixel mode, utilizing 2 x 2 pixel binning. The initial unit cell parameters were determined by least-squares fit of the angular settings of the strong reflections, collected by a 4.4 degree scan in 15 frames over three different parts of reciprocal space (45 frames total). After one complete hemisphere of data collection, the first frames were recollected in order to improve the decay corrections analysis. Processing was carried out by the use of the program SAINT, which applied Lorentz and polarization corrections to three-dimensionally integrated diffraction spots. The program SADABS was utilized for the scaling of diffraction data, the application of decay correction, and an empirical absorption correction based on redundant reflections.

The structures of **2** and **6** were solved by using the direct methods procedure in the Siemens SHELXTL program library, and refined by full-matrix least squares methods with anisotropic parameters for all atoms, except the methyl hydrogens at the C4 and C8

positions of **2**. The hydrogens of the C4 and C8 atoms of **2** were generated at calculated positions, with thermal parameters based on the carbons to which they are attached.

### **3.5 Mass Spectra**

Pneumatically assisted electrospray (ES) was performed with either DCM or a mixture of 90/10 dichloromethane/methanol as the mobile phase at a flow rate of 10 $\mu$ L/min employing a Brownlee Microgradient syringe pump. Samples were prepared by reacting 10 $\mu$ l ( $8.727 \times 10^{-5}$  mol) Fe(NO)<sub>2</sub>(CO)<sub>2</sub> with  $1.7454 \times 10^{-4}$  mol of imidazole ligand in either 10mL DCM or MeOH and were introduced by loop injection (10 $\mu$ L). Data was acquired in MCA mode. Full scan positive ion ES experiments (MS and MS/MS) were performed with a Micromass Quattro-LC triple quadrupole instrument. The PEEK tubing and fittings were replaced with either stainless steel or teflon. A Rheodyne 7125 HPLC injection valve was connected to the ES probe with ~10cm of teflon tubing to allow sample introduction to take place as close as possible to the exit of the stainless steel ES capillary. Operating parameters were as follows: source temperature 80°C, cone voltage (CV) 5 - 15V (normally 35V or greater) and a capillary voltage of 4 - 4.5 kV (normally 3 - 3.5kV). Argon was used as the collision gas for MS/MS experiments at a gas cell pressure of ~  $2 \times 10^{-3}$  mBar.

### **3.6 Synthesis of Complexes**

#### **Synthesis of Dinitrosylidicarbonyliron(0)**

Dinitrosyldicarbonyliron(0) was synthesized by a modified method of Seel.<sup>62</sup>

Twenty five milliliters of Ironpentacarbonyl (0.20 mol) was dissolved in 400mL of methanol, along with 10g (0.44 mol) sodium metal and 17g (0.25 mol) sodium nitrite. The solution was refluxed until the distillate no longer showed a yellow colour. The methanol was distilled off at 70°C to leave a dry yellow product, Na[Fe(NO)(CO)<sub>3</sub>]. 400mL of distilled H<sub>2</sub>O was added and 17g (0.25 mol) of sodium nitrite. The solution was purged with a slow flow of CO<sub>2</sub> and the yellow/orange gas evolved was collected in a series of 3 U-tubes as a brick red solid, at -78°C in a dry ice/acetone bath. The yield was 20g (60%). MW = 171.88g/mol;  $d = 1.56 \text{ g/cm}^3$ ; m.p. = 21.6 °C; IR (in ether):  $\nu(\text{NO})$ : 1810 cm<sup>-1</sup>, 1767 cm<sup>-1</sup>;  $\nu(\text{CO})$  : 2087 cm<sup>-1</sup>, 2038 cm<sup>-1</sup>.

### Synthesis of Diimidazole dinitrosyliron(0) (1)

Fe(NO)<sub>2</sub>(CO)<sub>2</sub> (0.1mL,  $8.727 \times 10^{-3}$  mol) was added to a solution of 0.10g (0.01745 mol) of imidazole dissolved in 1mL of ether. Gas evolved, and within two minutes the solution turned from a red to a green colour. The solvent was removed by reduced pressure. The solid was washed three times with ether and decanted each time. After the final wash, the solid was dried under reduced pressure at room temperature. Yield 68 %; MW 250g/mol ; M+ 250 m/z, 222 (M+ -NO), 191 (M+ - 2NO), 184 (M+ - Im), 154 (M+ -NO, Im); IR: $\nu_{(\text{NO})}$  1680, 1622 cm<sup>-1</sup>; EPR: g 2.0344,  $a_{n1}$  3.3,  $a_{n2}$  2.4, 2 X  $a_{n3}$  2.1 G.

### Synthesis of Di(1-methylimidazole)dinitrosyliron(0) (2)

$\text{Fe}(\text{NO})_2(\text{CO})_2$  (0.1mL,  $8.727 \times 10^{-3}$  mol) was added to a solution of 0.120mL (0.01745 mol) of 1-methylimidazole dissolved in 1mL of ether. Gas evolved, and within two minutes the solution turned from a red to a green colour. The solvent was removed by reduced pressure. The solid was washed three times with ether and decanted each time. After the final wash, the solid was dried at reduced pressure and at room temperature. Yield 87 %; MW 280 g/mol ; M+ 280 m/z, 250 (M+ - NO), 220 (M+ - 2NO), 168 (M+ - NO, 1-MeIm) ; IR  $\nu_{(\text{NO})}$  1673, 1616  $\text{cm}^{-1}$ ; EPR g 2.0275, 2 X  $a_{n1}$  2.9, 2 X  $a_{n2}$  2.6 G.

### Synthesis of Di(4-methylimidazole)dinitrosyliron(0) (3)

$\text{Fe}(\text{NO})_2(\text{CO})_2$  (0.1mL,  $8.727 \times 10^{-3}$  mol) was added to a solution of 0.120g (0.01745 mol) of 4-methylimidazole dissolved in 1ml of ether. Gas evolved, and within two minutes the solution turned from a red to a green colour. The solvent was removed by reduced pressure. The solid was washed three times with ether and decanted each time. After the final wash, the solid was dried under reduced pressure at room temperature. Yield 62 %; MW 280 g/mol; M+ 280 m/z, 250 (M+ - NO), 220 (M+ - 2NO), 168 (M+ - NO, 1-MeIm), M+ 477 m/z, 477 (M+), 447 (M+ - NO), 417 (M+ - 2NO), 395 (M+ - 4-MeIm), 365 (M+ - NO, 4-MeIm), 335 (M+ - 2NO, 4-MeIm); IR  $\nu_{(\text{NO})}$  1677, 1620  $\text{cm}^{-1}$ ; EPR g 2.0336,  $a_{n1}$  3.1,  $a_{n2}$  2.5, 2 X  $a_{n3}$  2.2 G.

### **Synthesis of Di(benzimidazole)dinitrosyliron(0) (4)**

Fe(NO)<sub>2</sub>(CO)<sub>2</sub> (0.1mL, 8.727 x 10<sup>-3</sup> mol) was added to a solution of 0.173g ( 0.01745 mol) of benzimidazole dissolved in 1mL of THF. Gas evolved, and within two minutes the solution turned from a red to a green colour. The solvent was removed by reduced pressure. The solid was washed three times with ether and decanted each time. After the final wash, the solid was dried under reduced pressure at room temperature. Yield 68%; MW 352 g/mol ; M+ 352 m/z, 322 (M+ - NO), 292 (M+ - 2NO), 234 (M+ - benzim), 204 (M+ - NO, benzim), 585 m/z (M+), 555 (M+ - NO), 525 (M+ - 2NO), 477 (M+ - benzim), 437 (M+ - NO, benzim); IR  $\nu_{(NO)}$  1682, 1625 cm<sup>-1</sup>; EPR g 2.0341,  $a_{n1}$  3.8,  $a_{n2}$  2.4, 2 X  $a_{n3}$  1.9.

### **Synthesis of Di(5,6-dimethylbenzimidazole)dinitrosyliron(0) (5)**

Fe(NO)<sub>2</sub>(CO)<sub>2</sub> (0.1mL, 8.727 x 10<sup>-3</sup> mol) was added to a solution of 0.213g ( 0.01745 mol) of 5,6-dimethylbenzimidazole dissolved in 1mL of THF. Gas evolved, and within two minutes the solution turned from a red to a green colour. The solvent was removed by reduced pressure. The solid was washed three times with ether and decanted each time. After the final wash, the solid was dried under reduced pressure at room temperature. Yield: 81 % ; MW: 408 g/mol; M+ 408 m/z, 378 (M+ - NO), 348 (M+ - 2NO), 262 \*, 232 (M+ - 5,6dimethylbenz), 202 (M+ - NO, -5,6dimethylbenz); IR: $\nu_{(NO)}$  1683, 1625 cm<sup>-1</sup>; EPR g 2.0344,  $a_{n1}$  3.9, 2 X  $a_{n2}$  2.2.

**Synthesis of dinitrosylcarbonyltriphenylphosphineiron(0)**

$\text{Fe}(\text{NO})_2(\text{CO})_2$  (0.45mL,  $4.11 \times 10^{-3}$  mol) was added *via* a syringe to a stirred solution of triphenylphosphine (1.11g,  $4.23 \times 10^{-3}$  mol) in diethylether (10 mL), in an Erlenmyer flask fitted with a rubber septum . The flask received a positive pressure of nitrogen via a syringe. The dark red solution was stirred overnight at room temperature. The solvent was removed under reduced pressure and the dried red solid was washed with methanol.

**Synthesis of Dinitrosyl-bis(triphenylphosphine)iron(0). (6)**

0.02 ml (  $1.23 \times 10^{-4}$  mol) of 1-methylimidazole was added to a solution of 0.01g ( $1.23 \times 10^{-4}$  mol)  $\text{Fe}(\text{NO})_2(\text{CO})(\text{PPh}_3)$  dissolved in 5 ml of diethylether in a glass test tube. The red solution was stoppered and turned dark red/green after one day, during which, large cubic crystals formed. A dark red crystal was obtained which provided the X-ray crystal structure of **6**. Yield, IR and EPR were not performed.

## FUTURE WORK and CONCLUSIONS

First, and foremost, research into the methods of purification of these compounds should be undertaken. State of the art vacuum line techniques, similar to that presented by Burford,<sup>63</sup> would provide an excellent vehicle for advancement of this field. Electrochemical studies should be performed to further support the mechanistic pathway presented. Formation of an  $\text{Im}^-$  species would provide almost conclusive results that the process does occur by a catalytic 17-electron electron transfer chain mechanism (ETC). Also, the nature of the colour change from green to brown may be by an electronic means and electrochemistry may help support this idea. It is believed that either a one electron oxidation to the 17 electron complex, or one electron reduction to the 18 electron complex is the driving force for the colour change by some species in solution. Constant voltage experiments on bulk solutions may provide the means for a colour change of the solution. MS/MS experiments must be performed on the m/z peaks of **2**. The repeat unit of 147 mass units observed for these peaks is an iron containing compound, but is 36 mass units less than the repeat unit observed for **1**, which should be the smallest repeat unit for the series.

The syntheses of the  $\text{Fe}(\text{NO})_2(\text{L})_2$  [ L = imidazole **1**, 1-methylimidazole (1-MeIm) **2**, 4-methylimidazole (4-MeIm) **3**, benzimidazole (benzim) **4**, and 5,6-dimethylbenzimidazole (56benzim) **5** ] series of compounds open the door to further research of biologically relevant iron nitrosyl chemistry. One future goal, is to mimic NO

transport. Elegant studies performed by Doyle<sup>64,65</sup> and Kadish<sup>66,67</sup> have shown that the NO ligand may be removed from an iron or cobalt center of porphyrin complexes by oxidizing the metal center. The higher the oxidation state, the weaker the metal nitrosyl bond and the more readily NO is released. It may be a process similar to this that allows metal mediated transfer in the human body. The  $d^{10}$  iron nitrosyl compounds have very strong M-N bonds and will not easily relinquish NO. Oxidation of compounds **1 - 5** would only provoke further instability and so it is not likely that these complexes would be a good illustration of species that release NO. Complexes **1 - 5** may then be more representative of an iron molecule *after* receiving NO. The goal then is to create a molecule which would accept NO to create the final products **1 - 5**. The use of a series of iron carbonyl imidazole complexes of the form  $\text{Fe}(\text{CO})_3(\text{L})_2$  seem a likely choice as receptors of NO gas bubbled through solution. Substitution of three CO ligands by two NO ligands would create the 18 electron complexes of **1 - 5**.

The chemical sensitivity of the  $\text{Fe}(\text{NO})_2(\text{L})_2$  series of compounds has precluded purification and isolation of these products. However, studies of reaction mixtures have elucidated the 17-electron ETC mechanistic pathway by which they are formed. Supporting evidence of the pathway is provided by IR, EPR and Mass spectroscopic studies. X-ray crystallography of **2** has shown that the four coordinate complexes are of a *pseudo*-tetrahedral geometry.

## **APPENDIX A**

Table 1. Observed and calculated structure factors for 2

$h$	$k$	$l$	10Fo	10Fc	10s	$h$	$k$	1	10Fo	10Fc	10s	$h$	$k$	1	10Fo	10Fc	10s	$h$	$k$	1	10Fo	10Fc	10s	
2	0	0	1274	1240	19	10	10	0	43	59	43	14	4	1	57	21	56	8	10	1	295	300	9	
4	0	0	2418	2331	37	12	10	0	12	79	11	16	4	1	64	85	52	10	10	1	257	257	13	
6	0	0	1512	1397	24	1	11	0	0	10	1	-15	5	1	263	258	7	12	10	1	150	143	15	
8	0	0	78	38	31	3	11	0	33	27	32	-13	5	1	175	173	12	-11	11	1	64	47	53	
10	0	0	1052	1054	22	5	11	0	580	576	7	-11	5	1	52	77	38	-9	11	1	74	70	42	
12	0	0	784	817	10	7	11	0	444	455	10	-9	5	1	666	665	6	-7	11	1	142	133	28	
14	0	0	0	62	1	9	11	0	45	70	44	-7	5	1	579	584	5	-5	11	1	183	183	11	
16	0	0	31	48	30	11	11	0	112	99	31	-5	5	1	727	729	6	-3	11	1	143	157	15	
1	1	0	365	368	3	0	12	0	88	129	37	-3	5	1	554	585	6	-1	11	1	173	184	12	
3	1	0	1907	1939	17	2	12	0	93	76	26	-1	5	1	333	359	7	1	11	1	116	68	17	
5	1	0	747	742	6	4	12	0	0	5	1	1	5	1	253	244	6	3	11	1	260	260	11	
7	1	0	291	322	5	6	12	0	35	78	34	3	5	1	1172	1247	14	5	11	1	85	17	43	
9	1	0	200	184	11	8	12	0	55	61	54	5	5	1	849	866	7	7	11	1	0	34	1	
11	1	0	62	29	43	1	13	0	0	40	1	7	5	1	921	941	7	9	11	1	0	4	1	
13	1	0	133	167	14	3	13	0	263	275	11	5	1	98	45	16	11	11	1	0	5	1	11	
15	1	0	93	65	51	5	13	0	242	222	10	11	5	1	260	253	7	-8	12	1	0	66	1	
17	1	0	80	41	29	7	13	0	197	187	12	13	5	1	390	401	6	-8	12	1	174	165	13	
0	2	0	892	862	22	0	14	0	0	27	1	15	5	1	197	197	9	-9	12	1	189	193	15	
2	2	0	2746	2703	18	2	14	0	0	47	1	-14	6	1	217	218	9	-12	12	1	282	288	8	
4	2	0	1220	1217	9	4	14	0	34	37	34	-12	6	1	141	139	12	0	12	1	168	129	19	
6	2	0	577	570	5	-17	1	1	264	263	10	-10	6	1	473	463	6	2	12	1	333	335	8	
8	2	0	1776	1770	14	15	1	1	268	258	9	-8	6	1	250	257	9	4	12	1	81	84	27	
10	2	0	977	964	8	-13	1	1	118	111	18	-6	6	1	74	46	27	6	12	1	34	105	33	
12	2	0	81	53	25	-11	1	1	106	125	17	-4	6	1	877	859	7	8	12	1	259	262	10	
14	2	0	156	153	13	-9	1	1	194	205	9	-2	6	1	639	622	12	-7	13	1	0	34	1	
16	2	0	29	46	85	-7	1	1	609	674	6	0	5	1	394	426	8	-13	13	1	0	32	1	
1	3	0	1356	1299	10	-5	1	1	2354	2295	18	2	6	1	684	738	7	-3	13	1	77	101	34	
3	3	0	933	888	6	-3	1	1	1628	1632	12	4	6	1	246	217	12	-1	13	1	62	61	61	
5	3	0	241	215	9	-1	1	87	76	4	6	6	1	198	214	9	1	13	1	80	46	29		
7	3	0	381	380	6	1	1	1	1447	1448	10	8	6	1	485	499	5	3	13	1	0	30	1	
9	3	0	393	399	6	3	1	1	1799	1861	13	10	6	1	80	99	26	5	13	1	118	77	25	
11	3	0	184	181	11	5	1	1	1619	1613	11	12	6	1	331	321	7	7	13	1	85	19	36	
13	3	0	85	64	85	7	1	1	560	564	5	14	6	1	97	111	17	-14	14	1	90	135	26	
15	3	0	250	250	10	9	1	1	192	179	7	-15	7	1	110	109	19	-2	14	1	198	203	15	
17	3	0	63	31	57	11	1	1	177	148	12	-13	7	1	301	319	7	0	14	1	203	198	12	
0	4	0	1839	1760	20	13	1	1	359	348	7	-11	7	1	0	31	31	1	2	14	1	108	84	22
2	4	0	1402	1371	16	15	1	1	455	443	8	-9	7	1	330	333	8	4	14	1	56	40	56	
4	4	0	253	262	6	17	1	1	230	226	11	-7	7	1	584	568	7	-16	0	2	105	135	32	
6	4	0	397	389	5	-16	2	1	77	48	38	-5	7	1	154	185	15	-14	0	2	226	199	31	
8	4	0	538	537	6	-14	2	1	113	100	22	-3	7	1	753	734	7	-12	0	2	329	324	10	
10	4	0	620	615	6	-12	2	1	384	408	10	-1	7	1	226	209	9	-10	0	2	500	479	9	
12	4	0	645	646	7	-10	2	1	614	627	6	1	7	1	764	745	8	-8	0	2	786	780	11	
14	4	0	140	128	15	-8	2	1	502	501	5	3	7	1	467	462	8	-6	0	2	547	516	11	
16	4	0	166	191	14	-6	2	1	654	643	6	5	7	1	543	525	8	-4	0	2	774	804	9	
1	5	0	546	515	5	-4	2	1	304	278	5	7	7	1	430	422	8	-2	0	2	3067	3055	27	
3	5	0	321	290	6	-2	2	1	478	471	6	9	7	1	281	293	8	2	0	2	226	226	7	
5	5	0	529	527	6	0	2	1	1004	1007	8	11	7	1	431	437	6	4	0	2	1176	1123	24	
7	5	0	381	374	6	2	2	1	36	31	36	13	7	1	220	231	9	6	0	2	184	183	10	
9	5	0	211	207	8	4	2	1	304	294	4	15	7	1	97	83	37	8	0	2	1372	1369	15	
11	5	0	214	208	9	6	2	1	273	246	6	-14	8	1	181	174	14	10	0	2	1511	1542	17	
13	5	0	0	22	1	8	2	1	398	404	6	-12	8	1	222	207	11	12	0	2	422	414	10	
15	5	0	231	220	9	10	2	1	637	626	6	-10	8	1	191	186	15	14	0	2	170	186	18	
0	6	0	388	326	7	12	2	1	109	99	18	-8	8	1	374	393	7	16	0	2	215	203	17	
2	6	0	706	698	9	14	2	1	141	143	21	-6	9	1	25	3	25	-17	1	2	49	38	49	
4	6	0	993	987	8	16	2	1	48	42	47	-4	8	1	369	377	7	-15	1	2	95	108	22	
6	6	0	0	23	1	-17	3	1	177	175	19	-2	8	1	966	989	15	-13	1	2	197	185	13	
8	6	0	710	728	6	-15	3	1	314	314	9	0	8	1	672	639	7	-11	1	2	210	206	10	
10	6	0	384	387	6	-13	3	1	209	213	10	2	8	1	194	189	9	-9	1	2	625	616	11	
12	6	0	247	240	8	-11	3	1	43	42	43	4	4	8	1	209	212	10	-7	1	2	103	31	16
14	6	0	119	121	15	-9	3	1	381	388	6	6	8	1	197	200	10	-7	1	2	800	792	6	
1	7	0	184	178	18	-7	3	1	1190	1199	12	-11	9	1	93	87	24	7	1	2	371	358	5	
3	7	0	512	511	7	-5	3	1	1017	1024	8	8	8	1	9	88	52	25	9	1	2	307	288	6
5	7	0	329	324	7	-3	3	1	834	831	6	12	8	1	2	286	290	10	-13	7	2	115	114	7
7	7	0	432	414	10	-1	3	1	255	236	6	14	8	1	1	121	143	18	3	1	2	403	388	3
9	7	0	116	109	18	-13	3	1	128	138	16	-13	9	1	78	8	34	5	1	2	950	949	8	
11	7	0	108	102	24	3	3	1	130	136	11	-11	9	1	93	87	24	5	1	2	392	353	4	
13	7	0	0	24	1	5	3	1	1987	1951	12	-9	9	1	2	371	358	5	-15	7	2	121	128	16
15	7	0	155	133	25	-7	3	1	852	859	6	-7	9</											

-9	9	2	375	361	7	10	2	3	46	14	46	-6	8	3	379	365	8	-13	1	4	88	83	22	0	6	4	784	785	7	
-7	9	2	381	367	7	12	2	3	39	13	39	-4	8	3	524	521	9	-11	1	4	304	300	8	2	6	4	354	364	5	
-5	9	2	525	530	7	14	2	3	62	80	61	-2	8	3	759	771	7	-9	1	4	153	163	12	4	6	4	437	432	5	
-3	9	2	260	246	9	16	2	3	0	37	1	0	8	3	551	580	6	-7	1	4	63	74	25	6	6	4	643	661	5	
-1	9	2	432	415	7	-15	3	3	185	130	13	2	8	3	354	341	9	-5	1	4	386	378	4	8	6	4	471	478	7	
1	9	2	650	659	8	-13	3	3	153	137	27	4	8	3	187	195	10	-3	1	4	1662	1655	11	10	6	4	230	225	8	
3	9	2	338	334	14	-11	3	3	355	343	7	6	8	3	259	249	8	-1	1	4	2455	2500	12	12	6	4	0	58	1	
5	9	2	208	204	13	-9	3	3	600	616	7	8	8	3	352	351	7	1	1	4	412	418	3	14	6	4	87	63	21	
7	9	2	337	339	7	-7	3	3	863	891	7	10	8	3	432	442	7	3	1	4	293	298	4	-15	7	4	0	65	1	
9	9	2	76	62	29	-5	3	3	621	616	5	12	8	3	79	68	33	5	1	4	465	416	5	-13	7	4	7	7	7	
11	9	2	232	221	10	-3	3	3	41	12	40	14	8	3	102	89	24	7	1	4	568	542	5	-11	7	4	167	164	12	
13	9	2	192	187	15	-1	3	3	265	263	4	-13	9	3	58	52	57	9	1	4	150	156	8	-9	7	4	630	625	7	
-12	10	2	75	49	75	1	3	3	1080	1092	7	-11	9	3	76	43	41	11	1	4	396	393	6	-7	7	4	658	657	7	
-10	10	2	88	92	29	3	3	3	1452	1400	10	-9	3	198	183	11	13	1	4	122	121	15	-5	7	4	174	171	21		
-8	10	2	230	239	13	5	3	3	1330	1320	9	-7	9	3	375	358	8	15	1	4	0	32	1	-3	7	4	501	472	6	
-6	10	2	96	83	23	7	3	3	104	64	12	-5	9	3	84	70	23	-16	2	4	264	263	15	-1	7	4	312	314	5	
-4	10	2	409	410	7	9	3	3	297	285	5	-3	9	3	166	155	12	-14	2	4	304	282	9	1	7	4	658	664	6	
-2	10	2	415	403	7	11	3	3	357	356	11	-1	9	3	163	140	16	-12	2	4	402	399	7	3	7	4	786	805	10	
0	10	2	59	84	59	13	3	3	426	422	7	1	9	3	189	183	10	-10	2	4	205	201	8	5	7	4	481	484	6	
2	10	2	171	172	14	15	3	3	266	267	9	3	9	3	394	394	8	-8	2	4	485	483	6	7	7	4	362	364	10	
4	10	2	0	31	1	-16	4	3	112	109	38	5	9	3	118	87	16	-6	2	4	929	994	7	9	7	4	215	225	13	
6	10	2	92	92	24	-14	4	3	141	136	15	7	9	3	223	209	15	-4	2	4	1010	1023	7	11	7	4	219	233	9	
8	10	2	83	57	32	-12	4	3	137	148	15	9	9	3	68	68	67	-2	2	4	493	482	6	13	7	4	207	215	10	
10	10	2	36	84	35	-10	4	3	103	137	29	11	9	3	194	199	11	0	2	4	1389	1388	9	-14	8	4	175	176	12	
12	10	2	60	60	27	-8	4	3	300	313	7	13	9	3	214	214	11	2	2	4	544	542	4	-12	8	4	217	224	11	
-11	11	2	150	128	16	-6	4	3	340	355	5	-12	10	3	247	235	15	4	2	4	522	556	3	-10	8	4	72	19	42	
-9	11	2	280	274	9	-4	4	3	345	382	4	-10	10	3	153	140	15	6	2	4	1096	1079	8	-8	8	4	44	28	43	
-7	11	2	398	403	9	-2	4	3	778	773	6	-8	10	3	45	53	45	8	2	4	651	662	5	-6	8	4	116	112	22	
-5	11	2	78	89	26	0	4	3	1066	1082	8	-6	10	3	353	351	7	10	2	4	501	504	6	-4	8	4	465	468	8	
-3	11	2	119	93	16	2	4	3	455	451	4	-4	10	3	435	443	7	12	2	4	343	333	7	-2	8	4	704	719	7	
-11	11	2	106	104	21	4	4	3	564	595	5	-2	10	3	658	686	7	14	2	4	231	243	15	0	8	4	93	71	18	
1	11	2	227	214	10	6	4	3	886	913	6	0	10	3	123	94	15	16	2	4	274	276	9	2	8	4	78	103	26	
3	11	2	552	572	7	8	4	3	97	56	12	2	10	3	53	55	52	-15	3	4	35	9	34	4	8	4	189	185	10	
5	11	2	483	469	9	10	4	3	276	265	6	4	10	3	200	203	10	-13	3	4	136	134	14	6	8	4	245	234	8	
7	11	2	78	21	29	12	4	3	186	189	12	6	10	3	336	317	8	-11	3	4	233	227	11	8	8	4	548	554	7	
9	11	2	0	29	1	14	4	3	46	43	46	8	10	3	365	377	7	-9	3	4	439	408	6	10	8	4	93	94	21	
11	11	2	113	127	20	16	4	3	99	104	23	10	10	3	182	175	17	-7	3	4	278	256	7	12	8	4	104	111	36	
-8	12	2	79	53	38	-15	5	3	107	109	20	12	10	3	0	20	21	-5	3	4	451	480	5	14	8	4	0	104	1	
-6	12	2	93	38	24	-13	5	3	172	158	13	-11	11	3	70	57	57	-3	3	4	489	482	4	-13	9	4	84	90	84	
-4	12	2	95	42	22	-11	5	3	123	128	14	-9	11	3	56	93	56	-1	3	4	535	535	4	-11	9	4	301	294	13	
-2	12	2	0	12	1	-9	5	3	508	501	6	-7	11	3	140	116	20	1	3	4	1623	1595	10	-9	9	4	256	257	9	
0	12	2	80	78	38	-7	5	3	371	387	6	-5	11	3	169	152	14	3	3	4	687	670	5	-7	9	4	442	443	8	
2	12	2	104	43	41	-5	5	3	715	719	7	-3	11	3	152	146	14	5	3	4	399	227	4	-5	9	4	361	342	7	
4	12	2	80	101	27	-3	5	3	154	139	7	-1	11	3	107	96	18	7	3	4	246	235	4	-3	9	4	228	222	9	
6	12	2	49	63	48	-1	5	3	154	119	6	1	11	3	144	143	15	9	3	4	517	545	5	-1	9	4	648	648	8	
-7	13	2	235	226	13	9	3	3	1638	1642	14	5	11	3	113	98	17	13	3	4	304	0	1	7	3	9	4	393	391	7
-5	13	2	210	219	12	5	5	3	130	181	11	0	12	3	344	344	8	-6	4	376	383	4	-10	10	4	170	193	13		
-2	14	2	15	20	14	-12	6	3	31	43	31	2	12	3	80	57	27	-4	4	4	886	881	6	-8	10	4	38	12	38	
0	14	2	0	36	1	-10	6	3	503	512	6	4	12	3	251	248	9	-2	4	1252	1236	9	-6	10	4	314	319	16		
-2	14	2	0	10	1	-8	6	3	130	134	13	6	12	3	344	330	8	0	4	4	732	733	5	-10	4	486	485	11		
-17	1	3	176	159	14	-6	3	3	399	374	6	8	12	3	130	152	19	2	4	4	310	322	4	-2	10	4	100	25	27	
-15	1	3	211	198	14	-4	6	3	1085	1125	9	-7	13	3	14	34	13	4	4	4	587	576	5	0	10	4	117	111	17	
-13	1	3	103	104	21	-2	6	3	397	415	5	-5	13	3	0	9	1	6	4	4	635	652	4	2	10	4	195	214	11	
-11	1	3	633	634	7	0	6	3	376	359	5	-6	0	4	1353	1393	15	3	5	4	579	606	5	-8	12	4	82	2	31	
-16	2	3	96	72	57	-1	7	3	318	279	12	-4	0	4	1030	1013	12	5	5	4	96	110	13	-6	12	4	0	15	1	
-14	2	3	140	127	15	1	7	3	599	592	7	-2	0	4	1382	1441	9	7	5	4	60	35	59	-4	12	4	157	153		

7	1	5	94	26	13	-9	7	5	348	350	7	10	0	6	0	64	1	-8	6	6	358	356	6	-11	1	7	425	412	8
9	1	5	886	890	6	-7	7	5	129	97	15	12	0	6	87	104	86	-6	6	6	364	367	7	-9	1	7	674	674	12
11	1	5	700	702	7	-5	7	5	22	7	22	14	0	6	285	266	11	-4	6	6	631	628	6	-7	1	7	347	339	5
13	1	5	292	297	8	-3	7	5	313	316	5	16	0	6	228	254	26	-2	6	6	380	375	5	-5	1	7	410	402	4
15	1	5	101	100	20	-1	7	5	100	94	15	-15	1	6	71	50	42	0	6	6	192	187	8	-3	1	7	1159	1144	6
-16	2	5	119	62	21	1	7	5	123	115	15	-13	1	6	108	124	29	2	6	6	220	223	6	-1	1	7	733	831	3
-14	2	5	111	127	18	3	7	5	744	747	6	-11	1	6	142	161	13	4	6	6	487	485	4	1	1	7	1093	1112	8
-12	2	5	79	72	24	5	7	5	246	242	6	-9	1	6	129	127	18	6	6	6	490	489	5	3	1	7	850	796	12
-10	2	5	108	128	17	7	7	5	88	83	20	-7	1	6	103	49	14	8	6	6	439	440	7	5	1	7	157	116	6
-8	2	5	196	149	10	9	7	5	327	349	7	-5	1	6	328	303	4	10	6	6	0	37	1	7	1	7	692	696	5
-6	2	5	296	303	5	11	7	5	65	58	34	-3	1	6	86	92	8	12	6	6	103	127	17	9	1	7	840	811	6
-4	2	5	146	125	13	13	7	5	219	187	17	-1	1	6	448	459	2	14	6	6	126	142	15	11	1	7	543	534	5
-2	2	5	207	226	4	-14	8	5	247	246	5	1	1	6	100	111	5	-13	7	6	151	85	14	13	1	7	241	233	8
0	2	5	153	117	5	-12	8	5	135	135	16	3	1	6	238	238	5	-11	7	6	222	232	9	15	1	7	24	54	24
2	2	5	730	745	5	-10	8	5	0	58	1	5	1	6	154	137	7	-9	7	6	438	441	7	-16	2	7	107	94	22
4	2	5	388	379	4	-8	8	5	186	191	11	7	1	6	205	198	7	-7	7	6	221	206	11	-14	2	7	155	158	15
6	2	5	451	414	4	-6	8	5	89	116	31	9	1	6	246	221	6	-5	7	6	109	78	17	-12	2	7	141	139	14
8	2	5	61	76	26	-4	8	5	829	850	7	11	1	6	50	19	49	-3	7	6	265	265	6	-10	2	7	244	249	8
10	2	5	103	77	13	-2	8	5	701	680	7	13	1	6	0	37	1	7	6	506	512	5	-8	2	7	105	97	18	
12	2	5	187	176	10	0	8	5	193	178	10	15	1	6	74	87	27	1	7	6	789	776	7	-6	2	7	65	59	16
14	2	5	47	4	47	2	8	5	442	446	6	-16	2	6	289	291	9	3	7	6	526	512	5	-4	2	7	576	578	5
16	2	5	107	103	19	4	8	5	110	124	20	-14	2	6	413	397	7	5	7	6	79	87	16	-2	2	7	54	17	16
-15	3	5	24	49	24	6	8	5	321	324	7	-12	2	6	6	57	5	7	7	6	249	245	7	0	2	7	422	382	5
-13	3	5	154	143	19	8	8	5	631	638	6	-10	2	6	220	225	9	9	7	6	325	329	9	2	2	7	629	650	5
-11	3	5	434	429	7	10	8	5	97	86	20	-8	2	6	709	720	7	11	7	6	342	348	9	4	2	7	23	17	23
-9	3	5	996	1010	8	12	8	5	160	169	14	-6	2	6	933	949	6	13	7	6	169	149	19	6	2	7	98	104	9
-7	3	5	550	555	6	-13	9	5	109	127	21	-4	2	6	1001	1032	7	-12	8	6	64	72	43	8	2	7	84	87	15
-5	3	5	210	178	6	-11	9	5	122	143	27	-2	2	6	320	313	3	-10	8	6	0	49	1	10	2	7	83	103	17
-3	3	5	641	597	4	-9	9	5	92	13	30	0	2	6	198	179	4	-8	8	6	191	154	11	12	2	7	84	87	25
-1	3	5	605	649	4	-7	9	5	99	107	20	2	2	6	615	619	4	-6	8	6	281	272	9	14	2	7	68	41	32
1	3	5	1461	1494	8	-5	9	5	34	26	33	4	2	6	1074	1071	7	-4	8	6	275	275	8	-15	3	7	134	117	16
3	3	5	1331	1341	8	-3	9	5	72	58	52	6	2	6	791	794	5	-2	8	6	253	249	9	-13	3	7	313	321	8
5	3	5	106	119	7	-1	9	5	372	368	7	8	2	6	408	425	5	0	8	6	37	19	36	-11	3	7	556	564	7
7	3	5	470	460	4	1	9	5	0	49	1	10	2	6	21	6	21	2	8	6	191	202	9	-9	3	7	406	406	7
9	3	5	412	415	5	3	9	5	83	87	23	12	2	6	68	41	22	4	8	6	284	281	10	-7	3	7	53	60	28
11	3	5	487	482	6	5	9	5	143	123	12	14	2	6	235	238	9	6	8	6	287	298	7	-5	3	7	217	242	6
13	3	5	357	365	7	7	9	5	115	116	16	16	2	6	214	225	10	8	8	6	239	238	12	-3	3	7	251	277	5
15	3	5	148	150	15	9	9	5	32	70	31	-15	3	6	80	27	59	10	8	6	0	2	1	-1	3	7	1487	1440	10
-16	4	5	188	179	13	11	9	5	214	196	10	-13	3	6	84	92	24	12	8	6	92	70	27	1	3	7	1352	1329	7
-14	4	5	170	164	13	-10	10	5	62	72	49	-11	3	6	77	28	28	-11	9	6	188	189	14	3	3	7	205	214	6
-12	4	5	148	156	16	-8	10	5	152	164	14	-9	3	6	364	357	6	-9	6	2	216	213	10	5	3	7	653	640	5
-10	4	5	29	3	29	-6	10	5	486	482	8	-7	3	6	0	63	1	-7	9	6	334	335	8	7	3	7	261	248	5
-8	4	5	0	11	1	-4	10	5	329	329	7	-5	3	6	213	203	7	-5	9	6	80	47	25	9	3	7	393	380	4
-6	4	5	142	156	8	-2	10	5	503	508	8	-3	3	6	133	133	7	-3	9	6	416	421	8	11	3	7	566	561	4
-4	4	5	662	633	5	0	10	5	80	59	27	-1	3	6	533	565	6	-1	9	6	622	619	7	13	3	7	242	236	7
-2	4	5	236	237	5	2	10	5	72	80	26	1	3	6	440	442	3	1	9	6	439	420	7	15	3	7	0	16	1
0	4	5	62	70	21	4	10	5	555	567	6	-16	4	6	255	246	11	-6	10	6	209	193	10	0	4	7	669	601	8
2	4	5	202	199	5	-11	1	5	148	164	19	-12	4	6	152	124	2	-4	10	6	119	101	18	2	4	7	99	90	9
-15	5	5	84	114	27	1	11	5	180	176	14	-12	4	6	289	301	9	-1	10	6	37	33	36	4	4	7	342	331	4
-13	5	5	258	259	9	3	11	5	69	27	37	-10	4	6	264	248	8	0	10	6	116	113	25	6	4	7	331	329	4
-11	5	5	351	335	6	5	11	5	0	88	1	-8	4	6	493	493	6	2	10	6	105	105	16	8	4	7	134	119	16
-9	5	5	189	176	9	7	11	5	34	37	33	-6	4	6	896	904	6	4	10	6	199	201	10	10	4	7	205	214	7
-7	5	5	632	611	5	9	11	5	64	52	42	-4	4	6	512	518	4	6	10	6	0	63	1	12	4	7	105	108	13
-5	5	5	203	166	8	-8	12	7	0	23	1	1	5	8	536	520	4	-15	9	239	225	3	-2	8	9	0	36	1	
-3	5	7	841	828	6	2	12	7	254	261	10	3	5	8	137	148	9	-13	1	9	354	367	7	9	7	9	243	263	21
-1	5	7	635	657	5	4	12	7	310	332	12	5	5	8	145	150	11	-11	1	9	274	268	8	-12	8	9	77	67	32
1	5	7	344	365	4	6	12	7	2																				

11	7	7	92	104	21	-14	2	8	243	240	10	-8	8	8	178	197	12	5	3	9	308	309	4	-1	11	9	175	182	12	
13	7	7	171	167	13	-12	2	8	103	65	24	-6	8	8	329	317	7	7	3	9	378	379	6	1	11	9	30	7	30	
-12	8	7	0	40	1	-10	2	8	578	572	6	-4	8	8	285	277	12	9	3	9	575	562	5	3	11	9	14	20	13	
-10	8	7	0	10	1	-8	2	8	736	736	6	-2	8	8	143	146	15	11	3	9	267	272	16	5	11	9	37	61	37	
-8	8	7	242	228	9	-6	2	8	776	775	5	0	8	8	114	143	14	-14	4	9	98	82	25	7	11	9	113	84	22	
-6	8	7	649	629	7	-4	2	8	329	344	5	2	8	8	279	272	6	-12	4	9	95	94	24	-4	12	9	0	24	1	
-4	8	7	468	466	6	-2	2	8	230	249	3	4	8	8	212	200	8	-10	4	9	309	310	8	-2	12	9	48	15	48	
-2	8	7	114	125	14	0	2	8	965	971	5	6	8	8	348	343	7	-8	4	9	374	357	5	0	12	9	208	210	10	
0	8	7	299	292	7	2	2	8	1012	1062	6	8	8	8	20	13	20	-6	4	9	306	302	5	2	12	9	190	179	15	
2	8	7	79	34	24	4	2	8	845	867	5	10	8	8	21	91	21	-4	4	9	253	262	6	4	12	9	160	162	13	
4	8	7	503	525	5	6	2	8	364	366	4	12	8	8	127	136	24	-2	4	9	53	29	23	-14	0	10	55	1	54	
6	8	7	582	601	6	8	2	8	0	8	1	-11	9	8	137	144	17	0	4	9	480	510	4	-12	0	10	282	300	11	
8	8	7	230	216	8	10	2	8	155	134	9	-9	8	111	128	31	2	4	9	715	730	4	-10	0	10	479	489	9		
10	8	7	205	207	9	12	2	8	320	320	7	-7	9	8	0	21	1	4	4	9	361	331	4	-8	0	10	565	569	8	
12	8	7	165	163	12	-15	3	8	68	45	39	-5	9	8	198	191	10	6	4	9	166	153	9	-6	0	10	631	642	7	
-11	9	7	112	119	28	-13	3	8	76	72	32	-3	9	8	430	430	6	8	4	9	151	161	9	-4	0	10	315	324	6	
-9	9	7	262	248	9	-11	3	8	51	20	50	-9	8	9	282	298	7	10	4	9	180	175	20	-2	0	10	613	610	6	
-7	9	7	72	61	71	-9	3	8	213	207	8	1	9	8	269	272	7	-13	5	9	231	247	8	0	0	10	1110	1181	9	
-5	9	7	276	278	8	-7	3	8	133	124	10	3	9	8	202	214	9	-11	5	9	383	366	6	12	0	10	245	218	19	
-3	9	7	543	548	6	-5	3	8	239	229	5	5	9	8	0	40	1	-9	5	9	239	247	9	-15	1	10	71	24	36	
-1	9	7	61	45	42	-3	3	8	222	243	5	7	9	8	477	483	6	-7	5	9	248	253	7	-13	1	10	0	17	1	
1	9	7	89	73	34	-1	3	8	461	432	3	9	9	8	346	369	7	-5	5	9	458	461	7	-11	1	10	43	5	42	
3	9	7	104	103	16	1	3	8	563	544	4	11	9	8	118	116	21	-2	5	9	750	742	5	-9	1	10	104	120	14	
5	9	7	116	126	15	3	3	8	0	56	1	-10	8	116	111	24	-1	5	9	899	894	6	-7	1	10	93	73	14		
7	9	7	222	249	9	5	3	8	426	424	4	-8	10	8	225	215	11	1	5	9	83	99	14	-5	1	10	247	254	5	
9	9	7	204	208	17	7	3	8	185	164	8	-6	10	8	84	12	51	3	5	9	289	284	5	-3	1	10	40	46	27	
11	9	7	83	10	30	9	3	8	62	15	18	-4	10	8	0	12	1	5	5	9	585	580	5	-1	1	10	190	201	4	
-10	10	7	110	87	28	11	3	8	252	258	6	-2	10	8	115	107	15	7	5	9	318	314	5	1	1	10	0	75	1	
-8	10	7	238	210	10	13	3	8	147	145	33	0	10	8	0	39	1	9	5	9	328	293	7	3	1	10	68	48	67	
-6	10	7	156	156	13	-14	4	8	61	73	60	2	10	8	184	186	10	-12	6	9	157	180	11	5	1	10	0	24	1	
-4	10	7	419	413	7	-12	4	8	43	44	12	4	10	8	174	162	11	-10	6	9	200	195	9	7	1	10	30	30	29	
-2	10	7	238	253	9	-10	4	8	277	277	7	6	10	8	105	102	18	-8	6	9	283	281	6	9	1	10	106	49	40	
0	10	7	47	55	46	-8	4	8	584	596	5	8	10	8	108	105	19	-6	6	9	247	228	8	11	1	10	160	154	24	
2	10	7	467	481	6	-6	4	8	806	815	5	10	10	8	40	82	39	-4	6	9	331	322	6	-14	2	10	0	51	1	
4	10	7	461	465	6	-4	4	8	463	450	5	-7	11	8	0	3	1	-2	6	9	90	83	21	-12	2	10	78	105	26	
6	10	7	270	288	12	-2	4	8	122	108	8	-5	11	8	55	29	54	0	6	9	602	593	5	-10	2	10	602	588	6	
8	10	7	119	123	36	0	4	8	670	685	6	-3	11	8	327	334	7	2	6	9	459	461	4	-8	2	10	643	665	5	
10	10	7	4	11	3	2	4	8	905	905	5	-1	11	8	370	372	7	4	6	9	426	431	4	-6	2	10	506	503	4	
-9	11	7	0	6	1	2	4	8	641	650	4	1	11	8	311	325	7	6	6	9	174	160	8	-4	2	10	144	147	6	
-7	11	7	0	9	1	2	4	8	246	236	5	-3	11	8	38	64	37	8	6	9	155	175	10	-2	2	10	382	371	4	
-5	11	7	71	76	32	8	4	8	0	68	1	5	11	8	169	180	12	10	6	9	323	315	15	0	2	10	1098	1138	5	
-3	11	7	71	49	33	10	4	8	129	134	10	7	11	8	118	145	17	-13	7	9	175	175	13	2	2	10	1148	1189	8	
-11	11	7	208	194	11	12	4	8	267	256	9	-6	12	8	62	52	61	-11	7	9	156	153	12	4	2	10	473	506	13	
1	11	7	87	93	24	14	4	8	198	210	22	-4	12	8	82	41	28	-9	7	9	37	66	36	6	2	10	112	112	58	
3	11	7	59	34	45	-13	5	8	42	42	41	-2	12	8	116	117	22	-7	7	9	185	195	11	8	2	10	332	333	16	
5	11	7	116	134	16	-11	5	8	115	135	16	0	12	8	90	112	22	-5	7	9	343	334	7	10	2	10	417	410	14	
1	11	7	104	117	9	-9	1	11	107	109	15	2	8	8	11	111	155	18	-10	5	12	186	185	15	-1	5	13	187	155	13
3	10	9	95	14	18	-7	1	11	311	310	6	4	8	11	172	40	27	3	5	12	168	154	14	-11	5	13	95	71	21	
5	10	9	74	44	47	-5	1	11	833	847	6	-9	9	11	52	60	52	5	5	12	80	81	1	-9	5	13	268	267	12	
7	10	9	241	224	34	-3	1	11	842	853	4	-7	9	11	115	7	32	7	5	12	110	125	27	-7	5	13	261	257	16	
9	10	9	148	120	18	-1	1	11	540	551	5	-5	9	11	38	30	37	9	5	12	134	78	77	-5	5	13	186	130	22	
11	10	9	236	218	13	1	11	11	232	216	7	-3	9	11	111	155	18	-10	6	12	235	244	9	-3	5	13	143	131	22	
-14	4	10	77	95	49	3	1	11	714	734	11	-9	11	8	374	384	8	-8	6	12	121	113	19	-1	5	13	187	155	13	
-12	4	10	161	147	13	5	1	11	853	858	16	-6	11	11	0	22	1	8	6	12	246	250	20	-9	5	10	324	325	9	
-10	4	10	279	282	8	-4	2	11	24	26	23	-11	12	8	106	30	25	-4	8	12	110	109	25	-2	6	13	527	507	9	
-8	4	10	0	34	1	1	3	11	95	94	19	-13	1	12	96	30	25	4	8	12	178	68	27	2	8	13				

3	7	10	0	13	1	-13	5	11	256	261	8	-2	2	12	658	677	6	7	1	13	311	305	13	5	1	14	173	174	17
5	7	10	313	308	7	-11	5	11	163	164	11	0	2	12	992	1029	7	9	1	13	141	47	29	7	1	14	115	94	39
-10	8	10	93	80	20	-9	5	11	30	34	29	2	2	12	683	696	11	11	1	13	180	136	25	9	1	14	120	116	25
-8	8	10	123	119	15	-7	5	11	391	399	5	4	2	12	101	85	25	-12	2	13	34	22	33	11	1	14	148	117	33
-6	8	10	172	178	10	-5	5	11	440	437	6	6	2	12	103	91	29	-10	2	13	60	102	39	-12	2	14	106	120	44
-4	8	10	59	62	42	-3	5	11	426	441	5	8	2	12	224	230	13	-8	2	13	40	65	40	-6	2	14	196	145	19
-2	8	10	123	112	14	-1	5	11	281	275	7	10	2	12	472	484	16	-6	2	13	194	170	15	-4	2	14	431	443	7
0	8	10	146	120	15	1	5	11	36	33	36	12	2	12	348	351	15	-2	2	13	214	230	9	-2	2	14	366	357	7
2	8	10	294	290	6	3	5	11	205	185	12	-13	3	12	66	129	66	-2	2	13	197	187	8	0	2	14	160	152	10
4	8	10	297	294	10	5	5	11	424	424	9	-11	3	12	64	9	38	0	2	13	15	59	15	2	2	14	189	189	14
6	8	10	105	76	38	7	5	11	408	417	10	-9	3	12	302	303	7	2	2	13	249	250	8	4	2	14	197	208	13
-9	9	10	24	48	23	9	5	11	342	350	16	-7	3	12	361	368	5	4	2	13	101	90	26	6	2	14	191	146	22
-7	9	10	153	150	13	-12	6	11	191	178	10	-5	3	12	128	118	9	6	2	13	184	182	17	8	2	14	396	395	12
-5	9	10	256	247	9	-10	6	11	123	126	13	-3	3	12	186	197	19	8	2	13	78	34	45	10	2	14	359	350	26
-3	9	10	285	295	11	-8	6	11	174	180	10	-1	3	12	232	216	10	10	2	13	119	87	83	-7	3	14	177	112	23
-1	9	10	151	148	11	-6	6	11	0	38	1	1	3	12	74	35	27	12	2	13	120	73	36	-5	3	14	82	58	38
1	9	10	113	108	19	-4	6	11	68	81	30	3	3	12	21	85	20	-11	3	13	83	81	42	-3	3	14	232	222	11
3	9	10	81	40	28	-2	6	11	139	144	9	5	3	12	244	214	16	-9	3	13	208	207	8	-1	3	14	56	58	55
5	9	10	231	236	13	0	6	11	443	441	5	7	3	12	237	224	13	-7	3	13	348	340	7	1	3	14	398	409	6
-8	10	10	15	47	15	2	6	11	359	344	8	9	3	12	70	7	70	-5	3	13	368	366	23	3	3	14	390	401	8
-6	10	10	0	18	1	4	6	11	248	233	12	11	3	12	98	106	97	-3	3	13	362	369	9	5	3	14	149	164	15
-4	10	10	72	72	72	6	6	11	0	31	1	-12	4	12	220	232	8	-1	3	13	53	28	52	7	3	14	194	173	13
-2	10	10	117	104	16	8	6	11	121	116	31	-10	4	12	351	375	6	1	3	13	233	247	8	9	3	14	128	92	25
0	10	10	103	92	17	-11	7	11	92	100	23	-8	4	12	272	278	6	3	3	13	473	466	7	11	3	14	97	45	97
2	10	10	143	160	13	-9	7	11	116	71	18	-6	4	12	45	47	44	5	3	13	464	464	8	-6	4	14	51	32	50
4	10	10	86	141	35	-7	7	11	84	108	24	-4	4	12	167	167	12	7	3	13	355	360	11	-4	4	14	92	93	32
6	10	10	0	28	1	-5	7	11	388	397	7	-2	4	12	350	311	15	9	3	13	66	41	66	-2	4	14	386	386	10
-7	11	10	158	150	15	-3	7	11	291	288	9	0	4	12	407	397	7	11	3	13	205	166	18	0	4	14	408	425	7
-5	11	10	296	290	14	-1	7	11	145	116	9	2	4	12	509	525	7	-12	4	13	175	174	11	2	4	14	260	253	9
-3	11	10	210	210	10	1	7	11	157	156	13	4	4	12	424	435	8	-10	4	13	124	137	12	4	4	14	153	143	14
-1	11	10	192	164	13	3	7	11	157	131	19	6	4	12	71	8	40	-8	4	13	0	30	1	6	4	14	224	221	12
1	11	10	74	8	4	5	7	11	349	327	10	8	4	12	476	470	10	-6	4	13	233	190	18	8	4	14	305	302	10
3	11	10	86	122	27	7	7	11	388	385	14	10	4	12	397	411	11	-4	4	13	182	169	16	10	4	14	140	137	34
-5	14	14	366	361	14	-7	3	15	270	247	20	4	0	16	178	170	18	-2	6	16	194	162	50	3	5	17	133	118	28
-3	5	14	104	104	32	-5	3	15	233	206	19	6	0	16	100	114	33	0	6	16	176	182	26	5	5	17	164	164	20
-1	5	14	329	322	10	-3	3	15	94	38	21	8	0	16	241	226	15	2	6	16	50	5	49	-4	6	17	163	179	34
1	5	14	318	307	8	-1	3	15	221	217	9	-7	1	16	119	122	118	4	6	16	188	176	15	-2	6	17	102	73	38
3	5	14	243	219	12	1	3	15	333	337	7	-5	1	16	129	147	41	6	6	16	236	209	16	0	6	17	154	20	33
5	5	14	176	156	34	3	3	15	296	311	8	-3	1	16	81	36	24	-1	7	16	184	127	19	2	6	17	131	82	40
7	5	14	152	153	25	5	3	15	261	274	10	-1	1	16	117	125	18	1	7	16	245	231	20	-6	0	18	341	329	20
9	5	14	137	144	24	7	3	15	129	119	22	1	1	16	0	23	1	3	7	16	170	159	24	-4	0	18	364	344	14
-4	6	14	243	220	20	9	3	15	184	143	19	3	1	16	261	272	7	0	8	16	126	114	40	-2	0	18	145	119	16
-2	6	14	309	304	11	-6	4	15	103	10	41	5	1	16	78	45	32	-7	1	17	194	212	26	0	0	18	184	154	14
0	6	14	260	256	10	-4	4	15	184	164	30	7	1	16	112	130	22	-5	1	17	102	102	52	2	0	18	246	205	11
2	6	14	122	122	25	-2	4	15	288	273	14	9	1	16	52	32	51	-3	1	17	161	147	12	4	0	18	256	248	11
4	6	14	36	36	36	0	4	15	191	196	17	-6	2	16	371	382	11	-1	1	17	300	299	6	-5	1	18	119	29	32
6	6	14	262	247	17	2	4	15	61	38	61	-4	2	16	232	321	10	-4	2	17	83	29	35	-6	2	18	299	252	14
-3	7	14	251	272	47	-3	5	15	153	105	22	6	2	16	316	321	34	-3	2	17	193	19	2	-2	2	18	166	160	12
5	7	14	118	116	28	-1	5	15	201	169	15	8	2	16	189	193	19	-2	2	17	0	19	1	-2	2	18	166	160	12
7	7	14	80	79	79	1	5	15	371	364	8	-5	3	16	170	189	17	0	2	17	0	19	1	-2	2	18	166	160	12
0	8	14	166	155	27	3	5	15	303	318	9	-3	3	16	142	129	15	2	2	17	74	20	30	0	2	18	83	69	23
2	8	14	11	10	11	5	5	15	106	100	42	-1	3	16	139	154	12	4	2	17	95	73	19	2	2	18	235	245	8
4	8	14	121	122	40	7	5	15	75	75	43	0	4	16	115	78	18	7	3	17	134	86	19	-2	4	18	121	78	21
-7	1	15	357	369	12	-4	6	15	238	255	22	3	3	16	154	143	12	-5	3	17	108	65	28	-5	3	18	137	23	23
-5	1	15	112	134	28	-2	6	15	224	194	16	5	3	16	93	10	24	-3	3	17	181	174	19	-					

## **APPENDIX B**

## Observed and calculated structure factors for 6

$h$	$k$	$l$	10Fo	10Fc	10s	$h$	$k$	$l$	10Fo	10Fc	10s	$h$	$k$	$l$	10Fo	10Fc	10s	$h$	$k$	$l$	10Fo	10Fc	10s
1	0	0	950	965	12	6	6	0	31	20	31	11	2	1	85	85	21	-4	6	1	130	118	10
2	0	0	558	583	9	7	6	0	55	65	19	12	2	1	44	76	43	-3	6	1	45	64	22
3	0	0	428	425	5	8	6	0	112	71	14	13	2	1	97	109	14	-2	6	1	177	171	6
4	0	0	354	358	5	9	6	0	60	62	30	-13	3	1	0	11	1	-1	6	1	312	307	4
5	0	0	916	953	10	10	6	0	65	9	28	-12	3	1	47	12	47	0	6	1	356	355	4
6	0	0	1201	1253	16	11	6	0	0	11	1	-11	3	1	32	27	32	1	6	1	242	242	4
7	0	0	529	532	8	0	7	0	243	240	10	-10	3	1	150	132	9	2	6	1	42	25	24
8	0	0	193	192	10	1	7	0	237	245	9	-9	3	1	385	398	5	3	6	1	0	14	1
9	0	0	14	68	14	2	7	0	50	11	24	-8	3	1	202	206	5	4	6	1	140	135	6
10	0	0	259	243	9	3	7	0	0	18	1	-7	3	1	0	35	1	5	6	1	219	232	6
11	0	0	159	155	13	4	7	0	193	189	7	-6	3	1	25	39	25	6	6	1	307	308	5
12	0	0	212	214	12	5	7	0	114	108	10	-5	3	1	24	28	23	7	6	1	102	113	14
13	0	0	221	203	25	6	7	0	183	193	6	-4	3	1	385	395	3	8	6	1	36	17	35
14	0	0	94	73	94	7	7	0	72	86	25	-3	3	1	468	489	4	9	6	1	0	31	1
0	1	0	982	1015	10	8	7	0	0	10	1	-2	3	1	474	483	3	10	6	1	0	46	1
1	1	0	486	505	3	9	7	0	72	66	22	-1	3	1	320	308	3	11	6	1	135	153	17
2	1	0	771	791	5	10	7	0	68	8	2	0	3	1	44	47	11	-10	7	1	48	59	47
3	1	0	526	534	5	0	8	0	276	267	10	1	3	1	0	30	1	-9	7	1	115	103	19
4	1	0	730	725	6	1	8	0	161	153	9	2	3	1	35	27	18	-8	7	1	53	70	53
5	1	0	156	142	5	2	8	0	68	14	47	3	3	1	606	620	4	-7	7	1	140	118	8
6	1	0	523	521	5	3	8	0	30	20	30	4	3	1	356	342	3	-6	7	1	196	185	7
7	1	0	181	178	5	4	8	0	80	33	26	5	3	1	62	70	9	-5	7	1	109	104	9
8	1	0	138	122	8	5	8	0	121	92	18	6	3	1	279	262	4	-4	7	1	57	62	18
9	1	0	156	151	8	6	8	0	189	175	7	7	3	1	27	36	27	-3	7	1	32	35	31
10	1	0	146	133	9	7	8	0	148	153	8	8	3	1	25	37	25	-2	7	1	109	112	10
11	1	0	83	81	15	8	8	0	0	16	1	9	3	1	274	275	6	-1	7	1	169	168	8
12	1	0	118	121	13	0	9	0	99	137	19	10	3	1	191	190	8	0	7	1	258	260	8
13	1	0	92	79	16	1	9	0	37	25	36	11	3	1	0	56	1	1	7	1	92	84	15
0	2	0	428	861	9	2	9	0	150	124	11	12	3	1	58	36	26	2	7	1	113	105	12
1	2	0	426	429	4	3	9	0	198	189	8	13	3	1	0	31	1	3	7	1	30	29	2
2	2	0	332	350	3	4	9	0	129	107	12	-13	4	1	35	5	35	4	7	1	66	26	15
3	2	0	606	614	4	5	9	0	10	7	9	-12	4	1	0	21	1	5	7	1	172	166	7
4	2	0	816	835	6	6	9	0	90	78	19	-11	4	1	52	62	52	6	7	1	104	114	10
5	2	0	51	72	12	0	10	0	47	52	47	-10	4	1	215	203	9	7	7	1	73	90	15
6	2	0	165	167	6	1	10	0	54	53	54	-9	4	1	232	227	6	8	7	1	77	56	38
7	2	0	219	208	5	2	10	0	147	156	27	-8	4	1	127	137	7	9	7	1	0	41	1
8	2	0	321	316	5	-14	1	1	58	53	58	-7	4	1	61	60	12	10	7	1	83	29	27
9	2	0	254	260	5	-13	1	1	168	160	14	-6	4	1	54	55	10	-8	8	1	84	106	14
10	2	0	250	242	7	-12	1	1	149	133	10	-5	4	1	143	139	4	-7	8	1	75	51	15
11	2	0	104	111	12	-11	1	1	205	197	8	-4	4	1	276	281	3	-6	8	1	90	7	13
12	2	0	50	39	50	-10	1	1	221	204	7	-3	4	1	411	420	3	-5	8	1	9	10	9
13	2	0	30	41	29	-9	1	1	158	152	8	-2	4	1	166	173	2	-4	8	1	158	133	11
0	3	0	278	274	4	-8	1	1	345	329	5	-1	4	1	79	84	8	-3	8	1	187	183	8
1	3	0	218	206	3	-7	1	1	418	422	4	0	4	1	221	205	3	-2	8	1	95	115	15
2	3	0	369	364	3	-6	1	1	208	218	8	1	4	1	212	196	3	-1	8	1	64	13	33
3	3	0	443	441	3	-5	1	1	260	273	4	2	4	1	145	158	4	0	8	1	53	28	29
4	3	0	196	190	3	-4	1	1	1077	1088	10	3	4	1	353	358	3	1	8	1	108	123	22
5	3	0	38	30	17	-3	1	1	1189	1207	9	4	4	1	392	387	3	2	8	1	65	81	65
6	3	0	124	124	6	-2	1	1	464	475	3	5	4	1	213	196	4	3	8	1	197	179	10
7	3	0	87	94	13	-1	1	1	363	361	5	6	4	1	87	95	8	4	8	1	94	51	16
8	3	0	261	259	5	0	1	1	624	620	5	7	4	1	21	21	11	5	8	1	0	13	1
9	3	0	116	98	13	1	1	1	193	178	2	8	4	1	147	143	7	6	8	1	0	52	1
10	3	0	66	57	18	2	1	1	1653	1712	12	9	4	1	213	213	6	7	8	1	114	77	15
11	3	0	63	48	20	3	1	1	605	593	5	10	4	1	185	207	13	8	8	1	40	77	40
12	3	0	79	55	16	4	1	1	254	257	4	11	4	1	0	50	1	-6	9	1	35	24	35
13	3	0	0	17	1	5	1	1	268	271	5	12	4	1	0	26	1	-5	9	1	57	60	25
14	4	0	154	151	3	7	1	1	491	487	6	-11	5	1	73	68	47	-3	9	1	143	144	20
2	4	0	42	26	11	8	1	1	152	151	9	-10	5	1	117	136	13	-2	9	1	67	97	24
3	4	0	57	38	8	9	1	1	48	24	48	-9	5	1	128	131	10	-1	9	1	34	72	33
4	4	0	178	172	4	10	1	1	334	321	6	-8	5	1	76	48	23	0	9	1	113	103	13
5	4	0	50	43	12	11	1	1	113	129	12	-7	5	1	168	173	10	1	9	1	65	40	22
6	4	0	106	98	6	12	1	1	190	171	8	-6	5	1	141	138	7	2	9	1	51	59	35
7	4	0	141	147	6	13	1	1	163	135	10	-5	5	1	182	174	6	3	9	1	157	157	12
8	4	0	0	21	31	3	1	1	31	27	20	10	5	1	83	43	24	-9	6	1	117	115	25
9	4	0	71	23	18	-12	2	1	110	104	11	-3	5	1	312	321	5	5	9	1	46	33	46
10	4	0	0	4	1	-11	2	1	180	172	8	-2	5	1	255	242	4	6	9	1	71	52	70
11	4	0	91	76	24	-10	2	1	59	21	26	0	5	1	221	212	3	-3	10	1	62	23	35
12	4	0	113	69	20	-9	2	1	141	125	7	0	5	1	50	61	10	-2	10	1	57	24	57
0	5	0	138	139	6	-8	2	1	57	59	15	1	5	1	0	11	1	-1	10	1	0	13	17
1																							

-10	4	2	70	86	22	9	7	2	0	13	1	8	2	3	20	18	19	-5	6	3	178	178	6	5	0	4	300	307	8
-9	4	2	100	122	14	-9	8	2	34	6	33	9	2	3	120	127	11	-4	6	3	42	10	26	6	0	4	379	371	9
-8	4	2	0	15	1	-8	8	2	128	111	10	10	2	3	14	29	14	-3	6	3	56	69	22	7	0	4	150	134	13
-7	4	2	116	110	6	-7	8	2	138	144	8	11	2	3	186	183	10	-2	6	3	217	222	6	8	0	4	337	341	9
-6	4	2	193	192	4	-6	8	2	111	102	9	12	2	3	160	165	10	-1	6	3	418	413	5	9	0	4	245	249	11
-5	4	2	206	210	3	-5	8	2	52	45	26	13	2	3	72	43	48	0	6	3	271	275	5	10	0	4	221	231	13
-4	4	2	47	65	15	-4	8	2	73	63	17	-13	3	3	0	7	1	1	6	3	120	120	5	11	0	4	174	168	14
-3	4	2	137	135	8	-3	8	2	26	21	26	-12	3	3	66	58	27	2	6	3	37	25	23	12	0	4	118	73	18
-2	4	2	168	171	7	-2	8	2	59	23	27	-11	3	3	59	53	23	3	6	3	0	62	1	13	0	4	0	29	1
-1	4	2	207	198	3	-1	8	2	170	177	15	-10	3	3	171	174	7	4	6	3	100	101	10	-14	1	4	95	102	15
0	4	2	244	243	3	0	8	2	309	306	10	-9	3	3	246	249	6	5	6	3	273	268	6	-13	1	4	148	150	9
1	4	2	373	362	3	1	8	2	104	60	21	-8	3	3	204	208	5	6	6	3	216	214	8	-12	1	4	190	192	8
2	4	2	75	73	7	2	8	2	49	4	35	-7	3	3	64	64	10	7	6	3	110	101	12	-11	1	4	40	36	40
3	4	2	25	13	24	3	8	2	65	4	23	-6	3	3	83	75	8	8	6	3	24	16	23	-10	1	4	171	175	7
4	4	2	46	49	21	4	8	2	77	38	16	-5	3	3	223	222	3	9	6	3	0	32	1	-9	1	4	0	29	1
5	4	2	254	248	3	5	8	2	113	143	26	-4	3	3	673	674	5	10	6	3	62	42	62	-8	1	4	211	195	7
6	4	2	124	127	7	6	8	2	200	190	16	-3	3	3	537	538	6	-10	7	3	0	17	1	-7	1	4	375	378	5
7	4	2	94	79	9	7	8	2	62	60	27	-2	3	3	229	232	5	-9	7	3	65	62	23	-6	1	4	319	315	4
8	4	2	148	151	8	8	8	2	70	70	69	-1	3	3	121	120	5	-8	7	3	93	95	13	-5	1	4	220	209	4
9	4	2	0	12	1	-6	9	2	17	11	17	0	3	3	332	332	3	-7	7	3	199	208	6	-4	1	4	113	92	6
10	4	2	0	5	1	-5	9	2	66	22	20	1	3	3	511	511	4	-6	7	3	157	144	7	-3	1	4	443	451	4
11	4	2	0	60	1	-4	9	2	116	93	13	2	3	3	169	182	4	-5	7	3	115	104	9	-2	1	4	783	798	7
12	4	2	34	62	34	-3	9	2	143	136	19	3	3	3	564	570	5	-4	7	3	57	58	22	-1	1	4	206	195	3
-12	5	2	40	51	39	-2	9	2	117	95	13	4	3	3	207	212	5	-3	7	3	75	85	18	0	1	4	486	485	4
-11	5	2	145	109	24	-1	9	2	53	11	52	5	3	3	35	27	28	-2	7	3	218	212	6	1	1	4	563	554	5
-10	5	2	80	81	20	0	9	2	0	28	1	6	3	3	89	77	9	-1	7	3	365	351	8	2	1	4	131	136	7
-9	5	2	94	90	13	1	9	2	0	5	1	7	3	3	106	121	8	0	7	3	181	153	11	3	1	4	76	75	7
10	4	2	117	129	10	2	9	2	144	130	13	8	3	3	157	150	8	1	7	3	168	162	12	4	1	4	414	414	5
-7	5	2	166	174	7	3	9	2	142	143	11	9	3	3	235	230	7	2	7	3	0	18	1	5	1	4	143	134	9
-6	5	2	124	124	9	4	9	2	0	49	1	10	3	3	156	159	10	3	7	3	40	39	6	1	4	239	243	6	
-5	5	2	226	224	5	5	9	2	97	8	30	11	3	3	42	25	42	4	7	3	45	79	28	7	1	4	0	45	1
-4	5	2	172	164	7	6	9	2	36	28	35	12	3	3	120	76	19	5	7	3	138	141	10	8	1	4	56	48	21
-3	5	2	133	141	7	-3	10	2	141	109	18	-13	4	3	62	39	44	6	7	3	157	158	8	9	1	4	67	13	22
-2	5	2	125	112	15	-2	10	2	83	63	82	-12	4	3	0	8	1	7	3	54	9	53	10	1	4	135	144	11	
-1	5	2	256	248	3	-1	10	2	77	32	55	-11	4	3	140	124	37	8	7	3	91	30	23	11	1	4	72	89	20
0	5	2	273	273	3	0	10	2	71	25	21	-10	4	3	235	217	8	9	7	3	0	4	1	12	1	17	36	17	
1	5	2	212	206	3	1	10	2	108	78	34	-9	4	3	407	412	7	-9	8	3	54	77	36	-14	2	4	30	16	30
2	5	2	301	298	3	2	10	2	159	150	11	-8	4	3	201	206	6	-8	8	3	56	16	55	-13	2	4	32	48	32
3	5	2	166	175	4	-14	1	3	112	95	12	-7	4	3	159	159	5	-7	8	3	0	33	1	-12	2	4	0	45	1
4	5	2	80	95	8	-13	1	3	51	85	34	-6	4	3	82	99	11	-6	8	3	57	35	30	-11	2	4	168	171	11
5	5	2	132	132	5	-12	1	3	82	91	18	-5	4	3	260	270	3	-5	8	3	159	166	9	-10	2	4	286	288	6
6	5	2	167	144	7	-11	1	3	166	96	9	-4	3	3	537	544	5	4	8	3	209	232	10	-9	2	4	113	123	9
7	5	2	183	191	8	-10	1	3	9	49	9	-3	4	3	772	774	10	-3	8	3	122	139	12	-8	2	4	12	46	11
8	5	2	140	117	13	-9	1	3	125	123	7	-2	4	3	191	196	5	-2	8	3	63	62	63	-7	2	4	122	115	8
9	5	2	93	64	17	-8	1	3	227	216	6	-1	4	3	0	18	1	-1	8	3	36	72	36	-6	2	4	36	16	36
10	5	2	77	86	45	-7	1	3	519	517	6	0	4	3	110	85	6	0	8	3	90	67	44	-5	2	4	253	253	4
11	5	2	33	68	32	-6	1	3	74	80	15	1	4	3	237	242	4	1	8	3	136	145	13	-4	2	4	642	647	5
-11	6	2	16	24	16	-5	1	3	0	29	1	2	4	3	593	601	5	2	8	3	194	180	12	-3	2	4	23	26	22
-10	6	2	61	32	26	-4	1	3	187	194	5	3	4	3	77	371	4	3	8	3	224	200	11	-2	2	4	30	53	30
-9	6	2	41	14	40	-3	1	3	98	106	13	-8	5	3	140	129	9	3	9	3	153	130	24	12	2	4	30	53	30
6	6	2	23	12	1	3	141	140	15	-6	5	3	203	210	5	5	9	3	103	105	25	-12	3	4	62	90	35		
7	6	2	73	93	40	13	1	3	25	24	24	-5	5	3	137	142	7	-2	10	3	0	14	1	-11	3	4	137	132	10
8	6	2	0	13	1	-14	2	3	81	65	46	-4	5	3	236	233	5	-1	10	3	77	3	25	-10	3	4	203	198	6
9	6	2	37	54	36	-13	2	3	0	7	1	-3	5	3	142	127	6	0	10	3	118	43	13	-9	3	4	168	168	6
10	6	2	28	13	28	-12	2	3	148	144	10	-2	5	3	93	82	9	1	10	3	27	31	26	-8	3	4	0	22	1
-10	7	2	0	9	1	-11	2	3	100	109	12	-2	5	3	284	283	3	-14	0	4	170	129	31	-7	3	4	192	193	5
-9	7	2	37	38	37	-10	2	3	57	8	21	0	5	3	317	309	3	-13	0	4	241	245	11	-6	3	4	196	197	4
-8	7	2	67																										

1	4	4	134	114	5	2	8	4	68	14	31	0	3	5	318	307	4	-4	7	5	42	9	41	7	1	6	69	70	24	
2	4	4	277	271	4	3	8	4	82	17	20	1	3	5	633	639	5	-3	7	5	36	34	36	8	1	6	106	101	18	
3	4	4	269	276	4	4	8	4	66	120	41	2	3	5	482	489	4	-2	7	5	138	139	18	9	1	6	88	101	15	
4	4	4	134	132	6	5	8	4	175	145	16	3	3	5	60	40	21	-1	7	5	213	220	6	10	1	6	194	170	9	
5	4	4	172	175	5	6	8	4	70	104	26	4	3	5	0	22	1	0	7	5	60	14	59	11	1	6	150	146	11	
6	4	4	55	58	25	7	8	4	201	30	16	5	3	5	36	58	36	1	7	5	94	122	29	12	1	6	0	19	1	
7	4	4	31	35	31	-6	9	4	62	14	31	6	3	5	74	87	24	2	7	5	45	30	44	-14	2	6	0	39	1	
8	4	4	75	51	18	-5	9	4	0	38	1	7	3	5	211	212	9	3	7	5	44	59	44	-13	2	6	53	9	28	
9	4	4	57	17	24	-4	9	4	163	150	18	8	3	5	256	259	7	4	7	5	50	8	50	-12	2	6	75	103	30	
10	4	4	107	92	17	-3	9	4	158	149	18	9	3	5	129	97	17	5	7	5	106	94	14	-11	2	6	183	192	15	
11	4	4	27	67	26	-2	9	4	0	15	1	10	3	5	33	6	32	6	7	5	118	132	12	-10	2	6	231	228	7	
-12	5	4	85	128	27	-1	9	4	88	13	44	11	3	5	80	105	18	7	7	5	27	31	26	-9	2	6	63	50	18	
-11	5	4	175	178	10	0	9	4	0	50	1	12	3	5	0	12	1	8	7	5	31	43	31	-8	2	6	44	9	44	
-10	5	4	55	80	36	1	9	4	0	48	1	-13	4	5	56	7	55	-9	8	5	70	56	17	-7	2	6	107	84	8	
-9	5	4	75	63	16	2	9	4	163	165	12	-12	4	5	61	94	61	-8	8	5	53	40	31	-6	2	6	35	19	34	
-8	5	4	147	142	9	3	9	4	61	100	61	-11	4	5	155	145	11	-7	8	5	107	99	11	-5	2	6	269	264	4	
-7	5	4	173	181	7	4	9	4	0	13	1	-10	4	5	171	166	11	-6	8	5	95	108	11	-4	2	6	653	663	5	
-6	5	4	187	184	6	5	9	4	105	25	27	-9	4	5	319	307	6	-5	8	5	94	106	11	-3	2	6	182	190	4	
-5	5	4	378	377	5	-2	10	4	18	20	18	-8	4	5	265	267	8	-4	8	5	111	120	10	-2	2	6	39	45	23	
-4	5	4	197	185	7	-1	10	4	82	7	43	-7	4	5	90	101	9	-3	8	5	131	96	16	-1	2	6	105	100	6	
-3	5	4	210	203	9	0	10	4	0	17	1	-6	4	5	170	178	5	-2	8	5	118	109	15	0	2	6	68	89	8	
-2	5	4	112	113	13	-14	1	5	22	85	22	-5	4	5	473	477	4	-1	8	5	136	135	13	1	2	6	0	44	1	
-1	5	4	251	245	3	-13	1	5	45	40	45	-4	4	5	375	377	6	0	8	5	97	93	17	2	2	6	584	561	7	
0	5	4	148	147	5	-12	1	5	27	60	26	-3	4	5	378	386	5	1	8	5	73	85	35	3	2	6	382	375	5	
1	5	4	297	290	4	-11	1	5	140	140	9	-2	4	5	205	211	3	2	8	5	175	163	12	4	2	6	49	27	16	
2	5	4	317	311	4	-10	1	5	144	161	9	-1	4	5	85	81	7	3	6	5	120	114	15	5	2	6	62	58	14	
3	5	4	205	211	4	-9	1	5	44	13	44	0	4	5	207	208	4	4	8	5	46	89	45	6	2	6	147	145	8	
4	5	4	151	140	5	-8	1	5	143	152	7	1	4	5	651	642	6	5	8	5	101	43	24	7	2	6	81	88	14	
5	5	4	179	174	5	-7	1	5	186	176	6	2	4	5	468	459	5	6	8	5	99	68	24	8	2	6	246	248	7	
6	5	4	115	111	8	-6	1	5	362	348	4	3	4	5	165	175	5	-6	9	5	103	28	16	9	2	6	73	80	21	
7	5	4	144	148	7	-5	1	5	299	284	2	4	4	5	52	56	19	-5	9	5	61	55	31	10	2	6	0	9	1	
8	5	4	104	104	15	-4	1	5	167	173	5	5	4	5	0	16	1	-4	9	5	50	60	33	11	2	6	0	6	1	
9	5	4	121	126	39	-3	1	5	245	228	4	6	4	5	150	146	7	-3	9	5	0	23	1	12	2	6	78	73	23	
10	5	4	61	1	-2	1	5	209	204	4	7	4	5	278	278	5	-2	9	5	0	13	1	-13	3	6	0	4	1		
11	5	4	126	84	20	-1	1	5	303	296	3	8	4	5	274	256	11	-1	9	5	124	114	16	-12	3	6	164	148	14	
-11	6	4	99	76	20	0	1	5	589	578	5	9	4	5	193	184	8	0	9	5	0	48	1	-11	3	6	207	199	7	
-10	6	4	88	65	18	1	1	5	236	236	4	10	4	5	45	5	44	1	9	5	66	60	29	-10	3	6	289	287	6	
-9	6	4	68	76	17	2	1	5	228	219	5	11	4	5	57	38	38	2	9	5	0	79	1	-9	3	6	182	181	6	
-8	6	4	114	123	11	3	1	5	128	136	5	-12	5	5	0	15	1	3	9	5	0	5	1	-8	3	6	83	72	10	
-7	6	4	49	61	22	4	1	5	61	38	19	-11	5	5	89	51	20	4	9	5	0	4	1	-7	3	6	58	72	21	
-6	6	4	49	34	24	5	1	5	225	215	6	-10	5	5	0	11	1	-14	6	0	172	164	13	-6	3	6	161	171	4	
-5	6	4	103	98	8	6	1	5	287	273	9	-9	5	5	0	21	1	-13	0	6	178	171	12	-5	3	6	474	477	4	
-4	6	4	222	233	5	7	1	5	77	55	20	-8	5	5	27	45	27	-12	0	6	124	125	14	-4	3	6	533	531	4	
-3	6	4	158	163	7	8	1	5	154	152	9	-7	5	5	79	102	16	-11	0	6	64	47	31	-3	3	6	369	380	4	
-2	6	4	141	138	7	9	1	5	185	192	15	-6	5	5	229	224	6	-10	0	6	6	98	63	18	-2	3	6	89	88	8
-1	6	4	79	52	24	10	1	5	61	43	60	-5	5	5	165	161	5	-9	0	6	192	200	10	-1	3	6	124	113	5	
0	6	4	90	98	10	11	1	5	110	78	16	-4	5	5	110	116	8	-8	0	6	686	687	10	0	3	6	142	131	5	
1	6	4	109	107	6	12	1	5	63	88	37	-3	5	5	57	3	56	-7	0	6	245	260	12	1	3	6	364	363	4	
2	6	4	34	37	37	-10	2	5	22	42	22	1	5	5	205	199	15	-3	0	6	368	367	7	5	3	6	128	133	7	
3	6	4	71	79	35	-10	2	5	2	16	2	2	5	5	188	180	6	-2	0	6	625	643	14	6	3	6	67	46	13	
7	6	4	32	21	31	-9	2	5	80	76	15	3	5	5	149	150	6	-1	0	6	497	489	7	7	3	6	122	127	12	
8	6	4	74	35	22	-8	2	5	214	210	12	4	5	5	341	344	5	0	0	6	352	364	5	8	3	6	202	207	8	
9	6	4	92	17	22	-7	2	5	392	388	4	5	5	5	288	295	4	1	0	6	190	179	8	9	3	6	76	85	30	
10	6	4	0	29	1	-6	8	6	48	40	48	10	3	7	22	19	21	-6	8	7	63	45	25	3	2	8	86	70	11	
1	4	6	23	28	22	6	8	6	48	40	48	11	3	7	22	19	21	-6	8	7	63	45	25	3	2	8	86	70	11	
2	4	6	109	105	7	-6	9	6	83	66	22	-13	4	7	0	7	1	-5	8	7	99	109	10	4	2	8	117	129	9	
3	4	6	76	75	11	-5	9	6	134	110	12	-12	4	7	62	93	41	-4	8	7	157	177	7	5	2	8	199	196	8	
4	4	6																												

8	5	6	152	112	14	5	1	7	211	212	7	-6	5	7	170	164	7	-2	0	8	496	498	6	9	3	8	0	11	1
9	5	6	169	137	14	6	1	7	135	135	10	-5	5	7	200	203	7	-1	0	8	491	484	19	10	3	8	41	35	40
10	5	6	73	75	72	7	1	7	72	104	17	-4	5	7	159	158	8	0	0	8	187	191	7	-13	4	8	47	66	46
-11	6	6	33	47	33	8	1	7	162	163	9	-3	5	7	0	14	1	1	0	8	236	216	8	-12	4	8	78	12	31
-10	6	6	113	90	12	9	1	7	185	181	8	-2	5	7	148	168	9	2	0	8	191	180	13	-11	4	8	50	18	49
-9	6	6	25	15	25	10	1	7	121	132	13	-1	5	7	317	319	4	3	0	8	131	107	13	-10	4	8	122	90	13
-8	6	6	95	125	12	11	1	7	51	13	50	0	5	7	181	166	6	4	0	8	376	382	8	-9	4	8	81	119	80
-7	6	6	0	13	1	-14	2	7	55	77	54	1	5	7	317	307	4	5	0	8	547	558	9	-8	4	8	45	10	44
-6	6	6	39	38	38	-13	2	7	158	155	9	2	5	7	57	58	15	6	0	8	204	189	17	-7	4	8	67	79	29
-5	6	6	149	153	7	-12	2	7	6	18	5	3	5	7	175	171	7	7	0	8	83	48	22	-6	4	8	96	90	13
-4	6	6	28	21	28	-11	2	7	61	66	21	4	5	7	210	213	7	8	0	8	35	10	35	-5	4	8	126	125	7
-3	6	6	53	39	19	-10	2	7	28	5	27	5	5	7	12	8	11	9	0	8	0	8	1	-4	4	8	100	96	6
-2	6	6	99	60	21	-9	2	7	95	68	10	6	5	7	52	61	25	10	0	8	208	179	16	-3	4	8	123	125	6
-1	6	6	70	58	21	-8	2	7	213	214	5	7	5	7	105	95	11	11	0	8	164	172	26	-2	4	8	36	55	35
0	6	6	105	117	15	-7	2	7	275	273	5	8	5	7	44	17	44	-14	1	8	105	79	14	-1	4	8	0	7	1
1	6	6	106	113	9	-6	2	7	145	134	6	9	5	7	66	80	37	-13	1	8	102	89	14	0	4	8	30	45	30
2	6	6	80	83	10	-5	2	7	121	120	6	10	5	7	84	46	26	-12	1	8	56	19	25	1	4	8	198	207	5
3	6	6	161	164	6	-4	2	7	556	550	5	-11	6	7	38	7	37	-11	1	8	126	93	12	2	4	8	83	80	12
4	6	6	0	1	1	-3	2	7	61	73	13	-10	6	7	84	39	16	-10	1	8	93	84	21	3	4	8	55	90	20
5	6	6	60	39	31	-2	2	7	509	498	5	-9	6	7	155	143	10	-9	1	8	157	154	8	4	4	8	164	159	8
6	6	6	88	94	14	-1	2	7	341	328	3	-8	6	7	241	237	7	-8	1	8	282	292	5	5	4	8	102	105	14
7	6	6	107	82	25	0	2	7	105	102	7	-7	6	7	242	240	6	-7	1	8	31	43	30	6	4	8	63	58	19
8	6	6	65	94	37	1	2	7	150	137	5	-6	6	7	245	256	6	-6	1	8	157	145	5	7	4	8	31	34	31
9	6	6	0	67	1	-2	2	7	160	150	4	-5	6	7	108	110	11	-5	1	8	25	56	25	8	4	8	76	28	27
-10	7	6	51	42	37	3	2	7	294	286	5	-4	6	7	165	156	8	-4	1	8	223	217	4	9	4	8	97	108	20
-9	7	6	109	117	11	4	2	7	203	207	5	-3	6	7	191	183	8	-3	1	8	406	389	4	10	4	8	0	49	1
-8	7	6	181	184	7	5	2	7	234	243	6	-2	6	7	266	268	10	-2	1	8	322	310	5	-12	5	8	53	89	52
-7	7	6	170	150	8	6	2	7	96	86	13	-1	6	7	337	319	8	-1	1	8	36	62	35	-11	5	8	16	64	16
-6	7	6	144	134	10	7	2	7	0	11	1	0	6	7	294	302	6	0	1	8	62	53	11	-10	5	8	123	117	13
-5	7	6	178	172	7	8	2	7	68	78	21	1	6	7	159	167	8	1	8	141	146	7	-9	5	8	218	236	9	
-4	7	6	102	102	11	9	2	7	98	97	14	2	6	7	174	170	6	2	1	8	143	141	7	-8	5	8	170	169	8
-3	7	6	140	121	8	10	2	7	103	79	18	3	6	7	143	135	7	3	1	8	36	5	35	-7	5	8	110	114	16
-2	7	6	221	217	6	11	2	7	91	62	18	4	6	7	184	181	7	4	1	8	244	238	6	-6	5	8	214	194	7
-1	7	6	228	226	7	-13	3	7	67	56	66	5	6	7	210	215	8	5	1	8	343	343	6	-5	5	8	120	98	10
0	7	6	253	261	7	-12	3	7	99	70	20	6	6	7	160	150	13	6	1	8	79	79	17	-4	5	8	206	216	7
1	7	6	168	165	11	-11	3	7	168	178	13	7	6	7	46	28	46	7	1	8	30	70	30	-3	5	8	316	332	6
2	7	6	59	60	59	-10	3	7	148	137	8	8	6	7	92	72	25	8	1	8	89	106	15	-2	5	8	438	449	7
3	7	6	109	87	44	-9	3	7	148	133	6	9	6	7	79	86	29	9	1	8	36	8	35	-1	5	8	191	194	4
4	7	6	166	171	16	-8	3	7	94	99	15	-10	7	7	79	68	17	10	1	8	171	153	10	0	5	8	73	67	21
5	7	6	181	184	16	-7	3	7	109	103	9	-9	7	7	28	28	2	11	1	8	128	126	13	1	5	8	130	122	10
6	7	6	119	153	12	-6	3	7	38	14	38	-8	7	7	58	71	42	-14	2	8	46	17	46	2	5	8	226	223	6
7	7	6	67	48	37	-5	3	7	460	461	5	-7	7	7	121	105	9	-13	2	8	25	25	24	3	5	8	258	256	6
8	7	6	0	23	1	-4	3	7	68	76	9	-6	7	7	50	39	49	-12	2	8	122	104	10	4	5	8	273	279	6
-8	8	6	147	126	12	-3	3	7	0	26	1	-5	7	7	37	23	37	-11	2	8	205	195	7	5	5	8	79	104	15
-7	8	6	87	57	12	-2	3	7	0	30	1	-4	7	7	70	72	17	-10	2	8	253	248	6	6	5	8	35	39	34
-6	8	6	35	24	35	-1	3	7	50	60	18	-3	7	7	0	40	1	-9	2	8	116	101	8	7	5	8	59	70	22
-5	8	6	60	34	18	0	3	7	33	67	25	-2	7	7	128	15	27	-8	2	8	140	138	8	8	5	8	155	163	10
-4	8	6	94	77	17	1	3	7	297	293	5	-1	7	7	115	111	31	-7	2	8	53	59	17	9	5	8	63	88	37
-11	6	8	24	29	23	-4	2	9	44	49	20	-7	6	9	16	17	17	-3	2	10	196	187	5	-3	6	10	40	41	40
-10	6	8	6	53	51	-12	3	9	335	356	4	-3	7	9	92	42	16	4	2	10	21	53	20	4	6	10	0	28	1
-9	7	8	154	149	8	-5	3	9	155	164	5	-2	7	9	122	132	14	-2	2	10	175	164	9	-2	6	10	84	94	17
-7	7	8	76	44	22	-10	3	9	26	65	25	-8	7	9	44	59	43	-1	2	10	203	203	5	-1	6	10	64	41	44
-4	7	8	80	84	22	-2	3	9	43	23	22	0	7	9	73	22	24	7	2	10	195	180	8	7	6	10	114	46	78
-3	7	8	182	187	9	-1	3	9	0	14	1	1	7	9	0	38	1	8	2	10	81	95	18	-9	7	10	58	48	25
-2	7	8	318	314	7	0	3	9	228	225	5	2	7	9	64	6	63	9	2	10	20	212	6	1	6	10	65	58	28
-1	7	8	124	105	17	1	3	9	416	402	5	-8	8	9	69	9	22	10	2	10	15	41	15	-7	7	10	106	116	11
0	7	8	33	20	32	2	3	9	23	200	225	-7	8	9	58	16	26	-13	3	10	58	5	57	-6	7	10	0	15	

-12	1	9	85	85	14	3	4	9	68	45	22	-2	0	10	676	677	8	-10	4	10	150	155	11	-8	1	11	96	93	10
-11	1	9	97	65	13	4	4	9	70	48	17	-1	0	10	270	252	8	-9	4	10	111	91	19	-7	1	11	262	263	6
-10	1	9	77	87	19	5	4	9	53	18	37	0	0	10	266	250	7	-8	4	10	105	85	14	-6	1	11	199	207	6
-9	1	9	194	203	6	6	4	9	118	124	9	1	0	10	125	124	8	-7	4	10	51	79	50	-5	1	11	64	80	18
-8	1	9	223	215	5	7	4	9	209	223	9	2	0	10	163	155	11	-6	4	10	178	161	9	-4	1	11	325	317	5
-7	1	9	251	249	5	8	4	9	151	124	11	3	0	10	331	329	9	-5	4	10	150	157	8	-3	1	11	296	303	5
-6	1	9	155	155	5	9	4	9	59	15	28	4	0	10	310	310	9	-4	4	10	128	120	6	-2	1	11	270	254	5
-5	1	9	155	157	9	-12	5	9	48	29	47	5	0	10	161	176	16	-3	4	10	64	90	14	-1	1	11	140	123	8
-4	1	9	328	319	5	-11	5	9	87	103	24	6	0	10	0	32	1	-2	4	10	235	237	7	0	1	11	157	161	6
-3	1	9	207	200	5	-10	5	9	70	55	33	7	0	10	32	32	31	-1	4	10	163	174	5	1	11	233	229	6	
-2	1	9	157	154	6	-9	5	9	153	160	11	8	0	10	85	88	84	0	4	10	14	57	14	2	1	11	126	136	9
-1	1	9	384	380	5	-8	5	9	211	221	8	9	0	10	210	213	13	1	4	10	44	40	44	3	1	11	157	160	9
0	1	9	14	51	14	-7	5	9	210	196	7	10	0	10	101	118	32	2	4	10	212	200	7	4	1	11	262	262	6
1	1	9	267	265	5	-6	5	9	71	79	20	-14	1	10	118	94	11	3	4	10	165	155	7	5	1	11	186	176	9
2	1	9	244	234	6	-5	5	9	278	279	6	-13	1	10	67	1	4	4	10	83	78	15	6	1	11	53	82	53	
3	1	9	282	284	6	-4	5	9	73	85	16	-12	1	10	0	38	1	5	4	10	0	54	1	7	1	11	18	36	17
4	1	9	239	228	7	-3	5	9	253	263	7	-11	1	10	59	62	22	6	4	10	10	15	10	8	1	11	116	64	13
5	1	9	122	103	11	-2	5	9	325	330	7	-10	1	10	74	9	74	7	4	10	19	52	19	9	1	11	98	82	17
6	1	9	19	8	18	-1	5	9	221	219	4	-9	1	10	85	83	20	8	4	10	68	83	35	-13	2	11	37	27	37
7	1	9	151	142	9	0	5	9	27	30	37	-8	1	10	305	315	5	9	4	10	74	57	25	-12	2	11	40	26	39
8	1	9	65	92	28	1	5	9	238	228	5	-7	1	10	155	159	8	-12	5	10	50	36	1	-11	2	11	12	83	12
9	1	9	109	118	19	2	5	9	176	186	7	-6	1	10	41	9	40	-11	5	10	48	45	48	-10	2	11	206	212	7
10	1	9	97	71	16	3	5	9	232	232	6	-5	1	10	134	121	8	-10	5	10	120	100	19	-9	2	11	265	267	5
-14	2	9	0	58	1	4	5	9	168	167	9	-4	1	10	108	89	7	-9	5	10	138	158	13	-8	2	11	64	19	17
-13	2	9	133	124	13	5	5	9	117	108	18	-3	1	10	261	256	4	-8	5	10	63	9	39	-7	2	11	0	41	1
-12	2	9	58	36	22	6	5	9	61	42	25	-2	1	10	464	463	5	-7	5	10	96	83	14	-6	2	11	66	79	14
-11	2	9	50	83	50	7	5	9	59	79	18	-1	1	10	138	119	11	-6	5	10	138	125	10	-5	2	11	0	16	1
-10	2	9	71	88	17	8	5	9	0	55	1	0	1	10	70	54	14	-5	5	10	140	116	12	-4	2	11	301	284	5
-9	2	9	155	141	7	9	5	9	0	45	1	1	1	10	85	90	11	-4	5	10	82	92	14	-3	2	11	334	329	5
-8	2	9	112	116	8	-11	6	9	40	28	39	2	1	10	73	63	15	-3	5	10	100	110	13	-2	2	11	106	114	24
-7	2	9	195	194	5	-10	6	9	88	57	24	3	1	10	161	159	8	-2	5	10	38	55	37	-1	2	11	13	31	13
-6	2	9	184	188	6	-9	6	9	149	160	9	4	1	10	259	237	7	-1	5	10	103	103	9	0	2	11	116	103	9
-5	2	9	0	21	1	-8	6	9	171	164	8	5	1	10	24	46	23	0	5	10	214	196	8	1	2	11	32	12	32
2	2	11	0	33	1	6	6	11	93	76	19	7	2	12	122	136	12	0	7	12	9	45	8	1	4	13	18	18	
3	2	11	173	177	7	-9	7	11	77	78	19	8	2	12	75	43	25	1	7	12	0	7	1	2	4	13	12	6	
4	2	11	280	280	7	-8	7	11	94	79	13	9	2	12	53	16	53	2	7	12	133	128	17	3	4	13	14	63	13
5	2	11	0	25	1	-7	7	11	80	46	21	-13	3	12	105	107	23	3	7	12	168	105	17	4	4	13	42	7	41
6	2	11	0	15	1	-6	7	11	63	15	63	-12	3	12	89	76	88	-6	8	12	0	19	1	5	4	13	76	84	17
7	2	11	67	36	39	-5	7	11	27	2	26	-11	3	12	34	18	34	-5	8	12	41	8	40	6	4	13	129	115	11
8	2	11	53	14	53	-4	7	11	48	59	48	-10	3	12	81	46	30	-4	8	12	86	80	16	7	4	13	0	85	1
9	2	11	55	66	41	-3	7	11	120	138	15	-9	3	12	82	71	18	-3	8	12	144	144	18	-11	5	13	116	80	24
-13	3	11	162	151	16	-2	7	11	167	177	14	-8	3	12	78	11	28	-2	8	12	79	102	21	-10	5	13	35	65	34
-12	3	11	150	151	15	-1	7	11	54	59	53	-7	3	12	198	202	6	-1	8	12	32	10	32	-9	5	13	180	142	15
-11	3	11	163	151	14	0	7	11	78	77	27	-6	3	12	193	196	5	0	8	12	0	12	1	-8	5	13	0	5	1
-10	3	11	36	71	36	-1	5	12	101	90	12	-13	1	13	99	54	14	-7	5	13	75	74	40	-5	1	11	10	11	40
-9	3	11	92	101	15	2	7	11	0	42	1	-4	3	12	45	7	34	-1	5	13	360	366	5	1	5	13	0	10	1
-8	3	11	162	155	8	-7	8	11	22	23	21	-3	3	12	26	25	25	-11	1	13	148	118	15	-5	5	13	57	4	29
-7	3	11	220	222	5	-6	8	11	106	95	15	-2	3	12	6	17	6	-10	1	13	216	216	7	-4	5	13	59	7	35
-6	3	11	335	338	5	-5	8	11	147	122	11	-1	3	12	0	8	1	-9	1	13	280	272	7	-3	5	13	37	39	37
-5	3	11	238	231	5	-4	8	11	33	1	34	0	3	12	301	302	5	-8	1	13	132	115	10	-2	5	13	77	66	24
-4	3	11	148	130	11	-11	0	12	0	33	1	8	3	12	0	32	1	1	0	13	230	226	6	6	5	13	124	74	20
-3	4	11	45	47	44	-10	0	12	181	169	15	-12	4	12	0	34	1	1	1	13	179	177	7	-10	6	13	58	73	36
-5	3	11	67	120	23	-9	0	12	222	223	11	-11	4	12	113	62	19	2	1	13	192	190	7	-9	6	13	178	158	10
-6	3	11	175	163	9	-8	0	12	436	438	9	-10	4	12	66	51	34	3	1	13	198	183	8	-8	6	13	148	140	10
7	3	11	130	149	13	-7	0	12	425	416	10	-9	4	12	72	80	22	4	1	13	126	107	12	-7	6	13	62	36	61
8	3	11	79	63	20	-6	0	12	111	116	15	-8	4	12	56	101	45	5	1	13	98	123	16	-6	6	13	0	12	1
9	3	11	0	36																									

6	5	11	66	66	19	-11	2	12	211	214	7	-4	6	12	0	6	1	3	3	13	25	5	24	0	0	14	127	117	17
7	5	11	63	64	24	-10	2	12	89	77	14	-3	6	12	109	94	18	4	3	13	75	27	21	1	0	14	189	179	10
-10	6	11	98	81	17	-9	2	12	26	23	26	-2	6	12	62	70	26	5	3	13	86	53	16	2	0	14	456	446	8
-9	6	11	131	142	11	-8	2	12	106	71	14	-1	6	12	47	44	46	6	3	13	95	118	20	3	0	14	320	326	7
-8	6	11	113	101	12	-7	2	12	224	230	6	0	6	12	165	179	9	7	3	13	46	79	40	4	0	14	58	32	58
-7	6	11	0	9	1	-6	2	12	428	429	5	1	6	12	146	143	14	-12	4	13	140	130	18	5	0	14	0	50	1
-6	6	11	61	19	33	-5	2	12	344	348	5	2	6	12	0	39	1	-11	4	13	108	107	31	6	0	14	0	62	1
-5	6	11	58	8	50	-4	2	12	91	102	14	3	6	12	43	79	42	-10	4	13	92	56	25	7	0	14	101	99	25
-4	6	11	71	58	22	-3	2	12	81	51	11	4	6	12	48	29	48	-9	4	13	76	98	20	-13	1	14	47	28	47
-3	6	11	263	276	8	-2	2	12	39	64	38	5	6	12	34	33	34	-8	4	13	0	11	1	-12	1	14	125	113	19
-2	6	11	172	151	9	-1	2	12	296	291	5	-8	7	12	75	104	17	-7	4	13	210	209	9	-11	1	14	54	23	28
-1	6	11	0	40	1	0	2	12	512	511	6	-7	7	12	57	27	33	-6	4	13	171	142	24	-10	1	14	159	155	9
0	6	11	69	73	22	1	2	12	249	243	6	-6	7	12	38	13	38	-5	4	13	0	34	1	-9	1	14	112	94	15
1	6	11	35	25	35	2	2	12	4	58	4	-5	7	12	57	23	56	-4	4	13	61	43	24	-8	1	14	37	28	36
2	6	11	44	81	43	3	2	12	37	6	37	4	7	12	97	92	20	-3	4	13	43	30	43	-7	1	14	76	87	21
3	6	11	226	227	8	4	2	12	97	97	11	-3	7	12	184	195	9	-2	4	13	69	47	15	-6	1	14	184	180	8
4	6	11	155	160	15	5	2	12	43	66	42	-2	7	12	106	113	14	-1	4	13	118	119	8	-5	1	14	57	26	27
5	6	11	59	6	35	6	2	12	219	215	10	-1	7	12	61	53	31	0	4	13	164	164	9	-4	1	14	249	245	6
-3	1	14	215	207	7	-7	6	14	48	14	47	-2	4	15	0	33	1	-2	2	16	0	47	1	-2	2	17	0	17	1
-2	1	14	62	56	20	-6	6	14	63	48	39	-1	4	15	199	190	9	-1	2	16	140	124	10	-1	2	17	0	4	1
-1	1	14	130	134	15	-5	6	14	58	53	31	0	4	15	228	227	7	0	2	16	111	105	12	0	2	17	28	17	27
0	1	14	207	215	7	-4	6	14	50	8	34	1	4	15	65	45	25	1	2	16	93	87	15	1	2	17	117	131	11
1	1	14	52	21	27	-3	6	14	105	62	17	2	4	15	17	32	16	2	2	16	0	4	1	2	2	17	124	112	16
2	1	14	230	230	6	-2	6	14	50	6	49	3	4	15	0	4	1	3	2	16	51	37	27	3	2	17	95	59	16
3	1	14	200	199	7	-1	6	14	94	79	24	4	4	15	85	20	24	4	2	16	59	69	37	4	2	17	33	5	32
4	1	14	27	5	27	0	6	14	106	42	26	5	4	15	104	89	16	5	2	16	139	128	12	-10	3	17	0	26	1
5	1	14	108	117	14	1	6	14	37	22	37	-10	5	15	45	77	45	-11	3	16	80	68	31	-9	3	17	51	33	51
6	1	14	138	103	13	2	6	14	0	8	1	-9	5	15	113	94	28	-10	3	16	65	17	65	-8	3	17	0	68	1
7	1	14	16	18	16	3	6	14	0	5	1	-8	5	15	64	6	45	-9	3	16	54	11	58	-7	3	17	210	194	13
-13	2	14	111	127	20	4	6	14	0	32	1	-7	5	15	81	66	24	-8	3	16	103	104	23	-6	3	17	142	141	13
-12	2	14	117	123	18	-7	7	14	72	49	25	-6	5	15	98	113	16	-7	3	16	155	181	13	-5	3	17	10	62	10
-11	2	14	74	87	54	-6	7	14	35	47	34	-5	5	15	46	24	46	-6	3	16	138	132	10	-4	3	17	77	68	19
-10	2	14	85	44	20	-5	7	14	0	26	1	-4	5	15	108	130	15	-5	3	16	12	48	11	-3	3	17	59	8	58
-9	2	14	0	11	1	-4	7	14	106	93	14	-3	5	15	136	101	18	-4	3	16	65	65	28	-2	3	17	89	116	16
-8	2	14	158	144	8	-3	7	14	143	134	12	-2	5	15	0	5	1	-3	3	16	63	40	22	-1	3	17	179	175	11
-7	2	14	239	256	6	-2	7	14	114	100	16	-1	5	15	79	86	32	-2	3	16	78	73	17	0	3	17	97	126	14
-6	2	14	224	223	7	-1	7	14	18	28	17	0	5	15	141	75	76	-1	3	16	203	195	9	1	3	17	0	36	1
-5	2	14	113	104	8	0	7	14	97	18	26	1	5	15	68	12	29	0	3	16	109	86	12	2	3	17	93	57	26
-4	2	14	62	12	17	1	7	14	0	54	1	2	5	15	95	44	19	1	3	16	51	10	34	3	3	17	0	14	1
-3	2	14	95	56	24	-12	1	15	0	25	1	3	5	15	95	111	16	2	3	16	40	50	40	4	3	17	64	53	23
-2	2	14	66	47	20	-11	1	15	110	113	16	4	5	15	0	35	1	3	3	16	0	42	1	-9	4	17	0	15	1
-1	2	14	216	210	7	-10	1	15	123	89	11	-8	6	15	46	50	46	4	3	16	98	67	16	-8	4	17	100	106	28
0	2	14	281	280	6	-9	1	15	114	124	14	7	6	15	0	10	1	5	3	16	105	76	26	-7	4	17	191	213	17
1	2	14	221	209	7	-8	1	15	213	210	7	-6	6	15	0	5	1	-10	4	16	97	76	24	-6	4	17	134	155	17
2	2	14	38	46	37	-7	1	15	0	64	1	-5	6	15	94	91	16	-9	4	16	0	54	1	-5	4	17	77	40	33
3	2	14	0	50	1	-6	1	15	76	44	18	-4	6	15	188	209	10	-8	4	16	43	27	42	-4	4	17	84	53	28
4	2	14	83	62	16	-5	1	15	81	91	16	-3	6	15	173	146	16	-7	4	16	72	12	32	-3	4	17	89	21	27
5	2	14	127	148	13	-4	1	15	177	183	7	-3	7	15	76	77	30	1	4	16	64	50	33	-7	5	17	73	14	49
6	2	14	143	129	10	-3	1	15	130	139	11	-2	7	15	35	21	35	2	4	16	32	32	32	-6	5	17	49	14	49
-5	3	14	93	111	10	6	1	15	61	8	39	0	7	15	0	30	1	4	16	35	53	34	-4	5	17	54	34	24	
-4	3	14	56	22	32	-7	2	15	56	40	47	-6	6	16	63	75	40	-3	5	16	110	98	20	-4	6	17	101	119	42
3	3	14	0	14	1	-6	2	15	107	110	12	-5	6	16	168	185	12	-2	5	16	97	79	22	-3	6	17	105	91	53
4	3	14	51	32	50	-5	2	15	0	31	1	-4	6	16	231	245	10	-1	5	16	71	81	32	-2	6	17	0	30	1
5	3	14	77	66	21	-4	2	15	136	114	9	-3	6	16	53	53	0	5	16	39	63	39	-1	6	17	0	10	1	
6	3	14	94	64	15	-3	2	15	231	224	7	-2	6	16	0	67	1	5	16	79	36	78	-11	0	18	144	121	16	
7	3	14	36	53	36	-2	2	15	61	50	22	-1	6	16	44	21	30	1	2	16	76	85	27	-10	0	18	72	119	35
-11	4	14	103	27	36	-1																							

5	5	14	56	47	56	-5	4	15	80	68	19	-5	2	16	142	128	10	-5	2	17	144	161	10	-7	2	18	61	72	26
-9	6	14	57	18	56	-6	4	15	45	53	44	-4	2	16	48	45	39	-4	2	17	207	204	8	-6	2	18	0	33	1
-8	6	14	69	26	29	-3	4	15	36	32	36	-3	2	16	0	48	1	-3	2	17	68	42	28	-5	2	18	67	49	56
-4	2	18	0	15	1	-4	4	18	31	94	30	2	1	19	101	68	17	-4	4	19	0	31	1	-8	2	20	97	105	18
-3	2	18	25	5	25	-3	4	18	35	23	35	-9	2	19	59	63	59	-3	4	19	117	34	22	-7	2	20	98	99	25
-2	2	18	62	115	28	-2	4	18	51	2	50	-8	2	19	53	35	31	-2	4	19	105	129	26	-6	2	20	59	31	34
-1	2	18	115	120	13	-1	4	18	46	22	46	-7	2	19	52	7	42	-1	4	19	94	131	60	-5	2	20	10	17	10
0	2	18	53	37	42	0	4	18	70	40	69	-6	2	19	68	16	28	0	4	19	43	21	42	-4	2	20	0	26	1
1	2	18	68	13	30	1	4	18	57	19	30	-5	2	19	84	83	31	-9	0	20	68	16	67	-3	2	20	103	64	17
2	2	18	0	5	1	-7	5	18	56	35	56	-4	2	19	113	116	15	-8	0	20	53	15	53	-2	2	20	66	118	54
3	2	18	51	27	51	-6	5	18	0	33	1	-3	2	19	44	19	44	-7	0	20	111	24	23	-1	2	20	90	88	19
-10	3	18	0	7	1	-5	5	18	73	83	34	-2	2	19	58	18	32	-6	0	20	125	136	19	0	2	20	60	34	34
-9	3	18	94	41	25	-4	5	18	53	93	53	-1	2	19	0	16	1	-5	0	20	110	123	26	-7	3	20	56	52	55
-8	3	18	73	103	42	-3	5	18	61	52	61	0	2	19	0	16	1	-4	0	20	89	25	47	-6	3	20	67	8	43
-7	3	18	0	79	1	-2	5	18	70	24	69	1	2	19	28	98	27	-3	0	20	95	59	68	-5	3	20	85	3	32
-6	3	18	75	59	36	-1	5	18	33	48	32	2	2	19	89	85	37	-2	0	20	51	24	50	-4	3	20	46	28	45
-5	3	18	71	69	71	0	5	18	79	56	44	-8	3	19	57	65	57	-1	0	20	0	5	1	-3	3	20	91	42	22
-4	3	18	77	76	19	-10	1	19	24	47	24	-7	3	19	102	106	21	0	0	20	47	72	47	-2	3	20	145	110	12
-3	3	18	0	44	1	-9	1	19	102	89	15	-6	3	19	0	82	1	1	0	20	78	93	78	-1	3	20	82	70	18
-2	3	18	53	73	53	-8	1	19	50	51	50	-5	3	19	0	13	1	-8	1	20	88	61	23	-6	1	21	82	78	20
-1	3	18	75	93	67	-7	1	19	0	13	1	-4	3	19	77	55	45	-7	1	20	0	30	1	-5	1	21	121	116	18
0	3	18	111	65	15	-6	1	19	88	35	21	-3	3	19	0	34	1	-6	1	20	29	52	29	-4	1	21	96	84	18
1	3	18	37	29	36	-5	1	19	135	113	11	-2	3	19	130	120	12	-5	1	20	105	90	15	-3	1	21	27	32	27
2	3	18	34	19	33	-4	1	19	83	63	23	-1	3	19	117	92	14	-4	1	20	0	29	1	-2	1	21	31	7	30
3	3	18	38	23	38	-3	1	19	40	36	40	0	3	19	9	15	9	-3	1	20	69	12	25	-5	2	21	0	78	1
-8	4	18	53	41	52	-2	1	19	0	42	1	1	3	19	19	29	18	-2	1	20	39	28	39	-4	2	21	62	51	29
-7	4	18	0	3	1	-1	1	19	49	11	49	-7	4	19	102	121	23	-1	1	20	71	29	71	-3	2	21	7	7	7
-6	4	18	64	7	64	0	1	19	80	34	22	-6	4	19	113	56	21	0	1	20	0	30	1						
-5	4	18	47	55	47	1	1	19	106	131	33	-5	4	19	0	9	1	1	1	20	58	41	57						

## REFERENCES

- 1.Richter-Addo, G.B.; Legzdins, P. Metal Nitrosyls, Oxford University Press, New York, 1992, pgs. 336-337.
- 2.Tokiwa, H.; Nakagawa, R.; Horikawa, K.; Ohkubo, A. *Environ. Health Perspect.* 1987, 73, 191.
- 3.Feldman, P.L.; Griffith, O.W.; Stuehr, D.J. *C&En* 1993, 23.
- 4.Koshland, O.E., jr. *Science* 1992, 258, 1861.
- 5.Clarke, M.J.; Gaul, J.B. *Structure and Bonding*. 1993, 81, 147.
- 6.Doyle, M.O.; Hoekstra, J.W. *J.Inorg.Biochem.* 1981, 14, 351.
- 7.Lancaster, Jr, J.R., Hibbs, Jr, J.B., *Proc.Natl.Acad.Sci. USA.*, 1990, 87, 1223-1227.
- 8.Richter-Addo, G.B.; Legzdins, P. Metal Nitrosyls, Oxford University Press, New York, 1992, pgs. 17-18.
- 9.Jezowska-Tresebiatowska, B.; Jezierski, A. *J.Mol.Struc.* 1973, 19, 635.
- 10.Enemark, J.H.; Feltham, R.D. *Coord.Chem.Rev.* 1974, 13, 339.
- 11.Chisholm, M.H.; Cotton, F.A.; Extine, M.W.; Kelly, R.L. *Inorg.Chem.* 1979, 18, 116.
- 12.Richter-Addo, G.B.; Legzdins, P. Metal Nitrosyls, Oxford University Press, New York, 1992, pgs 33-68.
- 13.Legzdins, P.; Malito, J.T. *Inorg.Chem.* 1975, 14, 1875.
- 14.Mason, J.; Mingos, D.M.P.; Sherman, D.; Wardle, R.W. *J.Chem.Soc., Chem.Comm.* 1984, 1223.
- 15.Schoonover, M.W.; Baker, E.C.; Eisenberg, R. *J.Am.Chem.Soc.* 1979, 101, 1880.
- 16.Enemark, J.H.; Feltham, R.D.; Riker-Nappier, J.; Bizot, K.F. *Inorg.Chem.* 1975, 14, 624.
- 17.Crease, A.E.; Legzdins, P.J. *J.Chem.Soc., Dalton Trans.* 1973, 1501.
- 18.Legzdins, P.; Rettig, S.J.; Sanchez, L. *Organometallics* 1988, 7, 2394.
- 19.Fjare, D.E.; Gladfelter, W.L. *J.Am.Chem.Soc.* 1984, 106, 4799.
- 20.La Monica, G.; Freni, M.; Cenini, S. *J.Organomet.Chem.* 1974, 71, 57.
- 21.Fenske, R.F.; Millet, M.C. *Organometallics* 1986, 5, 1243.
- 22.Johnson, B.F.G.; Bhaduri, S.; Connelly, N.G. *J.Organomet.Chem.* 1972, 40, C36.
- 23.Mond, R.L.; Wallis, A.E. *J.Chem.Soc.* 1922, 121, 32.
- 24.Seel,F. *Z.Anorg.Algem.Chem.* 1952, 269, 40.
- 25.Summerville, R.H.; Hoffman, R. *J.Am.Chem.Soc.* 1976, 98, 7240.
- 26.Bryar, T. McMaster University Ph.D. thesis.
- 27.Morris, D.E.; Basolo, F. *J.Am.Chem.Soc.* 1968, 90, 2531.
- 28.Allano, V.G.; Araneo, A.; Bellon, P.L.; Ciani, G.; Manassero, M. *J.Organomet.Chem.* 1974, 67, 413.
- 29.Hörsken, A; Zheng, G.; Stradiotto, M.; McCrory, C.T.C.; Li, L. *J.Organomet.Chem.* 1998, 558, 1.
- 30.Amoroso, D.; McCrory, C.T.C.; Zheng, G.; Li, L. unpublished results.
- 31.Basolo, F. *Polyhedron* 1990, 9, 1503.
- 32.Connelly, N.G. *Inorg.Chim.Acta. Reviews.* 1972, 47.

- 33.Sun, S.; Sweigart, D.A. *Adv.Organomet.Chem.* **1996**, *40*, 171.
- 34.Huang, Y.; Carpenter, G.B.; Sweigart, D.A.; Chung, Y.K.; Lee, B.Y. *Organometallics* **1995**, *14*, 1423.
- 35.Hershberger, J.W.; Klingler, R.J.; Kochi, J.K. *J.Am.Chem.Soc.* **1983**, *105*, 61.
- 36.Zielman, P.M.; Amatore, C.; Kochi, J.K. *J.Am.Chem.Soc.* **1984**, *106*, 3771.
- 37.Li, L.; Enright, G.D.; Preston, K.F. *Organometallics* **1994**, *13*, 4686.
- 38.McBride, D.W.; Stafford, S.L.; Stone, F.G.A. *Inorg.Chem.* **1962**, *1*, 386.
- 39.Reginato, N. 4<sup>th</sup> year Thesis project.
- 40.Atkinson, Black, J.ChemSoc. Dalton trans, 1996, 3491.
- 41.Richter-Addo, G.B.; Legzdins, P. Metal Nitrosyls, Oxford University Press, New York, **1992**, Chapter 2.
- 42.Martini, G.; Tiezzi, E. *Z.Naturforsch.* **1973**, *28b*, 300.
- 43.Jezowska-Tresebiatowska, B.; Jezierski, A. *J.Mol.Struc.* **1973**, *19*, 635.
- 44.Li, L.; Morton, J.R.; Preston, K.F. *Magn.Res in Chem.* **1996**, *33*, S20.
- 45.Martini, G.; Tiezzi, E. *Z.Naturforsch.* **1973**, *28b*, 300.
- 46.Richter-Addo, G.B.; Legzdins, P. Metal Nitrosyls, Oxford University Press, New York, **1992**, pg. 55.
- 47.Summerville, R.H.; Hoffman, R. *J.Am.Chem.Soc.* **1976**, *98*, 7240.
- 48.Amoroso, D.; McCrory, C.T.C; Li, L. unpublished results.
- 49.Allano, V.G.; Araneo, A.; Bellon, P.L.; Ciani, G.; Manassero, M. *J.Organomet.Chem.* **1974**, *67*, 413.
- 50.Amoroso, D.; McCrory, C.T.C; Li, L. unpublished results.
- 51.Van Berkel, G.J. in Electrospray Ionization Mass Spectrometry, pg 65-106, John Wiley and Sons, Inc., 1997.
- 52.Smith, R.W. McMaster University, McCrory, C.T.C. personal communication.
- 53.Gaskell, S.J.; *J.Mass.Spec.* **1997**, *32*, 677.
- 54.Hofmann, K. Imidazole and its Derivatives, Part 1. Interscience Publisher, Inc. New York, 1953, pg7-9.
- 55.Smith, R.W. McMaster University, McCrory, C.T.C. personal communication.
- 56.Jarvis, J.A.J.; Wells, A.F. *Acta Cryst.* **1960**, *13*, 1027.
- 57.Bauman, J.E., Jr.; Wang, J.C. *Inorg.Chem.* **1964**, *3*, 368.
- 58.Inoue, M.; Kishita, M.; Kubo, M. *Inorg. Chem.* **1965**, *4*, 626.
- 59.Bauman, J.E., Jr.; Wang, J.C. *Inorg.Chem.* **1964**, *3*, 368.
- 60.Rettig, S.J.; Storr, A.; Summers, D.A.; Thompson, R.C.; Trotter, J. *J.Am.Chem.Soc.* **1992**, *119*, 8675.
- 61.Foffani, A.; Pignataro, S.; Distefano, G.; Innorta, G. *J.Organomet.Chem.* **1967**, *7*, 473.
- 62.Seel, F. *Z.Anorg.Allg.Chem.* **1952**, *269*, 40.
- 63.Burford, N.; Muller, J.; Parks, T.M. *J.Chem.Ed.* **1994**, *9*, 807.
- 64.Doyle, M.P.; van Doornik, J.V.; Fundkes, C.L. *Inorg.Chim.Acta.* **1980**, *46*, L111.
- 65.Doyle, M.P.; Pickering, R.A.; Cook, B.R. *J.Inorg.Biochem.* **1983**, *19*, 329.
- 66.Mu, X.H.; Kadish, K.M. *Inorg.Chem.* **1990**, *29*, 1031.
- 67.Kadish, K.M.; Mu, X.H.; Lin, X.Q. *Inorg.Chem.* **1988**, *27*, 1489.